Characterization of Sugars and Glycans from Ovalbumin Using a Combination of Derivatization, High-Performance Liquid Chromatography and Mass Spectrometry

By

Xiaodong Shen

A Thesis Submitted to the Faculty of Graduate Studies in Partial Fulfilment of the Requirements for the Degree of Master of Science

Department of Chemistry
University of Manitoba
Winnipeg, Manitoba

THE UNIVERSITY OF MANITOBA

FACULTY OF GRADUATE STUDIES

*****

COPYRIGHT PERMISSION PAGE

CHARACTERIZATION OF SUGARS AND GLYCANS FROM OVALBUMIN USING A COMBINATION OF DERIVATIZATION, HIGH-PERFORMANCE LIQUID CHROMATOGRAPHY AND MASS SPECTOMETRY

BY

XIAODONG SHEN

A Thesis/Practicum submitted to the Faculty of Graduate Studies of The University of Manitoba in partial fulfillment of the requirements of the degree of

MASTER OF SCIENCE

ABSTRACT

A combination of derivatization, reversed-phase high performance liquid chromatography (RP-HPLC), and mass spectrometry techniques has been explored for the characterization of small sugars, medium-size oligosaccharides, and glycans detached from chicken egg albumin (ovalbumin) by hydrazinolysis. Derivatization methods using 2-aminopyridine (PA) and 1-phenyl-3-methyl-5-pyrazolone (PMP) were selected among a number of previously reported methods for labeling carbohydrates since both had shown a quantitative yield, a rapid reaction and a simple workup procedure. The PMP derivatization method was preferred over pyridylamination owing to the simplicity of the reaction involved and, most importantly, its better enhancement of ionization efficiency in fast atom bombardment (FAB), electrospray (ESI), and matrix-assisted laser desorption/ionization (MALDI-MS). In addition, the good quality and ease of separation of PMP-derivatives by HPLC are also advantages of using PMP rather than PA as a derivatizing reagent. The PA- and PMP-derivatives of mono-, di-, and trisaccharides yielded FAB spectra with low S/N ratios, whereas ESI and MALDI produced better spectra with 100 times less material used for FAB. In general, PMP-derivatives of di- and tri-saccharides gave rise to stronger signals than PA analogs. For oligosaccharides with more than three rings, only PMP-derivatives produced structurally related information, and only ESI and MALDI were utilized while FAB was dropped. Sensitivity studies were carried out using a standard oligosaccharide, tetraglucose. One purpose of these studies was to determine the minimum amounts of PMP-tetraglucose required to obtain informative full-scan ESI spectra and collision-induced dissociation tandem (MS/MS)

spectra. The other aim was to study the fragmentation patterns of PMP-derivatives. Qualitative fragmentation studies of PMP-derivatives were also carried out with typical N-linked oligosaccharides obtained commercially. PMP-derivatives of these standard oligosaccharides not only produce abundant molecular ions, but also informative sequence-related fragment ions in ESI-MS and ESI-MS/MS while the MALDI mass spectra mainly yielded molecular ions, such as $[M+H]^+$, and $[M+Na]^+$. With this information in hand, the derivatization method was then applied to N-glycans cleaved from ovalbumin, which has only one N-glycosylation site. Intact ovalbumin was first analyzed by ESI- and MALDI-MS prior to the characterization of PMP-glycans by ESI-MS and ESI-MS/MS. The combination of ESI- and MALDI-MS of intact ovalbumin and ESI of PMP-glycans gave rise to detection of 27 different glycoforms, indicating microheterogeneity of this glycosylation site.

ACKNOWLEDGEMENTS

First of all, I would like to express my sincere appreciation to my supervisor, Dr. Hélène Perreault for her support, and detailed guidance throughout the course of this project, and for sharing her rich and wide knowledge and experience with me. I would also like to thank Dr. Philip. G. Hultin for his never forgettable encouragement, suggestions, help, and patience as well as for our use of his HPLC system.

I also wish to express my thanks to Dr. K. G. Standing, Dr. W. Ens and their research group (Physics Department, University of Manitoba) for use of Manitoba-II instrument and my appreciation to Mr. W. D. Buchannon for help with the FAB experiments. My acknowledgments also go to Drs. J. L. Charlton, A. S. Secco, and F. E. Hruska (Chemistry Department, University of Manitoba) for our use of their HPLC system. I am very grateful for the assistance from Mr. M. McComb during my research work. My thanks also go to Dr. Y. She for help with MALDI-MS analysis. I would like to thank D. Asres, R. Manswell, and T. Williams for their help and for making these almost three years so enjoyable and colourful. I also want to express my appreciation to Micromass UK Ltd. for the use of the Quattro-II and Q-Tof mass spectrometers.

Finally, I wish to express my love to my parents for all they have done for me. I especially thank my mother who died when I was in England for her love which is invaluable in all of my life and for what she gave to me which could not be better.

TABLE OF CONTENTS

LIST OF FIGURES

LIST OF SCHEMES

LIST OF TABLES

ABBREVIATIONS

ABDEAE	4-amino-benzoic acid 2-(diethylamino)ethyl ester
ABEE	p-aminobenzoic acid ethyl ester
ABT	2-aminobenzenthiol
AET	2-aminoethanethiol
Asn	Asparagine
BA	Benzoic anhydride
BC	Benzoyl chloride
$BF_3 \cdot Et_2O$	Boron trifluoride etherate
^{252}Cf-PD	Californium-252 plasma desorption
CHCA	α-cyano-4-hydroxy-cinnamic acid
CID	Collision induced dissociation
CI-MS	Chemical ionization mass spectrometry
CID-MS/MS	Collision-induced dissociation-tandem mass spectrometry
C.V.	Cone voltage
DANSYL	Dimethylamine-1-naphthalenesulfonyl
DCI	Desorption chemical ionization
DHB	2,5-dihydroxybenzoic acid
DNPO	N, N-(2, 4-dinitrophenyl)octylamine
EI-MS	Electron ionization mass spectrometry
ESI	Elcectrospray ionization
Et_3SiH	Triethylsilane

eV	Electron volts
FAB	Fast atom bombardment
FD	Field desorption
Fuc	L-fucose
Gal	D-galactose
GalNAc	N-acetyl-D-galactosamine
GC-MS	Gas chromatography-mass spectrometry
Glc	D-glucose
GlcNAc	N-acetyl-D-glucosamine
Hex	Hexose
HexNAc	N-acetylhexosamine
HPAEC	High pH anion exchange chromatography
HPLC	High performance liquid chromatography
IgG	Human immunoglobulin
kV	Kilo volts
LC	Liquid chromatography
LC/ESI-MS	HPLC coupled to ESI-MS
LD	Laser desorption
LSIMS	Liquid secondary ion mass spectrometry
MALD	Matrix-assisted laser desorption
MALDI	Matrix-assisted laser desorption/ionization
Man	D-mannose

$[M+H]^+$	Protonated molecular ion
$[M-H]^-$	Deprotonated molecular ion
$[M+2H]^{2+}$	Doubly charged protonated molecular ion
$[M+Na]^+$	Sodiated molecular ion
$[M+2Na]^{2+}$	Doubly charged sodiated molecular ions
M_r	Molecular mass
MS	Mass spectrometry
MS/MS	Tandem mass spectrometry
m/z	Mass to charge ratio of an ion
NANA	N-acetylneuraminic acid
m-NBA	m-nitrobenzylalcohol
NeuGc	N-glycolyl neuraminic acid
NeuNAc	N-acetylneuraminic acid
NGNA	N-glycolyl neuraminic acid
NMR	Nuclear magnetic resonance
ORM	Oxidation, reduction, and methylation
PA	Pyridylamination, or 2-aminopyridine, or pyridylamino
PMAAs	Partially methylated alditol acetates
PMP	1-phenyl-3-methyl-5-pyrazolone
PMPMP	1-(p-methoxy)phenyl-3-methyl-5-pyrazolone
PPEADP	Phosphatidylethanolamine dipalmitoate
PSD	Post-source decay

QQQ	Triple quadrupole
RI	Refractive index
RP-HPLC	Reverse-phase high performance liquid chromatography
SA	3,5-dimethoxy-4-hydroxycinnamic acid, or sinapinic acid.
SA	Sialic acid
SI	Secondary ion
SIMS	Secondary ion mass spectrometry
S/N	Signal to noise ratio
TFA	Trifluoroacetic acid
Thr	Threonine
TIC	Total ion current
TLC	Thin-layer chromatography
TMSOMs	Trimethylsilylmethane sulfonate
TMSOTf	Trimethylsilyl trifluoromethane sulfonate
TMAPA	Trimethyl (p-aminophenyl)-ammonium chloride
TSI	Thermospray ionization
UV	ultra-violet
V	Volts
Xyl	D-xylose
z	Charge number of an ion

1. INTRODUCTION

1.1 Importance of Glycoproteins and Their Glycan Components

Many important cell membrane proteins and serum proteins contain carbohydrate chains; these proteins are termed glycoproteins [1]. Of the many proteins that have been characterized, greater than 50% are glycosylated [2]. Glycoproteins are complex macromolecules existing in a large diversity and are present in all forms of life: animals, plants, and microorganisms [3]. They comprise several important classes of macromolecules, such as enzymes, hormones, immunoglobulins, transport proteins, cell adhesion molecules, toxins, lectins, structural proteins, and even the recently discovered cytoplasmic and nucleoplasmic proteins. These important macromolecules perform diverse biological functions including enzymatic catalysis, hormonal control, immunological protection, ion transport, blood clotting, lubrication, surface protection, structural support, cell adhesion, intercellular interaction, and most important, in recognition in general [3]. Glycoproteins are more precisely defined as conjugated proteins [3]. The role of protein-bound carbohydrates in biological recognition, such as that in host-pathogen, cell-cell, and cell-molecule interactions, among other biological processes, has aroused great interest and the popularity of this field has been increasing over the recent years. It has been known for some time that carbohydrates have an effect on the physiochemical properties of proteins, such as viscosity, isoelectric pH, degree of hydration, solubility, thermal stability, and resistance to proteolysis. Recent findings, e.g. the alteration in the glycan structures in various developmental and pathological states of glycoproteins, have suggested that glycans have great biological significance. The direct involvement of

glycans in biological functions has been demonstrated. For example, the removal of the glycans from some glycosylated hormones, such as human chorionic gonadotropin (hCG), lutropin (LH), and thyrotropin (TSH), resulted in a drastically reduced biological response relative to that of native hormones [3]. Generally, glycans play two major roles, one of which is to confer certain physicochemical properties to proteins, and the other is to act as signals for cell-surface recognition phenomena [4].

Glycoproteins currently constitute an active area of research, and the functional significance of the carbohydrate moieties has become increasingly apparent. The interest in carbohydrate function has created a need for rapid, reliable and sensitive methods for carbohydrate detection and analysis [5]. Characterization of carbohydrates would lead to a new insight into the biological functions of glycans. Structural elucidation of complex oligosaccharides found in glycoproteins remains challenging. In contrast to the linear protein and nucleic acid biopolymers, sugar analysis involves characterization of sugar sequence, branching pattern, linkage positions, anomeric configuration, and ring forms of the monosaccharide units present, as well as three-dimentional structure and possible presence of sulfate or phosphate groups [6-8].

1.2 Nomenclature and Structural Rules for Oligosaccharides in Glycoproteins

Monosaccharides commonly encountered in glycoproteins are listed in Table 1.1 [4, 8].

When a D-mannopyranose is linked to a N-acetyl-D-glucosamine as shown in Fig.1.1, Man can be linked to the GlcNAc at four different positions: C-2, C-3, C-4, and C-6. In addition, a Man residue can take two anomeric configurations, α or β. The

Table 1.1 Monosaccharides commonly encountered in animal glycoproteins [4,8].

Monosaccharide	**Abbreviation**
N-acetylneuraminic acid	NeuNAc* or NANA
N-glycolyl neuraminic acid	NeuGc, or NGNA
Sialic acid (either NeuNAc or NeuGc)	SA*
D-glucose	Glc
D-galactose	Gal
N-acetyl-D-glucosamine	GlcNAc
N-acetyl-D-galactosamine	GalNAc
D-mannose	Man
L-fucose	Fuc
D-xylose	Xyl

* used in this thesis.

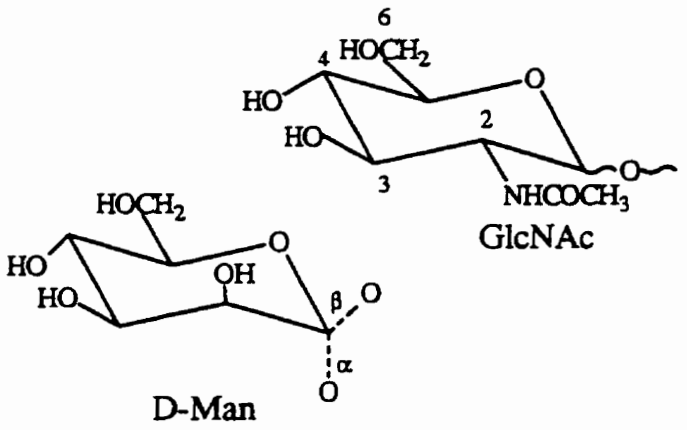

Fig. 1.1 Man can be linked to the GlcNAc at four different positions.

expression "Manβ1-4GlcNAc" represents a bond between C-1 of β-Man and C-4 of GlcNAc [5].

The glycans of glycoproteins can be classified into two groups since they can be linked to two different types of amino acids. The sugars called O-linked or mucin type are linked at serine, threonine, or (rarely) hydroxylysine residues of a polypeptide through a hydroxyl oxygen. The sugars classified as N-linked contain a GlcNAc at their reducing termini and are linked to the amide nitrogen of an asparagine residue found in the following sequence: Asn-X-Ser/Thr (Asn, asparagine; X, any amino acid; Ser, serine; Thr, threonine) [5,9]. N-linked sugars are more commonly found than O-linked sugars in mammalian glycoproteins, but a single glycoprotein may have multiple sugar chains, some of which are N-linked and some of which are O-linked [5].

Accumulation of structural data revealed that N-linked sugar chains conform to more structural rules than O-linked sugars [10]. All N-linked glycans contain a pentasaccharide, Manα1-6(Manα1-3)Manβ1-4GlcNAcβ1-4GlcNAc, as a common core. This core is called trimannosyl core and has been highly conserved during evolution. N-linked glycans can be further subclassified into three groups termed as glycotypes [11], differing only in the peripheral sugar residues, as shown in Fig. 1.2. Each glycotype is named according to the structure and the location of glycan residues added to the trimannosyl core [4]. These glycotypes are usually consistent at any one site [11]. Structural variations within a motif are termed glycoforms, which are often observed as a molecular distribution associated with microheterogeneity at a single glycosylation site [11], as a result of their biosynthesis in which several modifying enzymes compete for

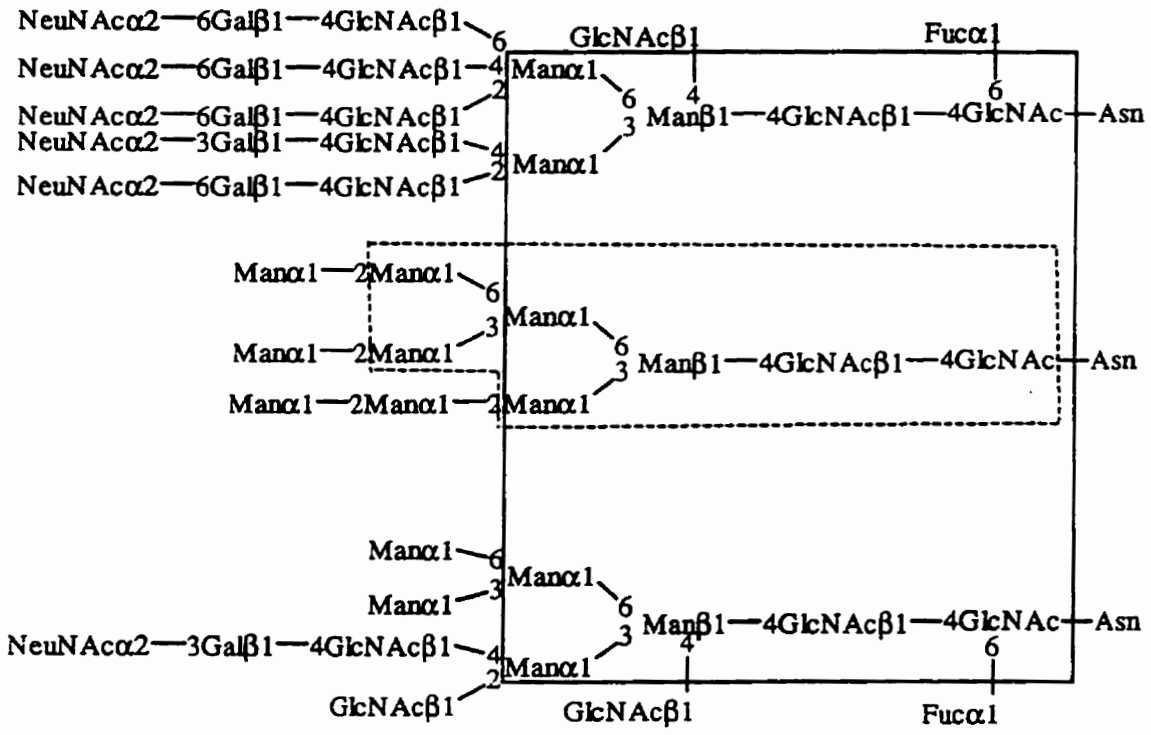

Fig. 1.2 The subgroups of N-linked sugar chains: (1) complex-type sugar chains; (2) high-mannose-type sugar chains; (3) hybrid-type sugar chains. The structure within the solid line is the pentasaccharide structure common to all N-linked sugar chains. The structure enclosed with a dotted line is the common heptasaccharide of high-mannose-type sugar chains. Structures outside the solid line can vary in their sugar chains [10].

common carbohydrate substrates [8]. The high-mannose-type structures contain from two to six additional mannose residues linked to the trimannosyl core [5]. The complex-type structures usually have from two to four branches attached to the two outer core mannose residues. The branches are distributed over the two terminating core Man residues. The complex structures are termed diantennary, triantennary, and tetraantennary, referring to the number of antennae. The basic branch structures are composed in most instances of one GlcNAc and one Gal residue. To complicate matters further each of these arms can terminate in SA. It is possible to have a tetraantennary complex glycoform with zero to four terminating SA residues [12]. Mammalian glycoproteins commonly carry complex oligosaccharides with 2-4 antennae, but pentaantennary and hexaantennary oligosaccharides have been described [5]. In addition, some complex-type glycans have an α-Fuc residue linked to the C-6 position of the proximal GlcNAc residue and a β-GlcNAc residue linked to the C-4 position of the β-Man residue of the trimannosyl core (bisecting GlcNAc).

The third group is called hybrid-type since the oligosaccharides have the structural features of both high-mannose-type and complex-type sugar chains. One or two α-Man residues are linked to the Manα1→6 arm of the trimannosyl core as in the case of the high-mannose-type, and the outer chains as in the complex-type are linked to the Manα1→3 arm of the core of this group. The glycans in this group also have an α-Fuc residue and the bisecting GlcNAc linked to the trimannosyl core, as in the complex type [10]. According to the biosynthesis pathway of asparagine-linked oligosaccharides, fucosyltransferase works only on substrates which have an unsubstituted GlcNAc in the

first antenna. Thus fucose may be added to the core of hybrid or complex oligosaccharide structures, but may not be added to high-mannose structures (which lack the GlcNAc of the first antenna). Fucosyltransferase will also not work on bisected structures [5].

It has been revealed that complex N-linked oligosaccharides tend to be located at N- terminus of proteins whereas high-mannose-types are located closer to the C- end of proteins. Furthermore, serum glycoproteins contain mainly complex-types while membrane glycoproteins have both complex- and high-mannose-type of oligosaccharides [13].

In contrast to N-linked glycans, O-linked glycans have fewer structural rules. They do not share a common core. Instead, they are based on several different cores and are more difficult to define. So far, these sugar chains can be classified into at least four groups according to their core structures (Fig. 1.3) [10]. Furthermore, O-linked sugars with GlcNAcβ1→6GalNAc and the GalNAcβ1→3GalNAc cores are found in a limited number of glycoproteins [10]. The O-linked sugars are usually short (2-10 residues), but longer chains may also occur. The sugar directly linked to the protein is frequently GalNAc (e.g., in mucins) or Gal (e.g., in collagens) [5]. O-linked structures in general appear to be less complex than N-linkages in the number of antennae and monosaccharides. However, they can be fucosylated and sialylated [12].

1.3 Release of Sugar Chains from Glycoproteins

The analysis of sugar chains involves identification of monosaccharide sequence, branching patterns, linkage positions, as well as anomeric configurations. There is no simple recipe for determing the structures of these compounds. Rather, a variety of

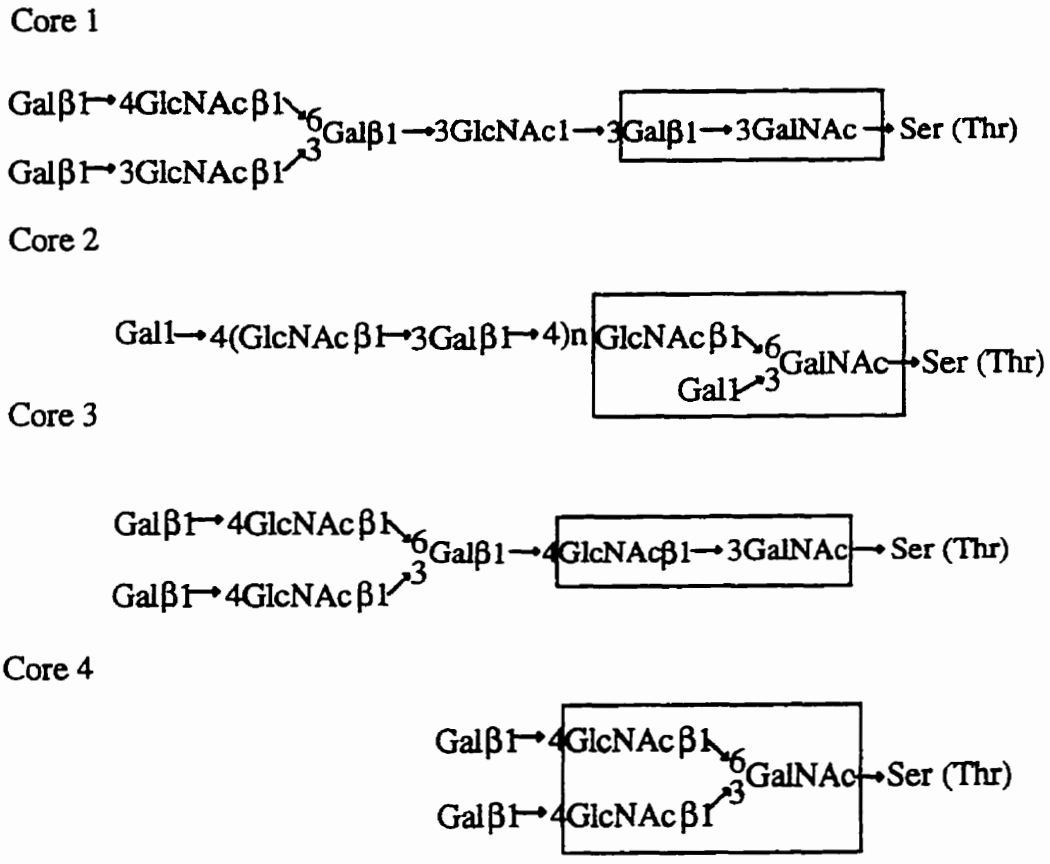

Fig.1.3. Four types of core structures found in O-linked sugar chains. The cores are enclosed by solid lines [10].

chemical and analytical methods have been used for acquiring complete structural information, and the particular procedures used depend largely on the nature and the type of starting material [7]. In most cases, structural analysis of the carbohydrate portion starts with cleavage of the sugar chains from the peptide backbone by either chemical or enzymatic methods. Cleavage is followed by fractionation of the mixture of glycans, and finally characterization of the individual components [7,14].

Chemical and enzymatic methods can be used to detach glycans from glycoproteins. Each has its advantages and disadvantages. The choice of method mainly depends on how much is already known about the structures of the oligosaccharides and their linkages to the protein, and also on the amounts of glycoprotein available [15].

1.3.1 Enzymatic Cleavage of the Oligosaccharide Portion from Glycoproteins

Until 1970, exhaustive pronase digestions had been used to convert glycoproteins into glycopeptides. However, digestions were usually incomplete and it was difficult to obtain pure glycopeptide samples due to the heterogeneities in the peptide and sugar chains [10]. Afterwards, it was considered more practical and useful to cleave the glycans from the polypeptide backbone and look at them separately. There are mainly two types of enzymes to cleave N-linked sugar chains. One type cleaves the linkage between the two GlcNAc residues in the core, producing an oligosaccharide with one GlcNAc residue at the reducing end, and leaving the other GlcNAc residue attached to Asn. The other type cleaves the linkage between the chitobiose unit and the peptide to yield the complete sugar moiety and a sugar-free peptide in which asparagine has been converted to aspartic acid [15]. The former type comprises the endo-β-N-acetylglucosaminidases, such as Endo-H,

Endo-D, Endo-F (F_1, F_2, F_3). Among these, Endo-H only cleaves high-mannose- and hybrid-type oligosaccharides, and the complex-type sugars are resistant to it. Endo-D digests only sugar chains in which the C-2 position of the α-(1→3)-linked Man of the trimannosyl core is unsubstituted. Endo-F including F_1, F_2 and F_3 cleaves high-mannose-, biantennary hybrid-, and biantennary complex-type sugar chains, while tri- and tetra-antennary complex-type sugars are resistant [15].

The second type of enzyme is based on peptide-N^4-(N-acetyl-β-glucosaminyl) asparagine amidase F, which has been given many shorter names: glycoamidase F, peptide N-glycosidase, PNGase, peptide N-glycosidase F, glycopeptidase F and N-glycanase [14,15]. This enzyme is extremely versatile and all commonly encountered N-linked sugars are susceptible to this enzyme except those occurring on C- or N-terminal asparagines [15]. The enzyme can not be guaranteed to release quantitatively all N-linked glycans and conditions for hydrolysis of a particular glycoprotein must be determined empirically [7].

However, it has been also reported that Endo-F_1 and Endo-H are similar in substrate specificity; both enzymes are nearly identical in their ability to hydrolyze high-mannose oligosaccharides and do not hydrolyze any of the complex N-linked oligosaccharides [16]. The substrate specificities of Endo F_2 and Endo F_3 are not well established, and they become more characterized as different substrates become available. An account of the specificity of each of these enzymes including PNGase F, Endo H and Endo F is presented in Fig. 1.4 [16].

Glycosidases and glycopeptidases can be used not only to release N-linked sugar chains, but also to identify glycosylation sites, in conjunction with protein primary

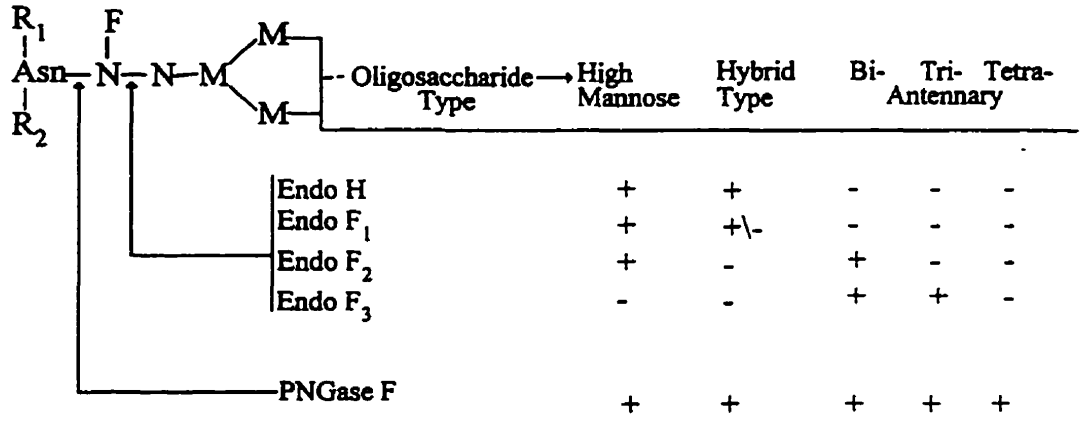

Fig. 1.4 Specificity of various endoglycosidases. Endoglycosidase specificity refers to any hydrolytic cleavage of the N-linked oligosaccharide core, including hydrolysis of the glycosylamine linkage by the amidase PNGase F, or the glycosidic cleavage of the di-N-acetylchitobiose moiety by endo-β-N-acetylglucosaminidases Endo H, Endo F_1, Endo F_2, or Endo F_3. The invariant pentasaccharide core of a N-linked glycan is shown to the left of the oligosaccharide type, and the type of attached oligosaccharide chain to the right. R_1, R_2, peptide bonds or H; N, GlcNAc; M, mannose; F, fucose; Asn, asparagine [16].

sequence analysis. This is because these two kinds of enzymes leave a marker on the protein or peptide at the glycosylation site after treatment. High-mannose- and hybrid-type structures are sensitive to Endo H. Treatment of glycoproteins or glycopeptides with this enzyme leaves behind a GlcNAc residue attached to any asparagine carrying an Endo H-susceptible oligosaccharide. PNGase F has relatively broad specificity and it converts glycosylated asparagine residues to aspartic acids after releasing the N-linked sugars from the polypeptide backbone. These enzymes can therefore be useful in revealing the occupied N-glycosylation sites and the general features of sugar chains at such sites [17].

In summary, endoglycosidases have restricted substrate specificities and generally are not suitable for obtaining a complete profile of Asn-linked oligosaccharides [14]. The best enzyme for the removal of all common types of N-linked oligosaccharides (even tetraantennary complex structures) from glycoproteins is PNGase, since its hydrophobicity enables it to gain access to the protein-oligosaccharide link which is often buried in a hydrophobic region of the protein [5].

Unlike for N-linked structures, there is no enzymatically-based method which releases all types of mono- or oligosaccharides which are O-linked to serine or threonine [18]. However, it has been reported that the O-linked disaccharide Galβ1-3GalNAc α-linked to serine or threonine can be cleaved from glycoproteins by endo-α-N-acetylgalactosaminidase from *Diplococcus pneumoniae*, also called O-glycanase, with a narrow substrate specificity [15,19]. An endo-α-N-acetylgalactosaminidase that seems to have a broader substrate specificity has been identified in culture supernatants of *Streptomuces*, but further work is required to verify the value of this enzyme as a

sequencing reagent [7].

1.3.2 Chemical Cleavage of the Oligosaccharide Portion from Glycoprotein

There are two commonly used chemical methods to cleave oligosaccharides from glycoproteins, namely, hydrazinolysis and β-elimination. Both take advantage of the high stability of glycosidic bonds to alkaline conditions [15].

1.3.2.1 Hydrazinolysis

Hydrazinolysis has been widely accepted as a technique for the nonselective and uniform release of N-linked oligosaccharides in high yield from glycoproteins [20]. Recently, a reexamination has revealed that under certain optimized conditions, O-linked oligosaccharides can also be selectively and effectively released [21].

The reaction mechanism by which hydrazinolysis functions to release N-linked oligosaccharides is still not clearly understood, and also the mechanism leading to the release of O-linked oligosaccharides has not yet been investigated at all, although a β-elimination has been suspected [22]. Reaction conditions under which N- and O-linked oligosaccharides can be released have been established empirically after thorough investigation using a range of glycoprotein standards whose glycosylation characteristics had been well defined previously [21]. Selective release of O-linked oligosaccharides with little release of N-linked oligosaccharides can be achieved with mild hydrazinolysis conditions. Hydrazinolysis can be used in three different ways, i.e. to release only O-linked oligosaccharides (60 °C for 5 h, during which 90% or more of O-linked oligosaccharides are released but less than 10% of N-linked oligosaccharides are cleaved), to release sequentially first O-linked, and then N-linked oligosaccharides, and to release all

N- and O-linked oligosaccharides (90 °C for 4 h, in which 85% or more of O- and N-linked oligosaccharides are released) [21,22]. It should be noted that hydrazinolysis may result in degradation of O-linked chains [21,22].

Although hydrazinolysis cleaves all classes of N-linked chains, it is not an ideal procedure. It can lead to low recoveries and a complex mixture of side reaction products [14,23]. The sialic acid linkage appears to be stable during hydrazinolysis, but certain N- and O- acyl substituents on sialic acids are labile [21]. The glycolyl group of NeuGc is more resistant to hydrazinolysis than the acetyl group of NeuNAc. However, it is impossible to avoid de-N-glycolylation. Therefore identification of sialic acid residues must be carried out on intact glycoproteins [24].

The reactions involved in hydrazinolysis and recovery of reducing oligosaccharides are summarized in Fig. 1.5 [20,23,25]. Through the hydrazinolysis reaction, however, N-acyl groups are removed concurrently from GlcNAc. After hydrazinolysis, the glycosylamine linkage of product (I) shown in Fig. 1.5 is very stable in aqueous solution even at acidic pH because the electron-donating effect of $-NH_2$ group stabilizes the linkage. In order to cleave this linkage, the product is N-acetylated to preclude the stabilizing effect of $-NH_2$ group by converting it to -NHAc, with acetic anhydride in a cold $NaHCO_3$ aqueous solution. The N-acetylation also reconverts glucosamine residues in the released oligosaccharides to GlcNAc residues. After N-acetylation, the oligosaccharides are mainly unreduced with a small fraction present as β-acetohydrazide derivatives (II) [22,23]. The latter have to be catalytically converted to unreduced oligosaccharides (III) with a trace of Cu^{2+} ions in a dilute acetic acid solution (Reaction 3) [22].

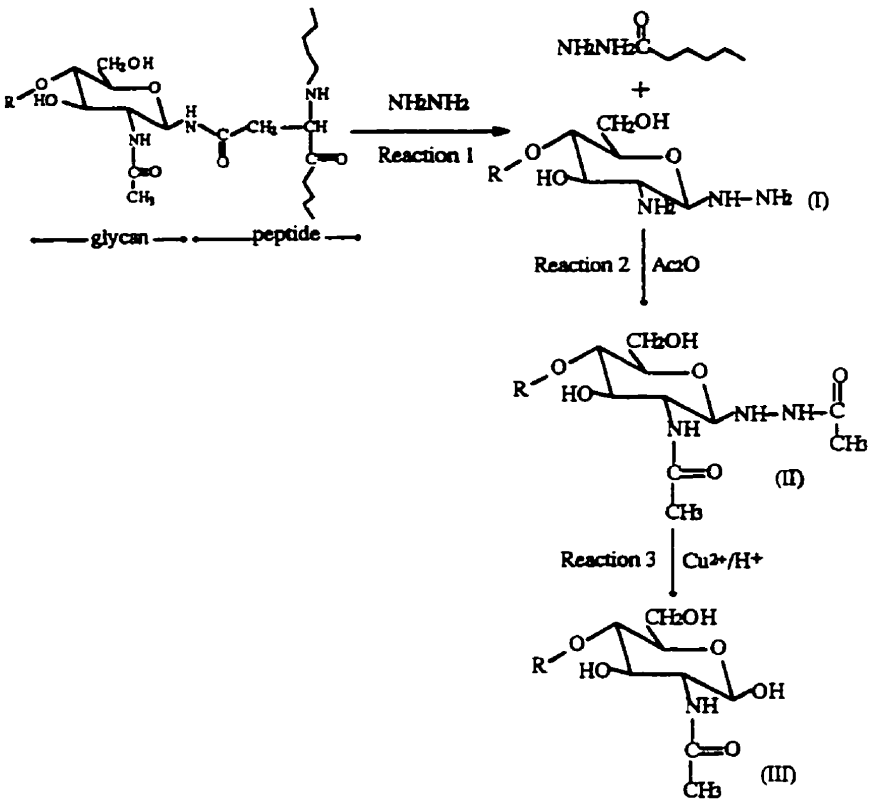

Fig. 1.5 Hydrazinolysis of N-linked sugar chains. R represents either hydrogen or sugars [20,23,25].

1.3.2.2 Reductive β-elimination

Discrimination between N- and O-linked sugar chains in glycoproteins had been traditionally based on mild alkaline borohydride treatment, which was considered to release only O-linked sugar chains. In contrast, N-glycosidic linkages between GlcNAc and asparagine were believed stable under mild conditions, although they have been known to be cleaved by alkaline borohydride under rigorous conditions [26]. It has now been shown that alkaline sodium borohydride treatment of proteins containing both N- and O-linked sugar chains (N, O-glycoproteins) gives O-linked sugars in good yields, but is accompanied by a simultaneous release of some N-linked sugar chains due to the reductive cleavage of the N-glycosylamide bond with sodium borohydride [26-28]. Likhosherstov has found that in the presence of cadmium acetate, O-linked oligosaccharides can be selectively cleaved by alkaline borohydride treatment, whereas the cleavage of N-linked sugar chains and peptide bonds is suppressed [28]. This treatment, in combination with a previously developed procedure for the release of the N-linked sugars by lithium borohydride [29], allows a sequential, and selective release of O-, and then N-linked sugar chains. O-glycosylation sites can also be identified by amino acid sequence analysis before and after reductive β-elimination. Reductive β-elimination releases O-linked oligosaccharides from glycosylated serine and threonine residues, and converts glycosylated serine residue to alanine, and glycosylated threonine to β-aminobutyric acid, while unglycosylated serine and threonine residues are not affected [17].

1.3.2.3 Trifluoroacetolysis

Another way to liberate N- and O-oligosaccharides involves treatment of

glycoproteins with a mixture of trifluoroacetic acid and its anhydride. Because of the complexity of the procedure, this method has not been widely used to cleave N- and O-linked sugar chains [15,19,24,30].

Apparently, in all cases the structure of the oligosaccharide should not be affected by the cleaving technique and subsequent chemical modification. In fact, desialylation, defucosylation, deacetylation, desulfation, and nonspecific cleavage at the reducing end are known to occur when chemical methods are used to release sugar chains or when enzymatic methods are followed by workup procedure under severe conditions (pH, temperature, chromatographic conditions for purification) [31].

1.4 Review of Current Analytical Methods for Glycans from Glycoproteins

Currently, characterization of oligosaccharide structures is laborious, insensitive, and time-consuming compared to established sequencing methods for the two other major biopolymers, proteins and nucleic acids, due to the limited amounts of oligosaccharides available, and to the complexity of composition and structure [32]. In addition, a glycoprotein has more than one carbohydrate structure attached to a single glycosylation site, so-called microheterogeneity, as a result of biosynthesis in which several modifying enzymes compete for common carbohydrate substrates [8]. This results in variable chain terminations, which complicates characterization [31,33].

A considerable amount of research has already been carried out in this area. A reliable method so far has been nuclear magnetic resonance (NMR) spectroscopy [31,34-36]. High pH anion exchange chromatography (HPAEC) has also been widely used [37,38]. Techniques involving the use of glycosidases in combination with sensitive

separation or analysis techniques to observe alterations before and after enzymatic treatment have proven to be very valuable [7]. Reverse-phase high-performance liquid chromatography (RP-HPLC) [39] and gas chromatography mass spectrometry (GC-MS) (40,41) are also commonly used techniques nowadays. However, with the advent of new soft ionization techniques such as electrospray ionization (ESI) [42,43] and matrix-assisted-laser desorption/ionization (MALDI) mass spectrometry [44-46], mass spectrometry holds a very important position in glycobiology, especially for structural elucidation of carbohydrate portions of glycoproteins.

1.4.1 Characterization of Oligosaccharide Structures by NMR

Where milligram quantities of material are available, ^{1}H and ^{13}C NMR have proven to be a powerful and nondestructive methods to provide primary structural information regarding anomeric configuration, linkage position, sequence, and composition [31,34,35]. However, many hours are needed to accumulate and interpret data [25]. The amount of pure oligosaccharide required to obtain an ^{1}H NMR spectrum in less than six hours of data acquisition time varies from 7 to 80 nmol depending on the magnetic field strength of the spectrometer available and the sensitivity of the receiver coil in the probe [31]. ^{13}C NMR spectroscopic studies require ten times more sample than ^{1}H studies [36].

The ^{1}H NMR spectrum obtained for a carbohydrate can be used as its "identity card". Comparison of the ^{1}H NMR spectrum of an unknown with that of a standard can identify the unknown. Several glycoprotein carbohydrate ^{1}H NMR databases are available for N-type glycopeptides, N-linked oligosaccharides, and O-linked oligosaccharide alditols

in D_2O. When the spectrum of the unknown does not match any of the spectra in the databases, efforts can be made to interpret the spectrum in terms of anomeric configurations and positions of glycosidic linkages using the structural reporter group concept [31]. Particularly useful structural reporter groups for ^1H NMR analyses include (1) the anomeric (H-1) protons, (2) the protons attached to the carbon atoms in direct vicinity of a linkage position, (3) the protons attached to deoxy carbon atoms, and (4) methyl protons, such as in N-acetyl groups [31].

An important advantage of NMR over other techniques is its nondestructive nature. After NMR analysis, the sample can be recovered unimpaired and used for other analyses. Furthermore, a mixture of closely related structures can be analyzed successfully. NMR however has certain limitations, therefore NMR should be the first, but never the only characterization step in the analysis procedure. It is also suggested that oligosaccharide composition be obtained by chemical analysis, that the M_r be verified by ESI- or MALDI-MS, and that anomeric configuration be determined by hydrolysis with specific exoglycosidases, in addition to NMR [31,36]. The most undesired limitation of NMR is its lack of sensitivity. At least 15 nmol of pure oligosaccharide are essential to obtain an NMR spectrum, but even at 600MHz, low intensity signals related to heterogeneity may not be observable. ^1H NMR may also fail to detect the presence of nonmagnetically active nuclei, such as in sulfate groups [31]. In general, NMR has proven to be most useful for small oligosaccharides. In most cases, NMR has been used in combination with various chemical methodologies [47]. With increasing size, it may be possible to define structural elements that extend from the core and backbone, but it is not

always possible to elucidate unambiguously the branch locations by NMR alone [31]. Furthermore, NMR requires a major commitment of personnel and facility resources, and large amounts of pure materials, as well as a fairly high degree of sophistication in experimental setup and interpretation. The use of NMR for oligosaccharide sequencing is far from routine [32].

It is necessary to emphasize that NMR spectroscopy of carbohydrates is not limited to studying ^{1}H nuclei. ^{13}C NMR spectroscopy is also very useful to fingerprint oligosaccharides [31]. Significant improvements in the interpretation of ^{1}H and ^{13}C NMR spectra of complex carbohydrates are due to the application of two-dimentional (2D) NMR methods. These newly developed methods have been stimulated, in large part, by rapid advances in computer technology and in the construction of high-field, superconducting magnets over the past decade. A multitude of 2D-NMR pulse sequences have been developed and applied to carbohydrate-containing molecules. The application of 2D-NMR simplifies complex spectra by increasing the spectral dispersion to make complete assignment of signals possible [36].

1.4.2 Characterization of Oligosaccharide Structures by High-Performance Anion-Exchange Chromatography (HPAEC)

The invention of high-performance anion-exchange chromatography (HPAEC) in the late 1980s revolutionized carbohydrate analysis [48]. This technique takes advantage of the weakly acidic nature of carbohydrates (pK_a values ranging from 12 to 14) to give highly selective separations at high pH, using strong anion exchange stationary phases [18]. The major advantages of HPAEC are (1) fast speed of analysis (within 15 min); (2)

high resolution (isomers differing only in linkage or branching position can be resolved); (3) high sensitivity (with pulsed amperometric detector (PAD), carbohydrates can be measured down to 10 pmol without pre- or postcolumn derivatization) [37,39,48].

The mechanism of separation is as follows [39]: under strong alkaline conditions (pH > 12), the hydroxyl groups of carbohydrates are partially ionized to form oxyanions. Because of the different pK_a values of carbohydrates, there is a variation in the interaction of these oxyanions with the strong anion exchange resins, enabling these carbohydrates to be eluted at different retention times and detected by measuring the current generated by the oxidation of carbohydrates at a gold electrode. Practical and sensitive detection has been made possible with the adopted "pulsed amperometric detection"(PAD). It is a very important adjunct to HPAEC. Frequently "HPAEC-PAD" has been used to describe this recently developed chromatographic technique [48].

Columns commercially available for HPAEC include CarboPac PA1, PA-100 and MA-1 columns designed by Dionex. Both CarboPac PA1 and CarboPac PA-100 are designed for rapid analysis of mono- and oligosaccharides. CarboPac PA1 is especially suited to the analysis of monosaccharides and the separation of linear homopolymers, whereas the CarboPac PA-100 is optimized for resolution and separation of oligosaccharides. Reduced carbohydrates are weaker acids than their nonreduced counterparts and poorly retained on the two kinds of columns mentioned above. Thus CarboPac MA-1 has been introduced to address this issue [48].

With GC-MS or other HPLC techniques, monosaccharides must be derivatized first in order to obtain sugar composition information. HPAEC-PAD eliminates

derivatization and associated sample preparation steps, thus making the composition analysis of glycoproteins much simpler and more accessible [18]. This technique has also been widely used for fractionation of monosaccharides and neutral or acidic oligosaccharides from glycoproteins, mapping of oligosaccharides released from glycoproteins, and for preparative purposes [39]. HPAEC-PAD can be used with other instrumentation, such as other HPLC methods (including RP-HPLC and/or size exclusion chromatography), NMR, capillary zone electrophoresis (CZE), SDS-PAGE, as well as some forms of MS [48].

However, a negative side of working in alkaline media is the potential for epimerization and degradation, well known for reducing carbohydrates. Especially for HexNAc-terminated oligosaccharides, this problem can be serious if the elution volume is large [37].

1.4.3 Characterization of Oligosaccharide Structures by Exoglycosidases

Sequential digestion of individual oligosaccharides with exoglycosidases of known and well-defined specificities is one of the most commonly used methods. This method is prominent in sequencing and structural elucidation of oligosaccharides, particularly N-linked glycans [7, 49]. This method is extremely sensitive, especially when applied to radiolabeled substrates [49].

Exoglycosidases cause hydrolysis, thus cleavage of terminal monosaccharides from the nonreducing end of sugar chains and cleavage of the sugar chains of glycoproteins. These enzymes have two kinds of specificities, the glycon specificity and the aglycon specificity, toward their substrates [50]. The products of their digestions are

oligosaccharide fragments, which the enzymes have produced by removing specific terminal residues. In order to achieve complete release of monosaccharide residues, a relatively high concentration of enzymes is required, with an extended incubation time. A structure can be deduced based on the information obtained from a series of digestion experiments with different exoglycosidases [7]. The amount of any pure oligosaccharide that is needed for enzymatic analysis largely depends on the labeling and detection methods used, but is usually on the order of 10-100 pmol [7]. The principal disadvantages of sequential digestion are that its application is an *ad hoc* process and requires the repeated isolation and determination of product hydrodynamic volume (prior to each incubation) [49]. Another problem which should be stressed is the contamination of the enzymes used for study with other glycosidases present [50]. Jacob and co-workers [7] have described simple chromatographic protocols to remove the commonly encountered contaminants, and to provide operationally pure enzymes.

A method different fundamentally from sequential methods was proposed by Edge and co-workers [49] for the application of exoglycosidase digestion to oligosaccharide structural analysis. This technique, called the reagent-array analysis method (RAAM) or enzyme array sequencing method, involves division of the purified oligosaccharide sample into aliquots, incubation of each aliquot with a precisely defined mixture of exoglycosidases, recombination of the products of each incubation, and a single analysis on the product pool. A specific enzyme mixture is called an enzyme array. The enzyme-array technique has other practical advantages over the sequential digestion technique in being much faster, using a smaller amount of sample (there is no sample loss associated

with repeated analysis and repurification) and having a very defined protocol. This eliminates the requirement for specific prior knowledge in designing the experimental procedure, making it easier to use routinely and also amenable to automation [49].

Usually, oligosaccharides released from glycoproteins before being subjecting to enzyme sequencing are radiolabeled with NaB^3H_4, or derivatized with 2-aminopyridine [7] or 2-aminobenzamide [51] to enhance sensitivity when combined with other analytical techniques such as Bio-Gel P_4 size exclusion chromatography, normal phase HPLC on amine-bearing columns, and capillary zone electrophoresis (CZE) [7].

The products from sequential digestion [7, 52-54] or RAAM [7,49] of radiolabeled oligosaccharide alditols as mentioned above are usually fractioned on a column of Bio-Gel P_4 to obtain a specific fingerprint which identifies the original structure. However, Bio-Gel P_4 chromatography, which separates oligosaccharides on the basis of hydrodynamic volume, is a relatively slow technique (6 to 24 h per run). Furthermore, since it is low-resolution approach, it is possible to work only with pure oligosaccharides and interpretation becomes difficult even when dealing with a binary mixture [2].

Recently, using MALDI in combination with RAAM, it was possible to obtain molecular mass and structural details of oligosaccharides from a few glycoproteins. This was accomplished by dividing a glycopeptide fraction from RP-HPLC into aliquots, performing digestions in parallel, and subjecting the products of each digest mixture to MALDI-MS analysis [2]. This approach enabled sequencing of all oligosaccharide structures at a particular glycosylation site simultaneously, and rendered approximate

quantitation of the individual structures possible.

In combination with fluorescent labeling with 2-aminobenzamide and normal phase HPLC, a series of sequential exoglycosidase digestions was performed on the total pool of IgG sugars, demonstrating the potential of this technology to elucidate a mixture of sugars without prior isolation of individual glycans [55]. RAAM, in conjunction with fluorescent labeling and normal phase HPLC, was applied to sequencing individual sialylated and neutral sugars [55] and to simultaneous sequencing aliquots of the total glycan pool from human erythrocyte CD59 [51]. Recently, coupled with fluorescent labeling with 2-aminobenzamide and capillary zone electrophoresis (CZE), RAAM was used to characterize different glycoforms which were still attached to normal human serum transferrin (hTf) and serum hTf from two patients with CDGC type I. This study suggested that the method may be useful for diagnosing diseases where glycoproteins are carbohydrate deficient [56]. This technology represents a fast, automated, and thorough strategy for profiling and analysis of sugars [55].

The use of this method probably will diminish in the future with the advances of sophisticated analytical techniques such as multi-dimensional NMR, ESI- and MALDI-MS. However, in the laboratories where these instruments are not available or when the amounts of material are limited, enzyme sequencing will continue to play a very important role in the structural characterization of carbohydrates [7]. However, sugar structures determined by RAAM are not always definitive, and the data should be interpreted very carefully.

1.5 Objectives of This Work

The main objective of this project is to adapt and use a combination of chemical derivatization, chromatographic and mass spectrometric methods for the characterization of oligosaccharides and glycans detached from a glycoprotein, i.e. chicken egg albumin (ovalbumin).

This main objective comprises secondary objectives:

- Search for (a) good derivatization method(s) which will be suitable for chromatography, UV detection and mass spectrometry of oligosaccharides.

· Application of the(se) method(s) to chromatographic and mass spectrometric characterization of small sugars and medium sized-oligosaccharides.

- From preliminary experiments, establishing a method for analysis of glycans detached from ovalbumin.

1.5.1 Derivatization for RP-HPLC of Carbohydrates

High-performance liquid chromatography has been widely used for the analysis of sugars. Although this technique does not allow for structure elucidation, it permits identification of unknowns relative to standards whose retention behaviour *vs.* structure have been already established. In HPLC analysis, as much as in other analytical techniques, high sensitivity is essential when the oligosaccharides are available in very limited quantities. Carbohydrate analysis by HPLC or other separation techniques coupled to ultra-violet (UV) detectors is rendered difficult by the absence of effective chromophores or fluorophores [57,58]. Early studies relied on refractometry or absorption in the UV region at 190-210 nm [58]. However, refractive index (RI) detectors have several limitations, namely, sensitivity to changes in solvent composition,

temperature, and pressure. Following this, a major shortcoming of RI detectors is their incompatibility with gradient elution [58]. UV detectors can be somewhat useful in carbohydrate analysis by HPLC, especially for those compounds bearing carboxyl groups. However, problems related to solvent UV-cutoff are often encountered. Pulsed amperometric detection (PAD), combined with high-pH anion exchange chromatography, has become a popular method for the analysis of native carbohydrates because of its high sensitivity. However, the relatively high pH of eluents has been known to cause some epimerization and degradation of reducing carbohydrates [37] as mentioned above in Section 1.4.2. For these reasons, derivatization plays a key role in HPLC of carbohydrates.

Pre-column derivatization is defined as the conversion of one chemical entity to another more suitable for the purpose of HPLC separation and detection [59]. A chemical derivatization method converts carbohydrates into derivatives which can be detected with higher sensitivity compared with their native analogs. Formation of such derivatives can also enhance the selectivity of detection. As an example, only reducing sugars can be derivatized upon modification of carbonyl groups [58]. Furthermore, derivatization can improve HPLC resolution of sugars. Because underivatized sugars are hydrophillic and have closely related structures, there are limitations in the ways they can interact differentially with the stationary and mobile phases. Tagging of sugars with aromatic groups renders oligosaccharides hydrophobic, thus permitting the use of RP-HPLC, which enables separation of oligosaccharide mixtures [58]. In addition, aromatic groups are very effective chromophores.

Usually, derivatization should be designed to satisfy the following requirements [58]:

1. The yield should be quantitative with a minimum extent of side reactions. In addition, the reaction should be well defined.

2. The reaction should be nondestructive to the other oligosaccharide constituents such as sialic acid, fucose, phosphorylated, and sulfated sugar residues.

3. A simple clean-up procedure prior to HPLC analysis should be required.

4. The introduced group should be chemically stable enough to allow subsequent reactions including exoglycosidase digestion, methylation analysis, periodate oxidation, partial acetolysis, and hydrazinolysis.

5. Derivatization should be specific to sugars but insensitive to other biomolecules such as lipids and proteins.

6. Convenient removal or replacement with another tag should be feasible when necessary.

It should be emphasized that for aqueous oligosaccharide samples, the derivatization reactions ideally should be rapid, mild, involve few transfer steps and proceed in aqueous media [60].

The reducing end aldehyde groups and hydroxyl groups of carbohydrates are the sites where derivatization reactions occur. Aldehyde groups are highly specific to reducing carbohydrates when other natural compounds also exist in a mixture, therefore most pre-column derivatization reactions are based on carbonyl derivatization [58]. Carbohydrate derivatization methods that have been used for HPLC are summarized below.

1.5.1.1 Carbonyl Derivatization

1) Carbonyl Derivatization into Imines (Schiff Bases) or Glycosylamines

Carbonyl groups of carbohydrates can be coupled with amines to form imines or glycosylamines, and the general reaction equations are shown in Fig. 1.6 [58]. Since the reactions are reversible, the products are somewhat unstable. On the other hand, by taking this advantage, regeneration of parent oligosaccharides can be made possible after HPLC separation as long as the derivatives are stable enough during chromatography. The derivatization reactions belonging to this category which have been reported are shown in Fig. 1.7 [58]. For example, in Fig. 1.7b the reducing groups were coupled with 5-dimethylamine-1-naphthalenesulfonylhydrazide (DANSYL-hydrazide) to form DANSYL-hydrazones in the presence of trichloroacetic acid. The DANSYL-oligosaccharides can be detected by fluorescence (Ex 350 nm/Em 500 nm) with a detection limit of nanogram quantities (10 pmol) [58,61]. Derivatives obtained with 2-aminopyridine by reductive amination are fluorescent, but intermediate imines are also fluorescent. The products, N-(2-pyridinyl)-glycosylamines, were stable enough to be separated by HPLC, and the sample could be regenerated afterwards by weak acid hydrolysis with 2% aqueous acetic acid [58, 62].

2) Reductive Amination [58]

The conversion of sugars into imines or glycosylamines as described above encounters problems relative to syn/anti-isomers, anomeric mixtures, and instability of the products, but these can be avoided by reduction of an imine into an amine, a single and more stable product. Some reductive amination reactions are shown in Fig. 1.8 [58].

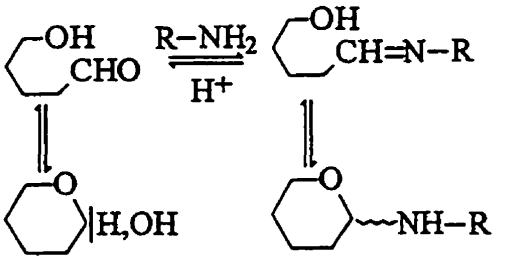

Fig. 1.6 Reaction of sugars with amines [58].

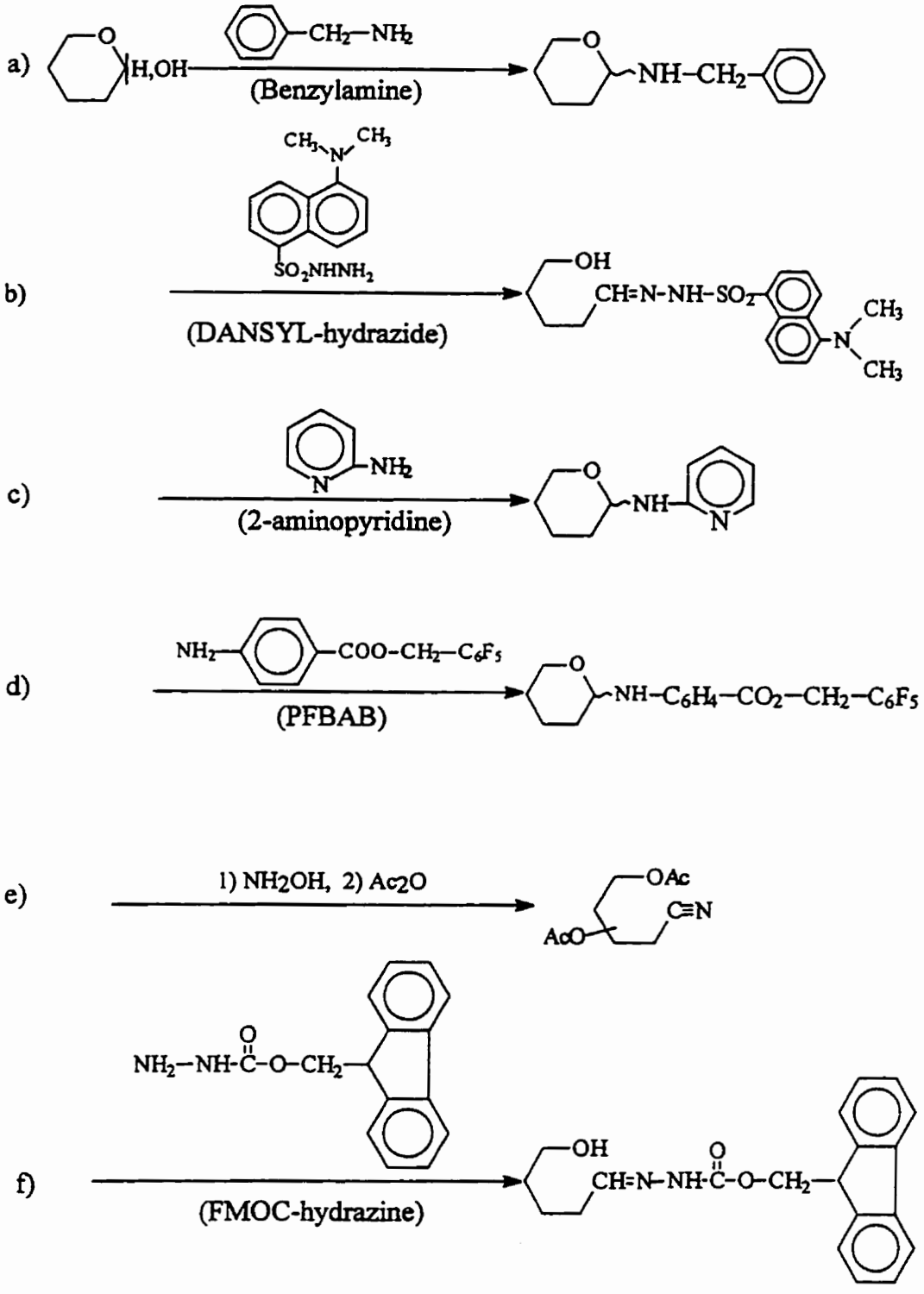

Fig. 1.7 Derivatization of sugars with amines [58].

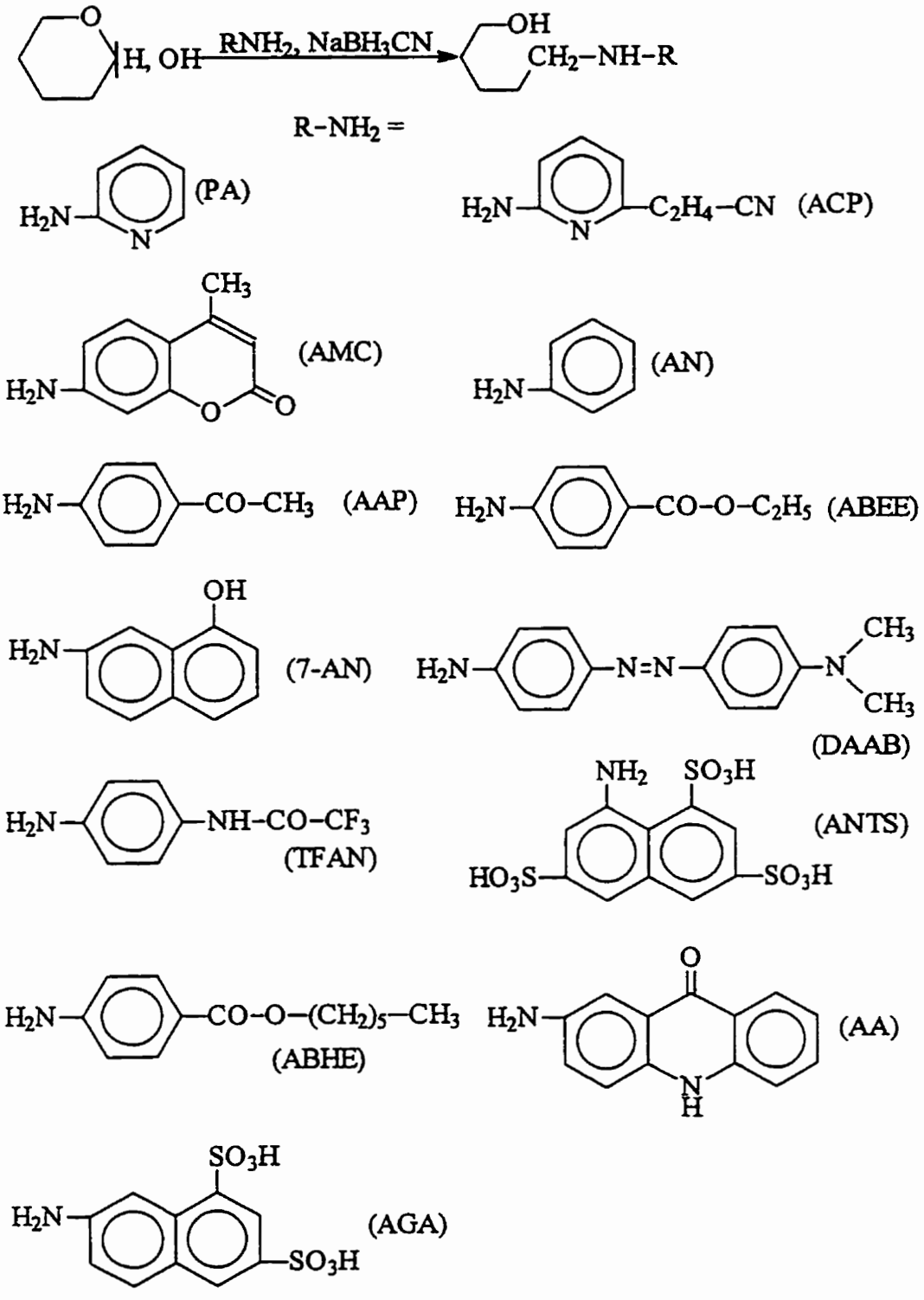

Fig. 1.8 Reductive amination of sugars [58].

These reactions can be conducted in one-step with aldehyde and amine in the presence of sodium cyanoborohydride ($NaBH_3CN$) or borane-dimethylamine complex ($BH_3 \cdot NH(CH_3)_2$), which is volatile and easy to remove [58]. Reactions can also be carried out in two-steps: formation of imines and then reduction [58]. Reductive amination introduces groups such as chromophores, fluorophores, charges, and hydrophobicity into oligosaccharides, providing high selectivity and sensitivity.

The analysis of oligosaccharides labeled with 2-aminopyridine is well-known for its excellent chromatographic separation and high fluorescence sensitivity [63, 64]. Moreover, pyridylamino (PA) derivatives are stable. Pyridylamination has been used in sugar component analysis, and characterization of sugar chains from glycoproteins and glycosphingolipids. The derivatization procedure has been improved and now a number of oligosaccharides of various structures, including sialylated oligosaccharides, can be pyridylaminated with recovery of more than 90% with minor side reactions [64]. PA-oligosaccharides have been separated by RP-HPLC and detected by fluorescence (Ex. 320 nm/Em. 400 nm). In most cases, fluorescent derivatives are detectable at the subpicomolar level by fluorescence detection, or by UV absorption. PA-sugar chains from glycoproteins were sufficiently stable for subsequent structure analysis such as Smith periodate oxidation, methylation analysis, and partial acetolysis [58]. From data of earlier HPLC analyses, a method for two-dimensional mapping was developed (65,66). The PA-oligosaccharides were separated and identified by size-fractionation and reversed-phase HPLC. The relation between the structure and elution position of HPLC is regular, so this method can provide information about an unknown oligosaccharide structure [67-69].

However, this reductive amination method involves a two-step labeling process and has a few additional shortcomings, such as time-consuming cleanup procedure and loss of sialic acid moieties [70]. An improved method claimed to circumvent this problem does not seem to produce quantitative yield [64, 70].

1.5.1.2 Hydroxyl Derivatization [58]

The hydroxyl groups of carbohydrates are also points where derivatization takes place, and chromophores are introduced by formation of ester or ether linkages (shown in Fig. 1.9). The derivatives of reducing carbohydrates comprise α and β anomers. Benzoyl reagents such as benzoyl chloride (BC) and benzoic anhydride (BA) have been used and the resultant perbenzoylated derivatives of carbohydrates were separated by HPLC, and detected at 230 nm or 254 nm.

1.5.1.3 PMP-Labeling

A number of other reactions have been reported as precolumn derivatization and some of them are summarized in Fig. 1.10 [58]. Recently, 1-phenyl-3-methyl-5-pyrazolone (PMP) [66-70] and its methoxy analog, 1-(p-methoxy)phenyl-3-methyl-5-pyrazolone (PMPMP) [70,76] have been used. The condensation products, bis-PMP-sugars (shown in Fig.1.11), or PMPMP-sugars, absorb strongly at 245 nm or 249 nm [70,71]. These derivatization methods have been used for sugar component analysis and for characterization of oligosaccharides from glycoproteins [71,76]. Both PMP and PMPMP derivatizing agents can be used to label sialic acid-containing oligosaccharides without causing desialylation [70], which constitutes a great advantage over the PA-derivatization method.

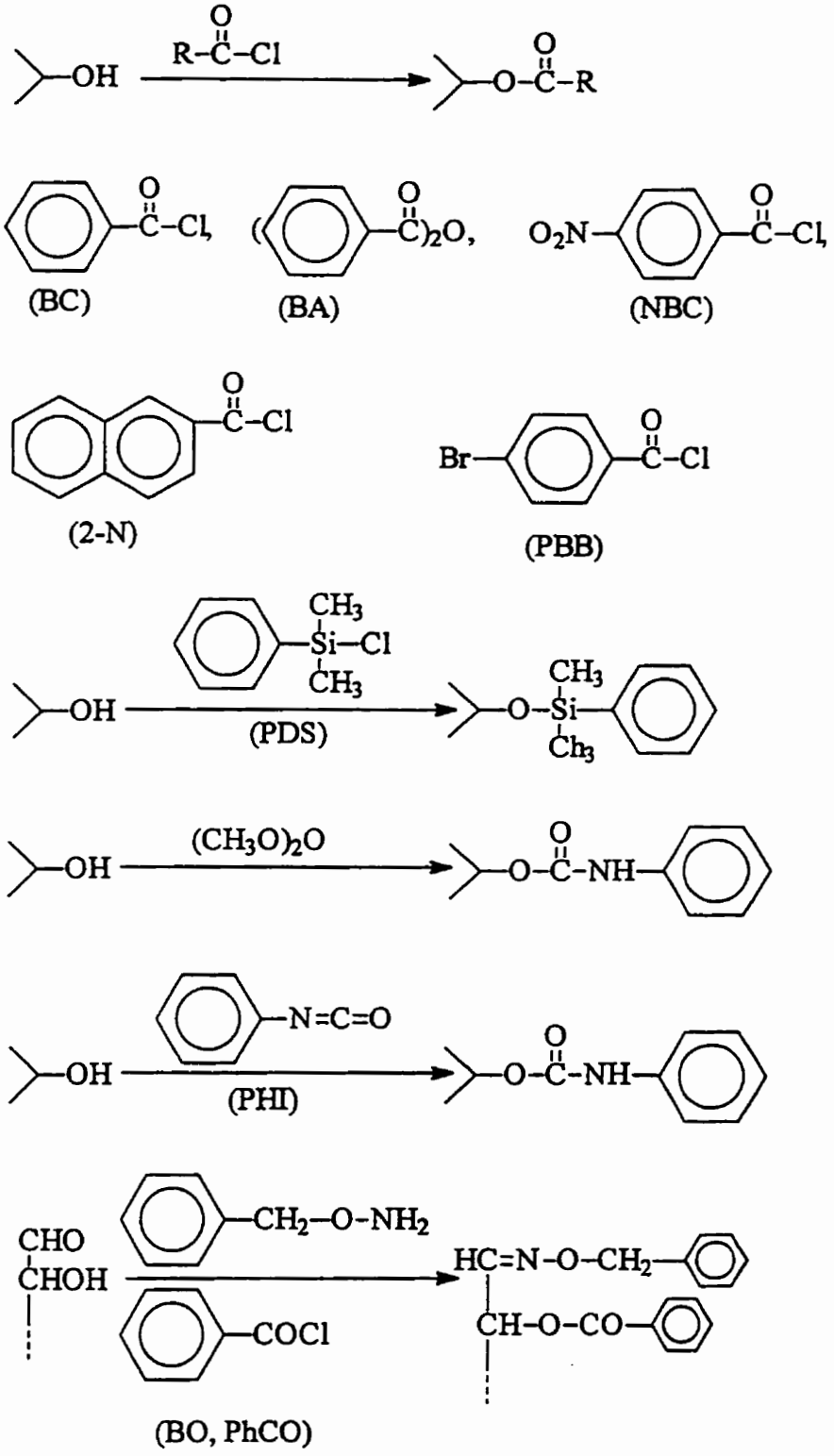

Fig. 1.9 Dervatization of sugars by the modification of hydroxyl groups [58].

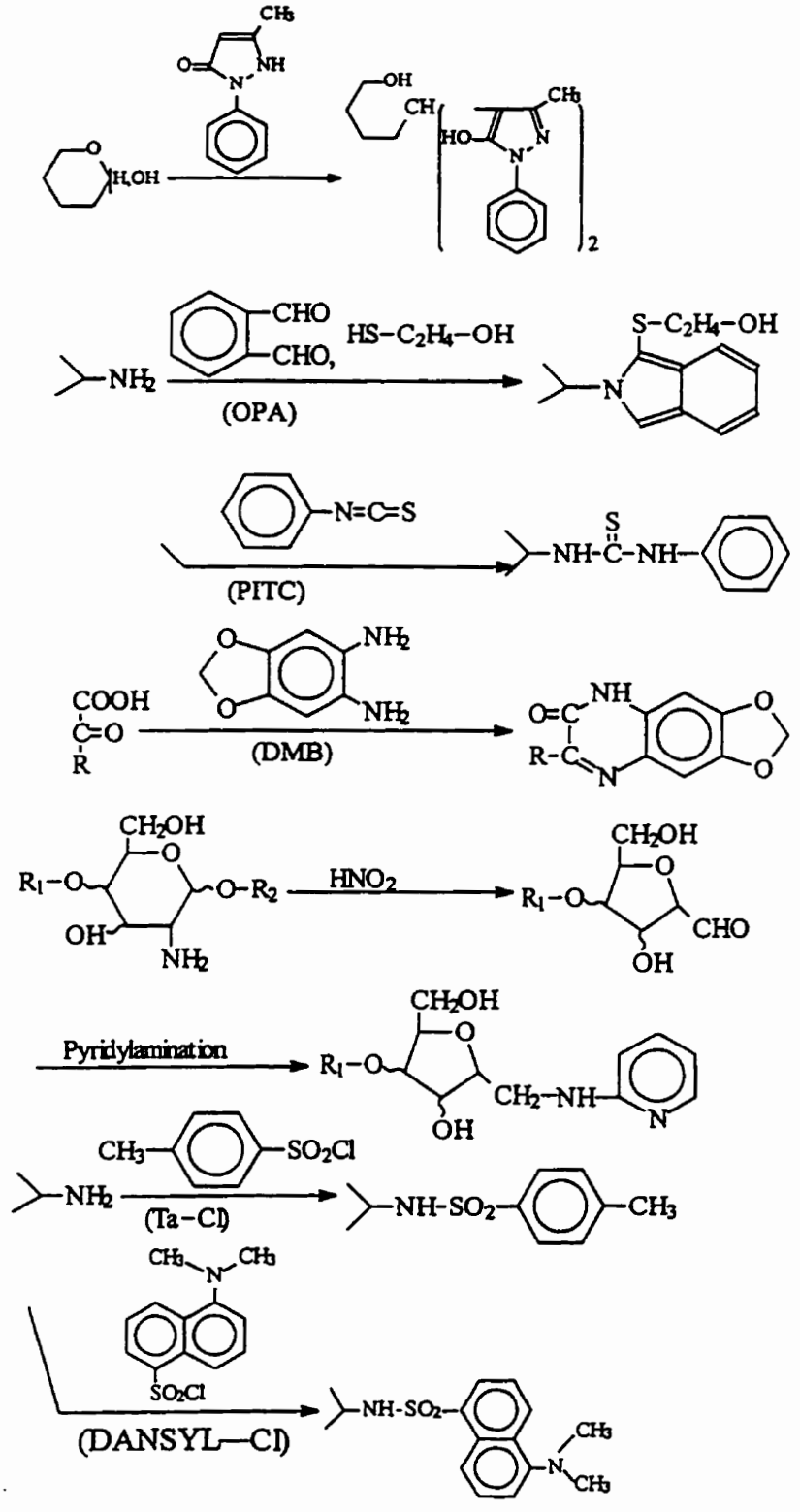

Fig. 1.10 Miscellaneous reactions for derivatization of sugars [58].

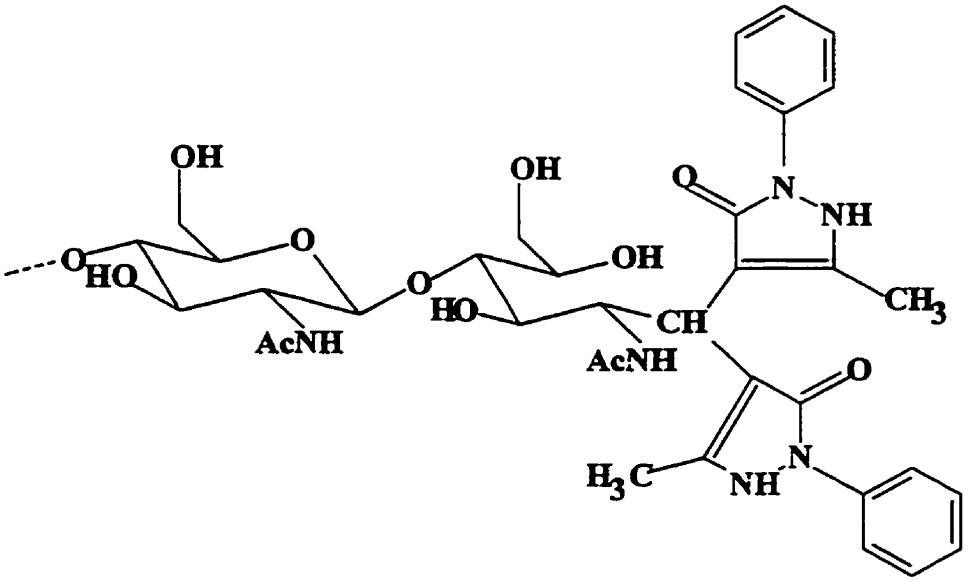

Fig. 1.11 General structure of the PMP derivatives.

1.5.2 Derivatization for Mass Spectrometry

Mass spectrometry (MS) is one of the key techniques used in carbohydrate analysis. As far as specific MS techniques are concerned, gas chromatography-mass spectrometry (GC-MS) and fast atom bombardment mass spectrometry (FAB-MS) have been for a long time the most important in terms of structural information they can provide, and the range of biological problems to which they can be applied. Together, these two techniques are able to define the complete primary structure of an oligosaccharide or glycoconjugate [77]. More recently, electrospray (ES) [42,43] and matrix-assisted laser desorption (MALD) [44-46] ionization methods have become more powerful than FAB-MS.

1.5.2.1 Currently Used Mass Spectrometry Ionization Techniques

1) Fast Atom Bombardment (FAB-MS)

There are several so-called "soft ionization" techniques: such as FAB, secondary ion (SI), field desorption (FD), desorption chemical ionization (DCI), californium-252 plasma desorption ^{252}Cf-PD), laser desorption (LD), thermospray (TSI), and electrospray ionization (ESI). FAB-MS was developed in early 1980s [78] and still holds a very important position in the analysis of biological molecules with masses up to about 5000 Da [79]. This technique can be used to analyze polar, non-volatile and thermally labile compounds [see Ref. 80 and references herein]. However, FAB exhibits poor ionization efficiency compared with ESI and MALDI and produces considerable ion source fragmentation [11].

In FAB, an accelerated beam of Xe^{o} atoms having kinetic energies of 8-10 keV is

fired from a gun towards the target, which has been previously loaded with a matrix containing the sample to be analyzed. When the fast atom beam collides with the matrix and the analyte, kinetic energy is transferred to the surface molecules, thus making many molecules of the analyte sputter out of the liquid into the high vacuum region of the ion source (Fig. 1.12) [81]. A significant number of these molecules are ionized during the sputtering process although some ions are preformed in solution as discussed below. When ion guns are used, the technique is sometimes called liquid secondary ion mass spectrometry (LSIMS) instead of FAB-MS, but the result is the same [77,82]. The sputtering ionization results from matrix-analyte interactions in a solution. Attachment of a proton or cation onto the analyte molecule (positive ion mode) or loss of a proton (negative ion mode) contributes to formation of pseudo-molecular ions, which produce intense signals in the mass spectra. During ionization, some internal energy imparted to the molecules leads to fragmentation [83].

The viscous and nonvolatile liquid matrix plays an essential role in FAB-MS. It promotes the diffusion of sample molecules to the surface of the matrix and formation of a stable, and reproducible ion current [78]. The matrix also serves to minimize sample damage from the high-energy particle beam by absorbing most of the incident energy and is believed to facilitate the ionization process [84]. Glycerol, or a mixture of glycerol and thioglycerol are the commonly used matrices for the analysis of carbohydrates and glycoconjugates [81].

Derivatives play an essential role in almost all FAB-MS studies of carbohydrates. They facilitate spectral interpretation, improve sensitivity, permit the analysis of salty

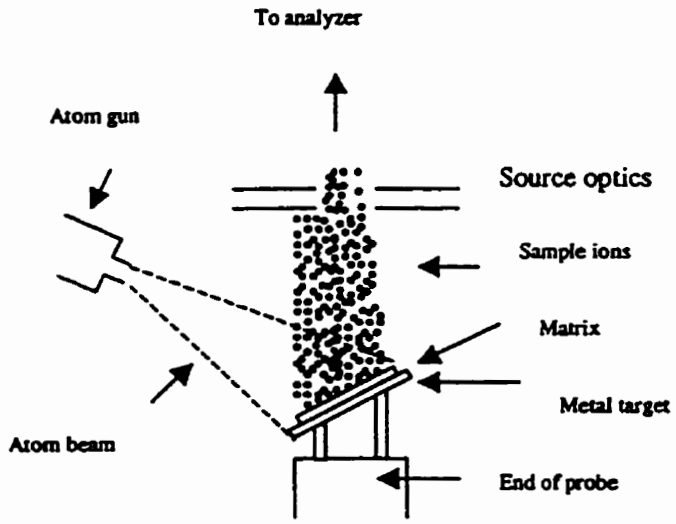

Fig. 1.12 Schematic representation of a FAB source [81].

samples, allow unambiguous sequencing, enable spectra to be obtained from very large molecules, and help in the location of O-acylated residues in oligosaccharides [81].

Sensitivities obtained in FAB analysis depend on both operators and samples. Experienced mass spectrometrists, when working with well purified samples, use between 0.1 and 5 µg of derivatized samples and between 1 and 10 µg of native samples (1-50 nmol) [85]. In addition, the higher the Mr, the greater the amount of sample required [81]. Furthermore, the higher the molecular mass of the sample, the greater the difference in minimum sample-loadings required to produce spectra from native samples and their derivatives. If M_r is > 4000, the difference becomes almost infinite, because underivatized polysaccharides and glycoconjugates of such a size hardly give a spectrum, whereas permethyl derivatives as large as 20,000 have been demonstrated to be amenable to FAB-MS [81].

2) Electrospray Ionization (ESI)

For the purposes of carbohydrate analysis, ESI is the most efficient and generally applicable technique currently available to transform these molecules from solution into gas-phase ions [33]. ESI is a relatively new ionization technique because it has only been used since 1988 [82]. The mechanism of this process is still under debate, but a consensus on some features has been reached. Electrospray makes use of high electric fields to aerosolize solutions, creating a fine mist with each droplet carrying an excess of surface charge. A heated, countercurrent bath gas at atmospheric pressure evaporates neutral solvent from the droplet surface, reducing its size, and therefore increasing its surface charge density. Eventually electrostatic repulsion disrupts the liquid surface, leading to the

ejection of smaller charged droplets or to the development of gas-phase ions [11,33].

In practice, solutions are directly infused through a stainless steel needle maintained at a potential of a few kilovolts at flow rate from 1 to 20 μL/min. This potential induces the surface charging of the emerging liquid and aerosol formation. The droplets migrate toward the nozzle through the countercurrent bath gas, which promotes solvent evaporation. The ions then pass through a skimmer and enter the analyzer as shown in Fig. 1.13 [33,86].

ESI provides two features important for biopolymer characterization: efficient ionization and multiple charging by proton or cation attachment in positive ion mode and proton subtraction in the negative ion mode [82]. The multiple charging effect makes the analysis of large molecules with M_r up to 100,000 to 150,000 Da possible using conventional mass analyzers with only a modest *m/z* range since the highly charged molecular ions, which typically exhibit little or no fragmentation, appear within the conventional *m/z* range of 1000-3000 u [82, 87]. Another distinct advantage of ESI-MS is that it provides effective coupling with powerful separation techniques such as liquid chromatography and capillary electrophoresis because it is a flow technique operating at atmospheric pressure. This allows direct separation and mass analysis of low picomole to femtomole quantities of biomolecules using microbore or capillary reversed phase HPLC coupled to ESI-MS (LC/ESI-MS) [see Ref. 82,88 and references herein].

A quadrupole mass analyzer is most commonly used in conjunction with ESI because of relatively low cost and ease of interfacing with this ionization technique. Other types of mass spectrometers are also amenable to coupling with ESI including magnetic

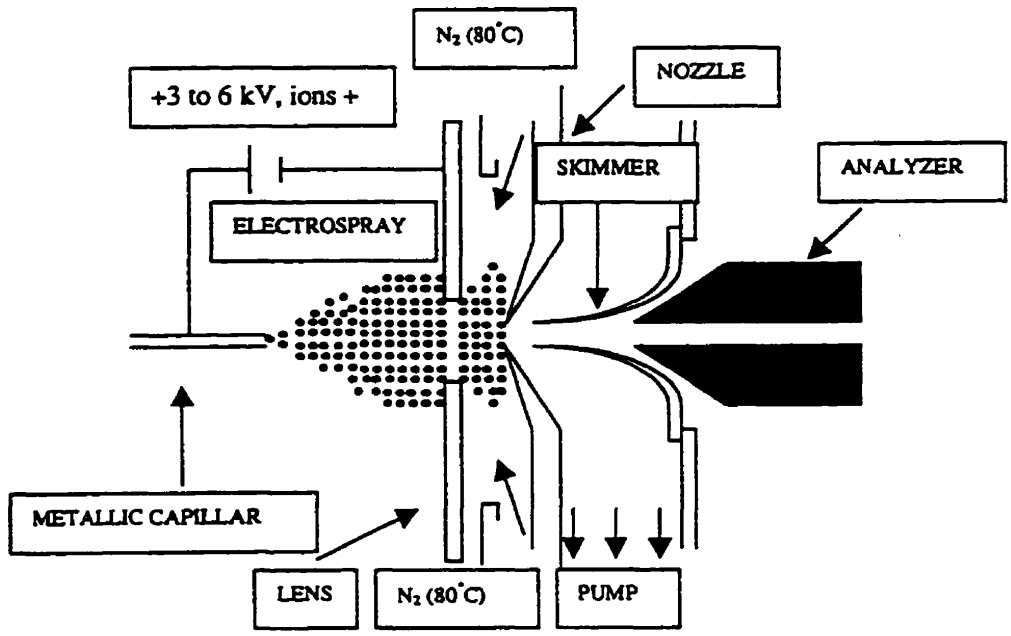

Fig. 1.13 Diagram of an electrospray source [86].

sectors, time of flight analyzers, quadrupole ion traps, and Fourier transform ion cyclotron resonance mass spectrometers [see Ref. 87 and references herein].

When using ESI for structural analysis and differentiation between isomers that often occur in natural compounds, collision-induced dissociation-tandem mass spectrometry (CID-MS/MS) is very useful, because unless in-source CID or CID-MS/MS is applied, ESI does not always generate fragment ions [89]. CID is a process whereby a small portion of the kinetic energy of the mass-selected parent ion is transformed into vibronic energy upon collision with helium or argon atoms for the purpose of promoting unimolecular decompositions [90]. In CID studies, a triple quadrupole (QQQ) mass spectrometer is commonly used. The first quadrupole (Q1) is operated in the mass analyzer mode and transmits only the desired parent or precursor ions. When the parent ions enter the central quadrupole (Q2), which is filled with molecules of an inert gas, i.e. argon, fragmentation occurs after collision and daughter or product ions are formed. Q2 is also termed the "collision-cell" and does not function as a mass analyzer like Q1. Emerging daughter (fragment) ions are accelerated toward the third quadrupole (Q3) which serves as a second mass analyzer followed by the detector [87,88]. A major advantage of CID-MS/MS is that mixtures can be analyzed in a manner that yields structural information related solely to the ions selected by Q1. This technique is particularly useful for the analysis of glycoconjugates, which commonly occur as heterogeneous samples. This method can give structural information on each individual component of a mixture [91].

Fragmentation patterns observed by ESI-CID-MS/MS are much the same as in

FAB-CID-MS/MS in either positive or negative ion mode, if the same analyzer instrument is used for both ionization techniques [89].

Although ESI-MS is definitely more sensitive than FAB, it is less sensitive than matrix-assisted laser desorption/ionization (MALDI). In most cases, a picomole of sample material can be identified using conventional mass spectrometry of ESI. Unlike with FAB and LSIMS, derivatization is not always required by ESI, while derivatization of oligosaccharides permits the analysis at lower sample levels [see Ref. 82 and references herein].

3) Matrix-Assisted Laser Desorption/Ionization (MALDI) Time-of-Flight (TOF) Mass Spectrometry

Besides ESI-MS, matrix-assisted laser desorption/ionization (MALDI) time-of-flight (TOF) MS, introduced in 1988 by Karas and Hillenkamp [92], appears to hold the greatest promise for the mass spectrometric analysis of biomolecules in the molecular mass range between a few thousand and a few hundred thousand Daltons [44].

MALDI involves pulsing a laser at the target loaded with the analyte co-crystallized with a large excess of matrix which absorbs at the laser wavelength used. Two commonly used wavelengths are 10.6 μm (CO_2 laser, IR) and 337 nm (N_2 laser, UV). A low concentration of analyte molecules, which usually only exhibit moderate adsorption of IR or UV, is embedded in a matrix consisting of highly absorbing species. In this way, the energy is transferred efficiently and controllably to the analyte molecules while they are spared from excessive energy obtained from irradiation which would cause their decomposition. In addition to absorbing the energy from laser light, the matrix also serves

to isolate the biomolecules from each other [44]. Under conditions of low intensity irradiation, little fragmentation is produced, which facilitates molecular mass determination. At higher irradiance, structurally significant fragmentation can be induced [93]..

The use of suitable matrix materials to promote efficient ionization is central to the success of MALDI-MS. 2,5-dihydroxybenzoic acid (DHB), 3-amino-4-hydroxybenzoic acid, or 3-hydroxypicolinic acid are commonly used for oligosaccharides and glycopeptides [see Ref. 93,94 and the references herein]. The other key to success of MALDI is how the analyte and matrix are co-crystallized. Since MALDI is quite a new technique, new matrices and crystallization methods are still under investigation, improving the analysis of oligosaccharides, glycopeptides, and glycoproteins as well as glycoconjugates [see Ref. 82 and the references herein].

In MALDI, the ions are generated by a pulsed laser beam, which makes the technique ideally compatible with time-of-flight mass analyzers [44], but not easily compatible with scanning mass spectrometers such as linear quadrupoles and sector instruments [87]. In a TOF mass analyzer, the mass-to-charge ratio of an ion can be measured by using its velocity. A packet of ions is accelerated to a fixed kinetic energy by an electric potential. The velocity of the ions will then be proportional to $(m_i/z_i)^{-1/2}$ where m_i/z_i is the mass-to-charge ratio of a particular ion species. The ions are then permitted to pass through a field-free region where they separate into a series of spatially discrete individual ion packets. Each ion packet travels with a velocity characteristic of its m/z value and arrives at the detector (at the end of the field-free region) at a different time,

proportional to $(m_i/z_i)^{1/2}$. The detector generates a signal as each ion packet strikes it [44].

The simplicity of the instrumentation and high sensitivity are the two major advantages of MALDI. The detection limit for glycopeptides has been achieved at the level of 500 femtomoles, and that for underivatized oligosaccharides at low picomole levels [see Ref. 82 and references therein]. However, because of problems with shot to shot reproducibility during MALDI and the large kinetic energy spread of the ions generated, the resolution (typically 100-400) and accuracy of mass determination (0.1%, internal calibration; 0.01% external calibration [93]) is significantly lower than that achieved with ESI and FAB-MS techniques [82]. Although MALDI allows the analysis of both native and derivatized oligosaccharides with great sensitivity, usually information is limited to molecular mass determination. However, it has been demonstrated that it is possible to determine the primary structure of oligosaccharides by combination of exoglycosidase analyses and MALDI-MS [95]. Also, it has been reported that post-source decay (PSD) MALDI-MS makes it possible to obtain sequence and branching information from native and derivatized sugars [24,45,96,97]. MALDI is also quite tolerant of the presence of buffers and salts [93].

In summary, ESI-MS is probably next to the most sensitive ionization technique, which is MALDI-MS, among several others. In terms of structural information, FAB may still be better for smaller molecules, but FAB is not able to ionize molecules larger than several thousand Daltons. Besides, FAB requires much larger sample amounts [89].

1.5.2.2 Nomenclature Used in Fragmentation of Carbohydrates [91]

A systematic nomenclature for labeling the types of fragmentations observed for

native and derivatized carbohydrates in FAB-MS spectra has been established by Domon and Costello [91], which is also applied to other ionization modes, such as ESI-MS and ESI-MS/MS [89,91]. This system has been devised by analogy to that used for peptides, although more complicated.

Two major types of cleavages are usually observed. One of these, also the simplest one, is cleavage of glycosidic bonds, yielding sequence information. The other is more complex, involving sugar ring cleavages, which are more commonly observed in CID-MS/MS spectra. Although more difficult to assign, the latter contain important structural information.

As shown in Fig. 1.14 (top), when the charge is retained on the non-reducing end, fragment ions are termed A_i, B_i, and C_i, where i represents the number of the glycosidic bond cleaved, counted from the non-reducing end. On the other hand, fragments with charge retained on the reducing end are termed X_j, Y_j, and Z_j, where j indicates the number of the glycosidic bond cleaved, counted from the aglycone unit, or from the reducing end sugar unit. The glycosidic bond linking to the aglycone is numbered 0.

The fragments formed with retention of glycosidic oxygen from the reducing end are Y-ions, and that from the non-reducing end are C-ions, whereas fragment ions formed without retention of glycosidic oxygen from the reducing end are Z-ions and that from non-reducing end are B-ions.

A_i and X_j labels are used to represent cross ring cleavages. Since several such fragmentations are possible, two superscripts k and l (i.e. $^{k,l}A_i$, $^{k,l}X_j$) are used to indicate the sugar ring bonds that have been broken and the ring bonds are numbered in the

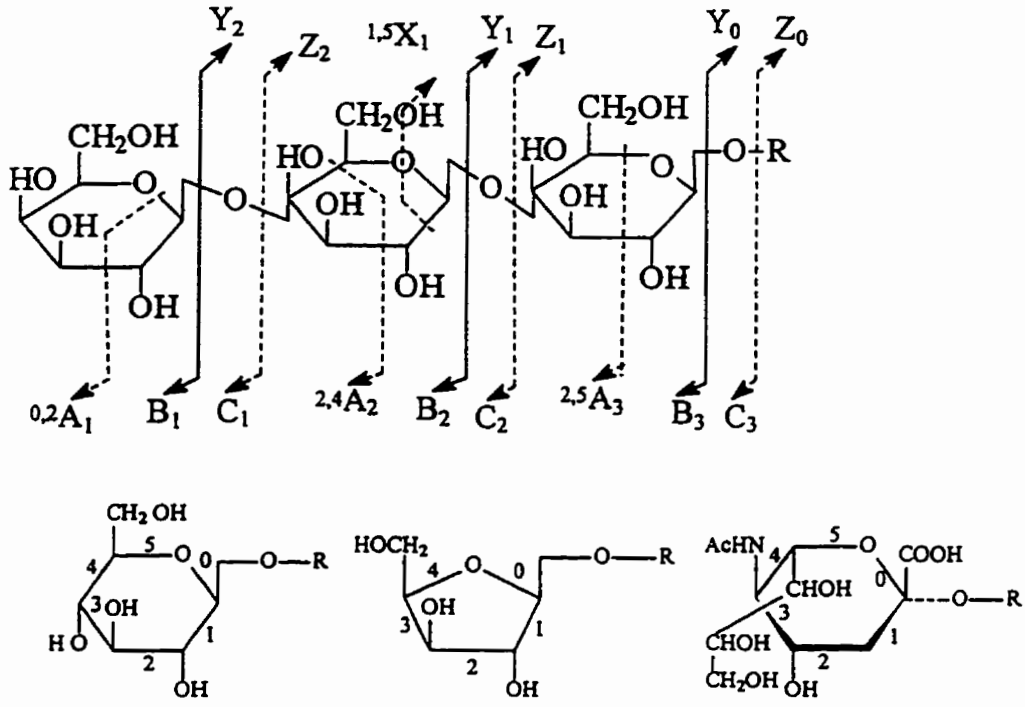

Fig. 1.14 Fragmentation encountered with carbohydrates [91].

bottom of Fig. 1.14. A_i-ions are seldom observed in the positive ion mode, while X_j-ions occur usually in positive ion spectra but rarely in negative ion spectra.

In the case of branched oligosaccharides (Fig. 1.15), the carbohydrate portion can be divided into the "core" and branches, called "antennae". The labels for the core portion are the same as used for linear oligosaccharides as described above and Greek letters α, β, γ are used to designate each branch with α being the largest and β, γ representing smaller branches in the order of decreasing molecular (fragment) mass. Fragmentation taking place on the α, or β-antenna are expressed as $A_{i\alpha}$, $B_{i\alpha}$, $C_{i\alpha}$, $X_{j\alpha}$,$Y_{j\alpha}$, $Z_{j\alpha}$, respectively. Fragment ions from the core portion are designated without Greek letters and the use of α, β, γ begins from the connection point of the core to the antennae. α', α'', and β', β'' are used when carbohydrates contain sub-branches with $\alpha' \geq \alpha''$, and $\beta' \geq \beta''$.

1.5.2.3 Chemical Derivatization for Mass Spectrometry

Unlike the usual approach to proteins, the analysis of carbohydrates involves chemical derivatization. The major goal for the early use of derivatization was to confer the necessary volatility to samples since they had to be in gas phase before ionization. Chemical derivatization was also used to enhance the information available from mass spectral data. The development of soft ionization techniques such as FAB, ESI and MALDI has overcome most volatility limitations. Chemical derivatization, however, still plays an important role since fragment ions from native carbohydrates do not always allow unambiguous determination of the sequence, and the poor ionization efficiency of underivatized samples limits their usefulness [42,98]. The reasons to use chemical derivatization for MS can be summarized as follows: (1) enhancement of volatility; (2)

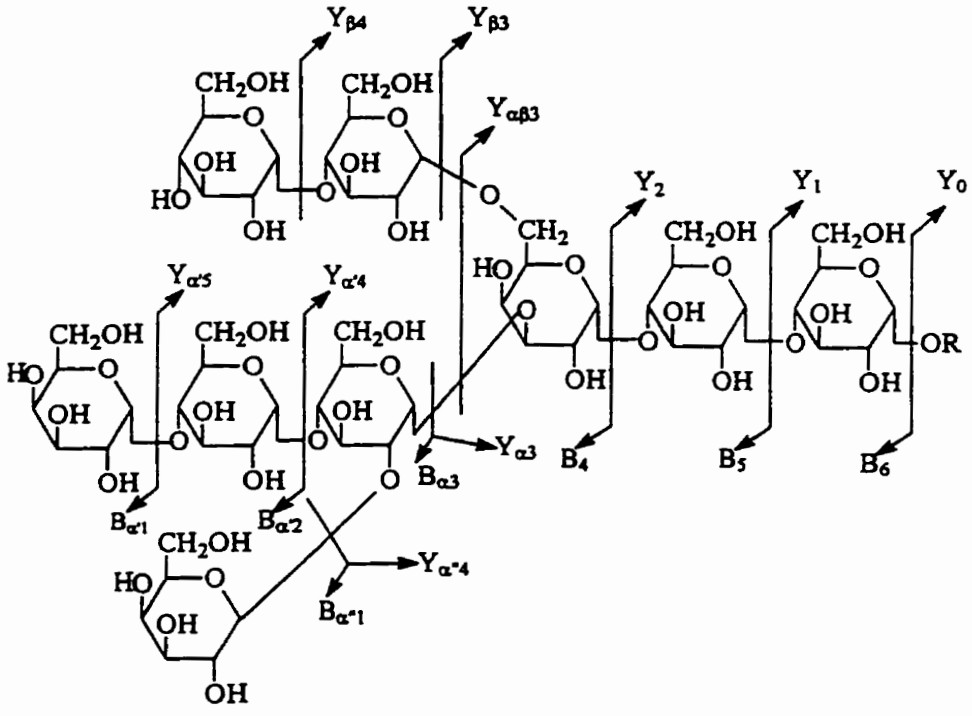

Fig. 1.15 The nomenclature of fragmentation for branched oligosaccarides [83].

enhancement of detectability ; (3) enhancement of separability; (4) modification of the fragmentation scheme: (a) enhancement of molecular ion production, and (b) enhancement of production of structurally informative ions; (5) possibility to localize functional groups [99].

A useful chemical derivatization reaction should be specific in that it should modify only the intended part of the molecule and should yield preferably a single stable product. It should be reasonably fast and simple to carry out and amenable to very small sample sizes. Ideally the derivatization reagents should also be reasonably stable and safe to handle. However, very few derivatization procedures meet all of these criteria [99].

Derivatization is still part of most FAB-MS strategies in carbohydrate analysis because (1) derivatives are easier to obtain free from salt impurities, which may prejudice the MS experiment, (2) sensitivity is significantly improved when hydrophobic moieties are introduced and (3) derivatized samples tend to fragment in very predictable ways, and lead to abundant fragment ions that can be assigned unambiguously [77]. For example, FAB-MS of native oligosaccharides is a well proven procedure for defining, via molecular ions, the compositions of components, including the number and types of modifying groups. Unfortunately, FAB-MS is not a reliable procedure for sequencing native oligosaccharides. The fragmentation of underivatized oligosaccharides is unpredictable, and fragment ions formed are of low abundance, or some molecules do not fragment at all. When fragmentation does occur, it may not be possible to assign unambiguous structures to the fragment ions [100,101].

The choice of the proper derivative for an analyte depends mainly on the nature of

the sample introduction/ionization technique to be used [102]. For instance, when the sample is introduced via a gas chromatograph or by a heated solid probe (electron impact), derivatives need to be volatile and/or thermally stable. Desorption ionization techniques such as FAB and secondary ion mass spectrometry (SIMS) work particularly well for the analysis of preformed ions. Therefore, derivatization is often directed toward formation of an ionic species and, in the case of FAB, directed toward increasing surface activity of the analyte by introduction of a hydrophobic group [102]. The best detectability with ESI-MS has been achieved with analytes that are either ionic in solution or that can be readily ionized in solution via Brønsted or Lewis acid/base chemistry. Neutral, non-polar molecules that are not easily ionized in solution by acid/base chemistry are not typically amenable to ESI-MS [103]. Derivatization, along with manipulation of solution chemistry to ionize or neutralize particular analytes, has the potential both to improve detectability of particular analytes in ESI-MS and to add selectivity to an analysis [103]. Reinhold et al. also indicated that, due to the weak acidity or basicity of most N- and O-linked glycans, free oligosaccharides do not efficiently charge by protonation or deprotonation. It is necessary, therefore, to use derivatization techniques, except for acidic carbohydrates [6,11,]. Derivatization helps carbohydrate structural analysis by ESI for two fundamental reasons. First, when using more volatile organic solvents, ESI shows significant increases in sensitivity, and second, methylation brings unique insight into structure when glycans are analyzed by collision-induced-dissociation (CID) [11].

1.5.2.3.1 Modifying Most or All Functional Groups

Methylation analysis, reductive cleavage, permethylation and peracetylation, as

well as periodate oxidation belong to this category. These derivatization methods involve modification of most or all functional groups and are discussed in detail below.

1) Derivatization for GC-MS Analysis

a) Methylation Analysis

Methylation analysis is one of the most powerful tools used for elucidating the oligosaccharide structure of glycoproteins [104]. Methylation was the first derivatization method developed for linkage analysis by mass spectrometry [82].

This procedure, as introduced by Lindberg and co-workers in the late 1960s [105], is based on treatment of the carbohydrate with Corey-Chaykovsky base (methylsulphinyl carbanion) and methyl iodide according to Hakomori [106]. Methylation of all free hydroxyl groups in an oligosaccharide is then followed by hydrolysis of glycosidic bonds, reduction with $NaBH_4$ (or $NaBD_4$) and acetylation of the exposed or newly formed hydroxyl groups [107]. The acetylated hydroxyls are those either involved in the linkages of the monosaccharide units in the oligosaccharide or linked to the oxygen within the sugar ring before hydrolysis. The partially methylated alditol acetates (PMAAs) are then separated by GC and analyzed by electron ionization mass spectrometry (EI-MS) and/or chemical ionization mass spectrometry (CI-MS), and identification of residues and linkages is obtained by comparison of retention times with known standards combined with molecular mass and characteristic fragmentation information [82].

A number of factors have been reported to influence the recovery of PMAAs [108], including undermethylation, side reactions occurring during methylation, liberation of substituents because of the strong alkaline conditions used, degradation or de-O-

methylation of the methylated sugar derivatives during acid hydrolysis, selective losses of volatile components during evaporation of solvents, loss of material by adsorption to glassware, and decomposition of the PMAAs (especially of hexosamine derivatives) during GC analysis. Furthermore, impurities derived from solvents or reagents may impair the identification and quantitation of PMAAs during GC-MS analysis [108].

b) Reductive Cleavage

Reductive cleavage is a relatively newer method, permitting the simultaneous determination of positions of linkage and ring form(s) in oligosaccharides [109]. This technique is based on methylation analysis, but differs from it in terms of the types of fragment ions eventually analyzed. The reductive cleavage procedure, as illustrated in Scheme 1.1 [47], produces partially methylated anhydroalditols which are readily characterized by performing GC/MS of their acetates.

Fragmentation patterns for these derivatives have not been established, but EI spectra do yield diagnostic fragment ions which can be used to identify the residues and linkages [82]. Total reductive cleavage is performed with triethylsilane (Et_3SiH) as the reducing agent and with either trimethylsilyl trifluoromethane sulfonate (TMSOTf) or a mixture of trimethylsilylmethane sulfonate (TMSOMs) and boron trifluoride etherate ($BF_3{\cdot}Et_2O$) as the catalyst [110]. Reductive cleavage with Et_3SiH and TMSOTf and subsequent in situ acetylation [111] are accomplished as previously described [47]. Reductive cleavage with Et_3SiH in the presence of TMSOMs and $BF_3{\cdot}Et_2O$ and separate acetylation are performed as described by Jun and Gray [112]. It was reported that reductive cleavage with TMSOTf gives isomerization products and probably incomplete

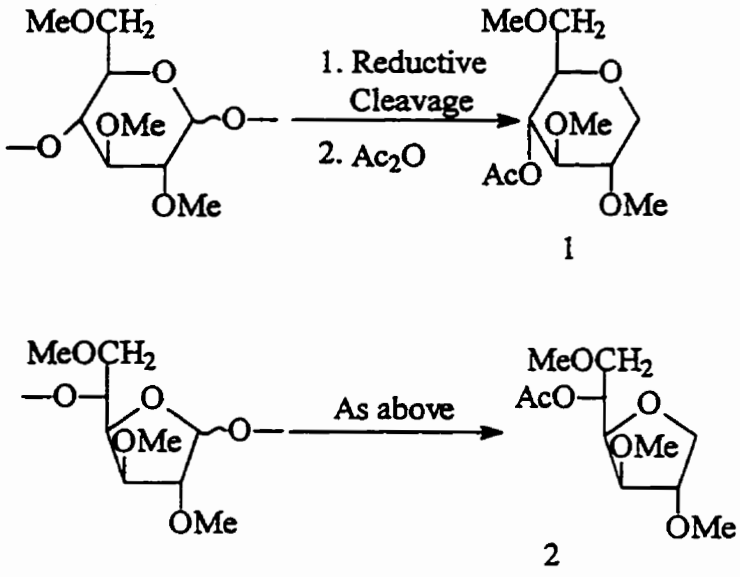

Scheme 1.1 Reductive cleavage [47].

cleavage, therefore reductive cleavage with TMSOMs and $BF_3 \cdot Et_2O$ as the catalysts is the preferred method [113].

2) Peracetylation and Permethylation

Peracetylation and permethylation are two of the most common derivatization procedures and take advantage of the reactivity of the numerous hydroxyl groups to yield highly modified apolar derivatives [114]. Peracetylation is one commonly used derivatization method permitting purification of the sample and resulting in concomitant increased surface activity and therefore enhanced sensitivity. The peracetyl-labile substituents, e.g. acyl are preserved. The reagent is prepared by mixing equimolar amounts of trifluoroacetic anhydride and acetic acid. If naturally O-acetylated residues are anticipated in oligosaccharides, the acetic acid can be replaced with ^2H-labeled acetic acid or propionic acid in order to define the presence and position of natural acetate groups [100]. The resulting mixed anhydride $CF_3CO\text{-}CO\text{-}COCH_3$ can, in principle, transfer either trifluoroacetyl or acetyl to a nucleophilic acceptor. In practice, all hydroxyl groups are almost exclusively acetylated [96]. Peracetylation by basic catalysis must be used to preserve acid labile groups such as sulfate. The reaction is carried out by dissolving the sample in pyridine or 1-methylimidazole, and then adding acetic anhydride (or ^2H-labeled acetic anhydride) to the mixture [77].

For positive mode FAB and LSIMS, permethylated and peracetylated samples are often dissolved in methanol or chloroform, and monothioglycerol or m-nitrobenzylalcohol (m-NBA) is used as the matrix [82]. The LSIMS spectra of permethylated and peracetylated samples often yield sodiated molecular species, $[M+Na]^+$, rather than

protonated molecules $[M+H]^+$. LSIMS analysis of permethylated oligosaccharides is particularly useful for the characterization of complex sugar structures, giving abundant B-type fragment ions at every HexNAc residue [82,116]. A systematic nomenclature for fragment ions was previously proposed by Domon and Costello [91].

For the analysis of high mannose oligosaccharides, peracetylation is preferred over permethylation to obtain sequence information. This is because permethylated derivatives are selectively cleaved only at the GlcNAc residues, while fragmentations occur all along the backbone for peracetylated compounds. However, additional fragmentation occurring in LSIMS spectra of permethylated compounds is not observed in spectra of peracetylated compounds [82].

Although peracetylation involves simple chemistry, it has the drawback of a significant molecular mass increase of the derivatized carbohydrates. Therefore, for oligosaccharides larger than six sugar units, permethylation is the method of choice and yields derivatives whose spectra allow the assignment of sugar sequence and branching, and also identification of 3-substituted HexNAc sugar units. In contrast to peracetyl derivatives, for which determination of the major structural parameters is straightforward owing to a complete set of B ions, permethyl derivatives require more extensive spectral interpretation since the same information is distributed over two incomplete B and Y ion series [117].

Peracetylation is an excellent method for recovering oligosaccharides from impure samples, e.g. urine extracts, salty samples. Once the peracetylated sample has been separated from water-soluble contaminations, it can be analyzed directly or converted to

the permethylated form [81].

ES-CID-MS/MS is a powerful new tool for structural elucidation of carbohydrates at the low-picomole level. Permethylation has been used in ES-MS to improve sensitivity. When combined with collision-induced dissociation (CID), permethylation yields sequence, linkage and branching information, even identification of specific isomers [11].

In summary, peracetyl and permethyl derivatives are ionized to give abundant molecular ions as well as reproducible and predictable fragmentation patterns which allow unambiguous sequencing and facile assignment of linkage positions. High sensitivity is achieved with both derivatization methods, in some cases two orders of magnitude better than with native samples [116].

3) Periodate Oxidation

Linkage information can also be obtained from MS or MS/MS of oligosaccharides by applying a well-known reaction in carbohydrate chemistry, the periodate oxidation [118]. The following sequence of reactions is carried out: (1) periodate oxidation, (2) borodeuteride reduction, and (3) permethylation (Fig. 1.16 [119]). Periodate cleaves between carbons carrying vicinal hydroxyl groups either cis or trans related to produce aldehydes, which are subsequently reduced with $NaBD_4$. The products formed depend on the position of substitution and linkages between monosaccharide residues. After this reaction, followed by permethylation, and FAB-MS, LSIMS or ESI-MS/MS, linkage positions can be deduced from primary and secondary sequence ions [82,101,120]. With respect to the extent of information acquired, ORM (oxidation, reduction, and methylation) parallels PMAA analysis, but the amounts of sample required are

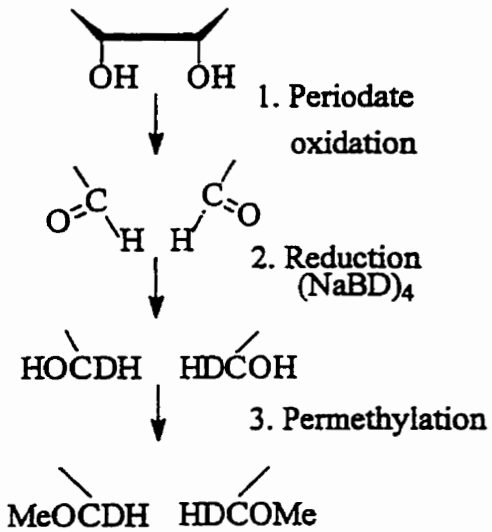

Fig. 1.16 Reaction steps for preparation of periodate oxidized samples for analysis by FAB mass spectrometry [119].

considerably less with ORM [33].

Angel and Nilsson [101] summarized, in a list, the names of the products obtained by ORM FAB analysis of non-reducing terminal and internal hexopyranosyl residues. The most abundant sequence ions are formed from the non-reducing terminal. Therefore, the linkage to a reducing hexose is determined best by subtracting the sequence ion with the highest *m/z* value from the molecular mass (M_r) which can always be determined [101, 120].

Peracetylated [119,101,121-123] rather than permethylated derivatives (after periodate oxidation, and borodeuteride reduction) have been used in order to direct fission to the carbon-oxygen bonds of the oligosaccharide backbone. The FAB mass spectra of the peracetylated derivatives give unique information not yielded in the spectra of the permethylated derivatives, in that fragmentation occurs on either side of the glycosidic oxygen atom, not only at the reducing terminal but also at internal linkages. Thus, since fragmentation is observed from both the reducing and non-reducing ends of the molecule, additional sequence information is obtained [121]. Borodeuteride reduction is utilized instead of borohydride reduction to differentiate a native primary alcohol function from one introduced by periodate oxidation followed by sodium borodeuteride reduction, and to distinguish 6-linked from 2-linked oxidized reducing terminal residues [121].

O- and N-linked oligosaccharides from bovine fetuin have been analysed by FAB after ORM [119]. A high-mannose glycan mixture isolated from a plant glycoprotein and a complex glycan mixture obtained from erythropoietin glycopeptide have been successfully analyzed by ES-MS after ORM [33].

One sugar structure in the O-linked oligosaccharide mixture from glycophorins of BALB/c mouse erythrocytes released as a mixture of alditol derivatives on reductive β-elimination was elucidated using the above method [122]. The structures of a number of oligosaccharides obtained from high-mannose glycoproteins have been analyzed [123].

1.5.2.3.2 Tagging of the Reducing Ends

The other category of derivatization is to tag the reducing end of sugars. Tags were originally introduced for improving sensitivity, for example, the pentafluoro-benzyloxime derivative was successfully used to characterize elicitor-active oligogalacturonides at low-microgram quantities isolated from plant cell walls [124]. Subsequently, a variety of tags has been used not only permitting sensitive detection during HPLC purification as ultraviolet or fluorescent chromophores but also promoting surface activity within the matrix during LSIMS as a hydrophobic tail [77,125].

1) Reductive Amination

The most commonly used derivatives are those formed by reductive amination with a hydrophobic chromophore to the free reducing terminus of an oligosaccharide. This is performed by formation of a Schiff base and subsequent reduction to the secondary amine as shown in Scheme 1.2 for derivatization with alkyl esters of p-aminobenzoic acid [125]. The chromophoric portion of the derivative is UV absorbing, thus permitting detection of the derivative using conventional HPLC-UV detectors. The MS analysis of aminated derivatives is superior to that of the underivatized oligosaccharides, since the introduction of a hydrophobic group greatly increases the surface activity of oligosaccharides in hydrophilic liquid matrices such as glycerol, thioglycerol, or

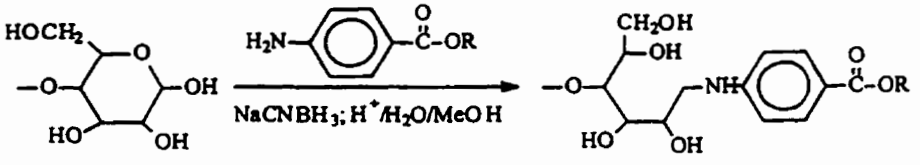

R = Me, Et, Bu, Hex, Oct, Dec, and Tdec

Scheme 1.2 Oligosaccharide derivatization with n-alkyl p-aminobenzoates [125].

triethanolamine, thus increasing the sensitivity in FAB- and LSIMS [85]. It also enhances pre-formation of ions in solution for ESI-MS analysis [46]. Furthermore, even though permethyl and peracetyl derivatization eases the difficulties of isolation and salt removal, these derivatives are of little use in subsequent separation of components of mixtures. In the case of larger oligosaccharides, reductive amination is particularly advantageous, since a large increase in the mass upon permethyl or peracetyl derivatization would preclude the detection of the molecular ions [85].

a) Derivatization with Alkyl Esters of P-aminobenzoic Acid

One of the most popular and successful labels for carbohydrates is the aminobenzoic acid alkyl ester group [85,125-127]. In addition to the obvious advantage of introducing an excellent UV chromophore at the free reducing terminus of oligosaccharides, this method also imparts hydrophobicity to the oligosaccharides. The increased hydrophobicity of these oligosaccharide derivatives allows the oligosaccharides to be separated by RP-HPLC as well as greatly increases the sensitivity of their detection [114]. Furthermore these derivatives serve to introduce a preferential site of protonation and more importantly, of deprotonation, which is of considerable analytical advantage in negative ion LSIMS analysis [125]. In the mass spectral characterization of these derivatives, the method chosen depends on the kind of information one wishes to obtain, and the amount of sample one wishes to use. In the positive ion mode, abundant molecular ions are produced with little fragmentation, so that a molecular mass profile of HPLC fraction components can be readily obtained by LSIMS by using approximately 5 pmol of sample. However, more importantly, in the negative ion mode the

fragmentation pattern obtained comprises several fragment ions, many of which contain the modified reducing terminus, thus providing sequence and branching information. In order to obtain this fragmentation pattern, around 50 pmol of derivatized sample are usually required [128].

Using this approach, the sequence of the neutral and acidic oligosaccharides expressed on 1 nmol of nicotinic acetylcholine receptor and the acidic N-linked oligosaccharides released from 2 nmol of human α_1-acid glycoprotein have been successfully determined [125]. It is proposed that this approach can be used to provide an "oligosaccharide map" of the gross oligosaccharide structures present on any serum or membrane-bound glycoprotein possessing N-linked oligosaccharides available at only picomole to low nanomole levels [125]. Furthermore, these derivatives with free nonreducing terminal moieties are directly amenable to sequence exoglycosidase digestion, thus the truncated structures could be analyzed by mass spectrometry, providing additional structural data such as linkage position and anomeric configuration [85,125]. The advantages of this protocol become obvious when very small quantities of oligosaccharides are available and losses of material due to sample transfer become noticeable.

Limitations of this method are that the derivatizing reagent must be prepared beforehand, the actual derivatization yield is not quantitative for longer chain alkyl esters, and significant sample workup must be performed prior to analysis [32].

b) Derivatization with 2-aminopyridine (PA)

2-aminopyridine (PA) has been extensively used to derivatize sugars for HPLC

separation and analysis, providing very high sensitivity as mentioned in Section 1.5.1.1. PA-oligosaccharides have also been analyzed by FAB-MS, and ESI-MS, as well as FAB-MS/MS and ESI-MS/MS [42,67,129,130]. It was reported that PA-derivatized maltopentaose showed a 3 to 10-fold sensitivity improvement in positive ion FAB-MS compared with the native sugar. While positive ion mode gave a 100-fold sensitivity increase in ESI-MS, negative ion mode yielded a 30-fold sensitivity improvement [42]. Both conventional FAB- and ESI- mass spectra showed only molecular ions, and no sequence-related fragment ions were apparent, and thus an oligosaccharide map could be provided [67,129]. For example, Carr and Reinhold prepared a mixture of linear polyglucoses (from corn syrup) which had been derivatized with 2-aminopyridine. The normal FAB mass spectrum contained the protonated molecular ions of oligomers with four, five and six, etc. monosaccharide units [129].

FAB-CID-MS/MS studies showed that selection and collision of the protonated hexamer yielded a diagnostic daughter ion spectrum [129]. Two series of reducing end fragment ions were obtained. One represented successive losses of terminal deoxyhexose units (Y-ions), while the other series was formed by scission of the pyran rings and protonation of the remaining reducing end oligomers ($^{1,5}X_i$-ions, 28 u higher than the Y-ions). This cleavage leaves a formyl group on the glycosidic oxygen. Nearly no fragments related to the nonreducing end of the molecule were apparent, probably because charge was strongly localized on the secondary amine of the aminopyridinyl group [129].

ESI-MS of PA-oligosaccharides was first reported by Suzuki-Sawada and co-workers [67]. They described both on-line LC/ESI-MS and fragmentation by CID. A PA-

glycan mixture cleaved from human immunoglobulin (IgG) was characterized and one component selected in this mixture was studied in detail by ESI-MS/MS [67]. The product ions were mainly due to fragmentation at glycosidic bonds. Types of hexoses and positional linkages could not be distinguished with these data alone, but the information provided by MS/MS was useful in corroborating the estimated structure [67]. Later on, Gu et al. [130] reported that molecular weights of PA-oligosaccharides were detectable by ESI-MS with a 1-pmol sample, and that the fragmentation pattern of PA-oligosaccharides obtained by applying in-source fragmentation, showed simple glycosidic cleavages with the positive charge retained on the PA site [89,130].

The other derivatizing agents used in reductive amination for MS include trimethyl (p-aminophenyl)-ammonium chloride (TMAPA) [42,116,117], aniline [127,45,131], benzylamine [45], 2-aminobenzamide [45], aminohexane[45], phosphatidylethanolamine dipalmitoate (PPEADP) [132], 2-amino-6-methylpyridine [133], 2-aminoethanethiol (AET) and 2-aminobenzenthiol (ABT) [see Ref. 57 and references therein], N, N-(2, 4-dinitrophenyl)octylamine (DNPO) [32,83], and N, N-dansyloctylamine [83]. The ionization efficiencies of TMAPA-, p-aminobenzoic acid ethyl ester (ABEE), and PA-derivatives have been investigated quantitatively by ESI- and FAB-MS, and compared with those of permethyl and peracetyl derivatives [42]. Among these derivatives TMAPA-derivatized maltopentaose showed extremely high sensitivity in positive ion ESI-MS, a 5000-fold improvement compared with native maltopentaose [42]. Derivatization with N,N-(2,4-dinitrophenyl)octylamine has demonstrated an at least 100-fold improvement in sensitivity relative to aminobenzoic acid alkyl ester derivatives

[32]. Recently, Takao and co-workers reported from experiments using a high-mannose-type N-linked oligosaccharide ($Man_8GlcNAc_2$) as a model showed that derivatization with 4-amino-benzoic acid 2-(diethylamino)ethyl ester (ABDEAE) gave 400-, 80-, and 20-fold increases in molecular ion abundance over the underivatized oligosaccharide and oligosaccharide derivatized with PA and ABEE, respectively. ABDEAE derivatization demonstrated a 1000-fold sensitivity increase over the underivatized oligosaccharide in MALDI-MS and 5000-fold in positive ESI mode [see Ref. 46 and references therein].

2) Derivatization with PMP or PMPMP

A MS sensitivity study on PMP and PMPMP oligosaccharides, relative to other types of derivatives has been conducted [57]. The derivatizing agents used included PA, ABEE, 2-aminoethanethiol (AET) and 2-aminobenzenthiol (ABT), in addition to PMP, and PMPMP. In FAB-MS, the PMP derivative in glycerol in aqueous methanolic solvent (positive ion mode) provided the second highest signal among the other derivatives of maltopentaose, with the ABEE derivative giving the highest response. In the negative ion mode, the PMP-derivative of maltopentaose not only gave intense molecular ion signals, but also detectable fragment ions from the nonreducing terminus corresponding to $^{2,4}A$-type fragments.

In positive ion ESI-MS, the spectrum of the PMP-derivative of maltopentaose gave the highest sensitivity among the other derivatives examined under optimized conditions. The relative intensities of PA derivatives were 5.8% of that of the PMP derivatives at a concentration of 1nmol/μL. The minimum amount of maltopentaose required was 0.9 ng. Honda and co-workers also checked the setting of voltages in the

ESI interface and noticed that the variation of the cone voltage had a serious effect on the response obtained for the PMP-derivatives of isomaltooligosaccharides. At 40 V, only the PMP derivative of glucose was observed, but the derivatives of larger oligosaccharides began to be observed with increasing cone voltage. At 400 V, the derivatives of isomaltooligosaccharides with up to 16 rings could be detected [57]. Higher voltages gave $[M+Na]^+$ signals in addition to $[M+H]^+$, even though the reaction mixture of derivatization had been subjected to desalting by electric dialysis. A high voltage setting is, however, considered to be favorable for the analysis of oligosaccharides derived from glycoproteins [57].

The usefulness of derivatization with PMP in LC/ESI-MS using thyroglobulin-derived oligosaccharides was demonstrated. The five peaks were eluted and separated. The mass spectra of these fractions showed the presence of high mannose-type oligosaccharides with six to nine mannose residues [57].

Recently, a combination of PMP-derivatization, liquid chromatography and MALDI-TOF-MS was applied for determination of carbohydrate heterogeneity in the humanizsed antibody CAMPATH 1H [134]. Preliminary work involved examination of native and PMP-derivatized standard carbohydrates by MALDI-MS. The native carbohydrates were observed as predominantly sodium and potassium adducted species. as expected. The derivatized materials in all but one case showed $[M+H]^+$ ions of reasonable intensity in addition to sodium and potassium adducted species. The LC profile and MALDI-MS data contributed to detection of twelve components. The mass spectra indicated that the derivatives were stable and did not significantly fragment under

MALDI-MS conditions [134].

1.5.3 Methodology Used in This Work

After considering the advantages and disadvantages of all derivatization methods described above, PA- and PMP-derivatives were chosen as the most practical ones to prepare. The preliminary work thus involved preparing PA- and PMP- derivatives of a series of mono-, di-, and tri-saccharides and comparing UV and MS sensitivities, as well as HPLC separation efficiencies. The results demonstrated that PMP-derivatives of small sugars were more worth preparing than PA-derivatives in terms of simplicity of the derivatization reaction and cleanup procedure, good quality and ease of separation by reversed-phase HPLC, as well as enhanced ionization efficiency in FAB-, ESI, and MALDI-MS.

Based on the above findings, linear tetraglucose and a few standard oligosaccharides obtained commercially were used as models of large oligosaccharides in order to address the sensitivity and study fragmentation patterns for PMP-derivatives using ESI-MS, ESI-MS/MS, and MALDI-MS.

Finally, intact chicken egg albumin (ovalbumin) and neutral glycans detached from ovalbumin were characterized by these recently developed MS techniques. The results from mass spectrometric experiments, especially involving ESI-MS and ESI-MS/MS, were emphasized.

Ovalbumin was used as a model glycoprotein in this project. Ovalbumin is the most abundant protein in egg white comprising 385 amino acid residues [135]. The total molecular mass of ovalbumin is 44287 [135,136] and the glycan portion in ovalbumin

accounts for 3.5% in weight [66]. The glycan moiety of ovalbumin has been scrutinized over the last 20 years [21,43,66,136-148]. There is only one N-glycosylation site, and no O-linked glycosylation site [21,43,137]. The carbohydrate moiety is attached to Asn-292 of the polypeptide chain whose molecular mass was reported to be 42699 [135], and the sequence of a glycopeptide shows it contains the Asn-X-Thr "recognition site" [135]. So far, about 35 different neutral sugars have been attributed to this glycoprotein [see Ref. 142 and the references therein]. Until 1992, only high-mannose- and hybrid-type oligosaccharides had been reported [21,43, 137,139]. However, recently complex-type oligosaccharides have also been found but rarely encountered. All these N-linked glycans contain neutral sugars without sialic acid [141-143, 146]. The main reason for choosing ovalbumin as a model is that it has only one glycosylation site. This eliminates the necessity to determine glycosylation sites and allows the study to remain focused on investigation of site-specific heterogeneity with regarding the limited time.

Studying the structures of these N-glycans requires their release from the protein backbone. As described above in Section 1.3, a number of different methods, chemical and enzymatic, exist for this purpose. Enzymatic cleavage of N-linked oligosaccharides with PNGase F offers several significant advantages over hydrazinolysis. Overall, the enzymatic procedure is simpler but much more costly than most other methods. A mild incubation with the enzyme releases all common classes of N-linked sugars. Usually, side reactions are unlikely to occur unless contaminating enzymes are involved. On the other hand, hydrazinolysis requires relatively harsh reaction conditions. Therefore when the asparaginyl-N-acetylglucosamide bond is cleaved, other undesirable reactions also occur,

such as release and partial degradation of O-linked sugars, de-N-acetylation, hydrazone formation, and in some cases, peeling and other side reactions. In addition, it is necessary to re-N-acetylate each oligosaccharide and to regenerate its free-reducing terminal before further characterization. Furthermore, labile derivatives such as O-acetyl groups of sialic acids are destroyed during hydrazinolysis [14]. However, hydrazinolysis has been chosen to release glycans in this project with the consideration that it is much less expensive than cleavage by enzymatic methods. It has been shown that hydrazinolysis, under certain reaction conditions, can cause complete cleavage of N- and O-glycosyl peptide linkages [21,22]. This occurrence is not relevant in the case of ovalbumin since only N-linked carbohydrates are present.

To maintain the fidelity of structures inherent with the starting material is a constant challenge during isolation of glycans [33]. In this project, special attention has been focused on the characterization of detached glycans and oligosaccharides, which have been chemically derivatized to impart molecular specificity during ESI- and MALDI-MS analyses. PMP-derivatization was selected among a number of reported methods to label the glycans for the reasons discussed above.

2. EXPERIMENTAL

2.1 Materials

The 1-phenyl-3-methyl-5-pyrazolone (PMP) reagent was purchased from ICN Biomedicals Inc. (Aurora, OH, USA) and used as obtained. Anhydrous hydrazine, 2-aminopyridine and borane-dimethylamine complex were obtained from Aldrich Chemicals (Wilwaukee, WI, USA). The small saccharides D(+)-galactose, D(+)-glucose, D(+)-mannose, D(+)-glucosamine, D(+)-galactosamine, D(+)-N-acetylglucosamine, L(-)-fucose, β-lactose, 2'-fucosyllactose, sialyllactose (a mixture of 3'- and 6'-N-acetylneuramin-lactose), tetraglucose (4-O-(4-O-[6-O-α-D-Glucopyranosyl-α-D-Glucopyranosyl]-α-D-Glucopyranosyl)-D-Glucopyranose), blue dextran, horse hemoglobin, ovalbumin (albumin, chicken egg, Grade V), myoglobin (from horse skeletal muscle, MW 16952,), bovine insulin (Mr 5733), Substance P (Mr 1347.6), 3, 5-dimethoxy-4-hydroxycinnamic acid (sinapinic acid, SA), α-cyano-4-hydroxy-cinnamic acid (CHCA) and Dowex -50W (H^+) were purchased from Sigma Chemical CO (St. Louis, MO, USA). Larger oligosaccharide standards M3N2 (conserved trimannosyl core), NGA3 (asialo-, agalacto-, triantennary) and NGA4 (asialo-, agalacto-, tetraantennary) were obtained from Oxford GlycoSystems (Rosedale, NY, USA) and used as received. Bio-Gel P-4 (minus 400 mesh) was from Bio-Rad (Richmond, CA, USA). All solvents were glass distilled, HPLC-grade and obtained from Mallinckrodt (Paris, KY, USA). Chromatographic paper (Whatman 3MM) was obtained from VWR Canlab (Mississauga, ON, Canada). Thin layer chromatographic (TLC) Baker-flex silica gel IB-F plates were obtained from J. T. Baker Inc. (Phillipsburg, NJ, USA). Sep-Pak C_{18} cartridges were

obtained from Waters (Waters Corp., Milford, MA, USA). Deionized, filtered water was obtained from a Barnstead Nano-Pure™ water filtration system supplied by a reverse osmosis feedstock.

2.2 Preparation of PA-Derivatives of Small Sugars [64,149,150]

The solutions of individual small sugars (0.3-5.5 μmol) or a mixture of six small sugars (1-5.5 μmol each) were evaporated to dryness in a 1.3 × 10 cm glass tube tapered at the bottom. The residue was thoroughly mixed with 10-100 μL of coupling reagent, which was prepared by mixing 552 mg of 2-aminopyridine with 200 μL of glacial acetic acid (reagents and syringe were warmed before use). The mixtures were heated at 90 °C for 60 min, and then cooled. Reducing reagent (70-350 μL, freshly prepared by dissolving 200 mg of borane-dimethylamine complex in a mixture of 50 μL of water and 80 μL of acetic acid) was added to the reaction mixture. The solutions were mixed, and heated at 80 °C for 50 min, then cooled to room temperature. Ammonium hydroxide (2.8 M) was then added to bring the pH to 10. Excess reagents were extracted three times with two volumes of chloroform. The pH of the aqueous phase was adjusted to 6.0 with acetic acid and the solution was evaporated to dryness by centrifuge-evaporation using a Savant Speed Vac with the 'no-heating' setting.

2.3 Preparation of PMP-Derivatives of Small Sugars [71,73]

The solutions of individual sugars (30 nmol-15 μmol) or a mixture of ten small sugars containing 1-5.5 μmol each were concentrated to dryness and dissolved in 0.3 M NaOH solution (10-500 μL). A 0.5 M methanolic solution (10-500 μL) of PMP was added to these solutions. The mixtures were vortexed, sealed and heated at 70 °C for 2 h.

After the reaction mixtures were cooled to room temperature, they were then neutralized by adding 10-500 μL of hydrochloric acid solution (0.3 M). Then 0.5 mL water and two volumes of chloroform were added. The organic phase was discarded after being vortexed and centrifuged (phase separation was enhanced by brief centrifugation). This extraction process was repeated twice more. The aqueous layer was evaporated to dryness using a centrifuge-evaporator (Savant Speed Vac), leaving a residue of PMP-sugars.

2.4 Isolation of Oligosaccharides from Ovalbumin

2.4.1 Hydrazinolysis and Re-N-Acetylation [20-22,63]

Anhydrous hydrazine (1 mL) was added to a dry sample of the glycoprotein (564 nmol, 25 mg) and the sample was heated at 95 °C for 4 h in an evacuated sealed side arm tube. The sample was shaken gently three or four times during heating. At the end of hydrazinolysis, excess unreacted hydrazine was removed under vacuum using Speed Vac at a temperature not exceeding ~ 25 °C. Toluene was added to assist removal of traces of residual hydrazine if the sample did not thoroughly dry under vacuum. Freshly prepared sodium bicarbonate solution (9.8 % wt/wt) and acetic anhydride were added to the residue. Five minutes later, another portion of the bicarbonate solution and acetic anhydride were added. The reaction mixture was left to stand for 30 mins at room temperature with occasional stirring. The volumes of reagents added are calculated based on the assumption that all possible amino groups are to be N-acetylated. For practical purposes it can be assumed that all of these derive from amino acids. A volume of acetic anhydride equal to a 5x molar excess over these amino groups should be added, and the volume of sodium bicarbonate is such as to render the final acetic anhydride solution

0.5 M. Dowex 50WX2 (H^+, 100-200 mesh) was added to the solution to bring the pH to 3 and thus remove amino acid derivatives and sodium ions. The resin and solution were poured into a small column (20 x 0.5 cm), which was washed with 5-fold bed volumes of water. The effluent and the washings were combined, and concentrated by rotary-evaporation and further dried by a centrifuge-evaporation at a temperature lower than 30°C.

An alternative method for re-N-acetylation was also used: Acetic anhydride (160 μL) was combined with a methanol-pyridine-water mixture (30:15:10, 2.2 mL) and used to acetylate the sample after hydrazinolysis [151]. The main advantage of this method is the volatility of the solvent system used. Moreover, it eliminates the desalting step. The glycans analyzed by off-line coupling of HPLC with MALDI-MS were re-N-reacetylated with this method after being cleaved from ovalbumin.

2.4.2 Separation of Glycans from the Peptide Moiety [20-22,52]

The N-acetylated samples were dissolved in small amounts of water and spotted on Whatman No. 3MM chromatographic paper. The paper was then subjected to descending chromatography using 1-butanol-ethanol-water (4:1:1) for 18 hours. Under these conditions, disaccharides and larger oligosaccharides are immobile and all of the degradation products from the peptide moiety move quite a distance on paper. The area at 0 to 5 cm from the origin was cut out and the oligosaccharides were recovered from the paper by elution with distilled water. The eluate was filtered (0.22 μm,Teflon filter), and concentrated to dryness. After N-acetylation, the oligosaccharide pool consists mainly of unreduced oligosaccharides with a small fraction present as the acetohydrazide

derivatives [22]. These latter are catalytically converted to the former as follows. The oligosaccharides pool after paper chromatography was redissolved in ~0.5 mL of 1 mM Cu (II) acetate in 1 mM acetic acid, and incubated at room temperature for one hour. After passage through a column of Dowex 50WX2 (H^+), the effluent and washings were combined and evaporated to dryness (the acetic acid can be removed by evaporation).

2.4.3 Separation of Neutral Sugars from Anionic Sugars [152]

The residue from the step above was dissolved in 0.5 mL of water and applied to a Bio-Gel P-4 column (20 × 1.5 cm). Water was used as the eluent at a flow rate of 20-30 mL/h. The material eluted within the void volume contained acidic oligosaccharides [7,152] separated from neutral oligosaccharides, which were retarded by the column according to the size. The pool of neutral glycans was collected and collection was stopped by the time it took for glucose to come out, which had been determined previously. The pool of neutral sugars was combined and evaporated to dryness. The sugar portion was checked by resorcinol-H_2SO_4 assay. The void volumn was determined with blue dextran or hemoglobin [153].

2.4.4 PA- or PMP-Derivatization of Larger Oligosaccharide Standards or Neutral Oligosaccharides from Ovalbumin

The oligosaccharide mixture isolated from ovalbumin as described above was subjected to PA- or PMP-derivatization using the methods described above but on a smaller scale, as well as each of M3N2, NGA3 and NGA4 standard oligosaccharides (10 μg each). In addition, for PMP-derivatization of larger sugars, the reaction time used was 30 min instead of two hours used for small sugars.

2.5 Thin-Layer Chromatography of PMP-Labeled Sugars [71]

The progress of the PMP-labeling reactions was monitored by TLC on silica gel plates. The presence of impurities could also be detected at the same time. A (40:10:1) mixture of chloroform-methanol-water was used as the eluent. The spots were visualized under the 254 nm UV light.

2.6 Reversed-Phase HPLC of Derivatized Carbohydrates

2.6.1 Reversed-Phase HPLC of PA-Derivatives of Small Sugars [65,68]

A mixture of D(+)-mannose, D(+)-galactose, D(+)-glucose, L(-)-fucose, β-lactose (5.5 μmol each) and 2'-fucosyllactose (1 μmol) was reacted with 2-aminopyridine as described above and the products were dissolved in 0.1 M ammonium acetate buffer. Aliquots corresponding to 1/400 of the total sample were injected into the HPLC system. A Waters model 600 HPLC system (Millipore Corporation, Malborough, MA, USA) equipped with a Waters 486 Tunable Absorbance UV detector and a Waters 746 Data Module was used. Reversed-phase HPLC of PA-derivatives was carried out with a Vydac 218TP54 Protein & Peptide C_{18} column (25 × 0.46 cm) (The Separations Group, Hesperia, CA, USA) at a flow rate of 1 mL/min. Solvent A was 0.1 M ammonium acetate buffer without pH adjustment (pH ~6.0), and solvent B was 0.5% n-butanol in solvent A (pH ~6.0). Initially, the mixture was 95:5 A-B. After injection of a sample, the proportion of solvent B was first increased linearly to 15% over 10 min, and then to 85% over 40 min. Detection was performed at 318 nm.

2.6.2 Reversed-Phase HPLC of PMP-Derivatives of Small Sugars [73]

A mixture of D(+)-mannose, D(+)-galactose, D(+)-glucose, L(-)-fucose, β-

lactose, D(+)-glucosamine, D(+)-galactosamine, D(+)-N-acetylglucosamine (5.5 μmol each), 2'-fucosyllactose (1 μmol) and sialyllactose (0.76 μmol) was reacted with PMP as described above. Aliquots corresponding to 1/200 of the total sample were injected into the HPLC system. A Spectra-Physics HPLC system (Thermo Instruments, San Jose, CA, USA), equipped with a model SP8450 uv/vis Spectra-Physics detector and a HP-3396A integrator (Hewlett Packard Canada Inc., Orangeville, ON), was used. An Inertsil ODS-3 column (15 × 0.46 cm, 5 μm particle size) was used (Phase Separations, Franklin, MA, USA). The flow rate was set at 1 mL/min and the wavelength at 245 nm. Solvents A and B were 0.1 M ammonium acetate (pH 5.5) with 10 and 25 % acetonitrile, respectively. A gradient of 45 to 100% buffer B over 55 min was used for separation.

2.6.3 Reversed-Phase HPLC Separation of PMP-Derivatives of Larger Oligosaccharides or Glycans from Ovalbumin

A Varian 9010 HPLC system (Varian, Lexington, MA, USA), equipped with a Varian 9050 UV/VIS detector and a Varian Star data processor, was used. The reversed-phase column was Hypersil ODS (25 × 0.46 cm, 5 μm particle size) (Sigma-Aldrich). Solvent A was 0.01 M TFA (trifluoroacetic acid) in water, and solvent B was 0.01M TFA in acetonitrile. Detection was at 245 nm. The gradient used consisted of increasing the proportion of B from 20 to 100% over 70 min at a flow rate of 1 mL/min. For larger standards, aliquots of 1/6 of the total sample (derivatization was carried out by using 10 μg of each of standards) were injected for analysis and the fractions corresponding to each peak were collected and concentrated by centrifuge-evaporation for ESI-MS analysis, and TFA was also removed during evaporation [141]. The same HPLC

procedure was applied to PMP-derivatized glycans from ovalbumin. Aliquots of 1/100 (for analysis) or 1/10 (for fraction collection) of the total sample were injected. Fractions collected were concentrated and reconstituted to a desired concentration for MALDI-MS analysis.

2.7 Mass Spectrometry

2.7.1 Fast Atom Bombardment Mass Spectrometry (FAB-MS) (Performed by X. Shen, and H. Perreault)

Positive ion mode FAB experiments were carried out with a VG Analytical 7070E mass spectrometer (Micromass, Manchester, UK). Samples (ca. 10 nmol) were loaded onto a stainless steel target and then a matrix of either glycerol alone or a mixture of glycerol-thioglycerol (1:1, v/v) was added and mixed with the sample. The FAB gun (Xe^{o}) was operated at 8 kV. The accelerating voltage was set at 6 kV. Conventional scans were at the rate of 2 s/decade and the *m/z* range covered was from 45 to 1000 u.

2.7.2 Matrix-Assisted Laser Desorption/Ionization Time-of-Flight Mass Spectrometry (MALDI-TOF-MS) (Performed by X. Shen, and H. Perreault)

MALDI-TOF-MS was performed in the linear mode on Manitoba II, an instrument built in-house in the Time of Flight Laboratory, Department of Physics, University of Manitoba, and described elsewhere [154]. The samples (1 μL, ca. 100 pmol) were loaded onto a stainless steel target with 1 μL of α-cyano-4-hydroxycinnamic acid (saturated in 1:1 acetonitrile water containing 0.1% TFA) as the matrix. The sample and the matrix were thoroughly mixed and co-crystallized (so-called dried-drop method) [92]. An accelerating potential of 25 kV was used. The samples were irradiated using a

N_2 laser beam at 337 nm. External calibration of the MALDI mass spectra was carried out from a second preparation on the same sample support using bovine insulin and substance P as external calibrants for the analyses of PMP-derivatives of sugars, and horse skeletal muscle myoglobin as a calibrant for the analyses of intact ovalbumin.

2.7.3 Electrospray Ionization Mass Spectrometry (ESI-MS)

2.7.3.1 Electrospray Ionization Mass Spectrometry (ESI-MS) for PA or PMP-Derivatives of Small Sugars (Performed by R. Bordoli, Micromass, Altringham,UK)

Sample-infusion ESI analyses were performed on a Micromass Q-Tof instrument (Micromass, Altringham, UK). Full-scan spectra were acquired over a *m/z* range 100 to 2000 u. Collision induced dissociation (CID) MS/MS experiments were conducted with argon at a gas pressure of 3×10^{-3} torr and a collision energy of 28 eV. Product ion scans were recorded.

2.7.3.2 On-Line HPLC/MS for PA- or PMP-Derivatives of Small Sugars (Performed by J. Langridge (Micromass, Altringham, UK))

A Micromass Quattro-II triple quadrupole mass spectrometer was used in these experiments. Full-scan data were acquired in the positive ion mode over a *m/z* range of 100 to 2000 u at the rate of 7 s/scan. The cone voltage was set to alternate between 50 and 100 V every second scan. An ABI Aquapore RP 300 column (100 × 1 mm) was used; the amounts of sample injected were one fifth of those used for HPLC-UV experiments in Section 2.6.1 and 2.6.2. The column effluent was monitored by an on-line UV detector at 245 nm for PMP-derivatives or at 318 nm for PA-derivatives. The flow rate was 50 μL/min and gradients were the same as used in RP-HPLC of PA- or PMP-derivatives

except that 50 mM NH_4OAc was used instead of 0.1M NH_4OAc.

2.7.3.3 Sensitivity Studies on Native and PMP-Derivatized Tetraglucose as a Model for Other Oligosaccharides by ESI-MS

A series of aqueous solutions of native and PMP-tetraglucose (4-O-(4-O-[6-O-α-D-glucopyranosyl-α-D-glucopyranosyl]-α-D-glucopyranosyl)-D-glucopyranose) was prepared, i.e. 10^{-3}, 10^{-5}, 10^{-6}, 10^{-7}, 10^{-8} M. The starting solution at 10^{-3} M was prepared first (PMP-tetraglucose solution was filtered with Teflon filter (0.22 μm)), and then diluted to yield 10^{-5}, 10^{-6}, 10^{-7}, 10^{-8} M solutions. Each of these solutions (20 μL) was injected into the mass spectrometer. The instrument used for these analyses was a Quattro LC from Micromass (Manchester, UK) equipped with a Z-spray™ electrospray source. Solutions were injected using a 20 μL Rheodyne loop, and the carrying solvent was 1:1 acetonitrile-water at a flow rate of 10-13 μL/min. A KD Scientific (KD Scientific Inc., Boston, MA, USA) syringe pump was used to provide the carrying solvent.

The samples were sprayed using a 3.50 kV needle voltage, and the cone voltage (declustering voltage) was set at 60 V for all experiments, unless specified. The source block and desolvation temperatures were set at 110 °C and 130 °C, respectively.

MS and MS/MS spectra were recorded in both the positive and negative ion modes, with scan rates of 300 u/sec and variable mass ranges for CID experiments. The pressure of argon in the gas cell was $2x10^{-3}$ torr, and the collision energy was set ranging from 35 to 90 eV.

2.7.3.4 ESI-MS and ESI-MS/MS of PA or PMP-Derivatives of Larger Sugar Standards (M3N2, NGA3, and NGA4) (Performed by X. Shen, And D. Boismenu,

(McGill University))

Most of these analyses were carried out with our instrument described in section 2.7.3.3 and some was carried out at McGill University with a Quattro II instrument from Micromass. The conditions were the same as used for tetraglucose. For native and PMP-NGA3, the mass spectrometer and all other conditions used were the same as used for tetraglucose, except that the carrying solvent, 49:49:2 water-methanol-formic acid was used for native NGA3.

2.7.3.5. On-line RP-HPLC/ESI-MS for PMP-NGA3

The HPLC system used was an Ultra Plus Pump Module from Microtech Science Inc. The column was a 25 × 0.46 cm Vydac 218TP54 Protein & Peptide C_{18} column (The Separations Group, Hesperia, CA, USA). The HPLC system was equipped with a Rheodyne injector (20 μL loop). A constant flow rate was set at 1mL/min, and the composition of the mobile phase was programmed as follows: The initial composition, 5% of acetonitrile in water, was kept for 5 min, then increased to 60% over 10 min, and kept at 60% for 20 min. Trifluoroacetic acid (TFA) was kept at a constant concentration of 0.04% throughout the separation.

2.7.3.6 ESI-MS of Intact Ovalbumin [43]

An ovalbumin solution was prepared by dissolving the sample in water first, and then adding acetonitrile and formic acid sequentially to reach a final concentration of 100 pmol/μL in acetonitrile-water (2:1) containing 2% formic acid. The amount of sample injected was 2 nmol. The mass spectra of ovalbumin were acquired by scanning from 500 to 2500 u in 7 s. Twenty scans were averaged to produce S/N and resolution

high enough to resolve oligosaccharide heterogeneity.

2.7.3.7 ESI-MS and ESI-MS/MS of PMP-Glycans Cleaved from Ovalbumin

The glycan derivatives were desalted using a Sep-Pak C_{18} cartridge. The cartridge was pre-conditioned by treatment with 5 mL water, 5 mL of acetonitrile, and 10 mL of water. The sample was then reconstituted with 0.5 mL of water and applied directly onto the cartridge. The sample was eluted with 5 mL of water, 5 mL of 20% aqueous acetonitrile, and 5 mL of pure acetonitrile [108]. The water fraction was discarded. The acetonitrile fractions were combined, passed through a Teflon filter (0.22 μm), and dried by centrifuge-evaporation. The residue was reconstituted in 100 μL of water for ESI-MS, or in 30 μL of water for ESI-CID-MS/MS (obtained from the same amount of ovalbumin). A 5 μL-aliquot containing the PMP-oligosaccharides detached from 4 mg ovalbumin was injected for ESI-CID-MS/MS, whereas an aliquot from 2.5 mg ovalbumin was injected for ESI-MS. The CID tandem mass spectra of selected $[M+2H]^{2+}$ ions of PMP-glycans were recorded. For this purpose, the precursors were individually selected by the first quadrupole, collided with argon in the second quadrupole, and the product ions (fragments) were mass-analyzed by the third quadrupole. The argon gas pressure was maintained at ca. 2×10^{-3} torr for this study and collision energies of 50-60 eV were used.

3. RESULTS AND DISCUSSION

3.1 Preliminary Work

The PA- and PMP-derivatization methods were selected among a number of reported methods for labeling carbohydrates since both involve quantitative yields, rapid reactions and simple cleanup procedures [57]. Preliminary work was carried out on characterization of PA- or PMP-derivatives of small sugars prior to studying derivatives of larger oligosaccharides, either obtained commercially or detached from ovalbumin. These oligosaccharides were available in very limited quantities, and therefore had to be characterized by methods which had been preassessed.

3.1.1 Labeling with PA or PMP

3.1.1.1 Labeling Carbohydrates with 2-aminopyridine

The reaction conditions for pyridylamination have been optimized by a thorough investigation regarding the effects of reagent concentration, temperature, time, etc., on the yield of PA-derivatives [64]. Borane-dimethylamine complex ($BH_3 \cdot NH(CH_3)_2$) was used rather than sodium cyanoborohydride ($NaBH_3CN$) for the reductive step of the PA-derivatization reaction, since the former is more volatile and thus more easily removed [58]. In addition, it was reported that the former gave the highest yield of PA-sugars and the smallest amount of by-products among the reducing reagents tested [64]. For the early experiments, a TSK gel HW-40F size exclusion column was tested to remove excess PA reagent [149]. However, since this method is time-consuming it was dropped, and extraction with chloroform was adopted [149].

3.1.1.2 Labeling Carbohydrates with PMP

The optimal concentrations of the reagent and NaOH to obtain quantitative yields for PMP-derivatives were found to be 0.5 and 0.3 M, respectively [71]. These concentrations represent large excesses of PMP and NaOH relative to the substrates, as is usually the case with precolumn labeling. The excess PMP reagent had thus to be removed prior to HPLC analysis. Chloroform was found by Honda et al..[71] to give good results for both extraction efficiency and product recovery. However, chloroform gave unsatisfactory recovery of some more hydrophobic monosaccharides such as xylose and fucose. Butyl ether was reported to give more complete recovery of the PMP-monosaccharides than chloroform since butyl ether is a less polar solvent [73]. We decided to use chloroform in our experiments since it yielded much clearer two-phase separations than butyl ether. The nebulous separations observed when using the latter resulted in sample loss.

3.1.2 Reversed-Phase HPLC of PA- and PMP-Labeled Small Sugars

3.1.2.1 Reversed-Phase HPLC of PA-Labeled Small Sugars

Fig. 3.1a shows the HPLC-UV chromatogram obtained after injecting a mixture of PA-mannose, galactose, glucose, fucose, β-lactose (14 nmol of each) and 2'-fucosyllactose (2.5 nmol). The retention times of the individual components had been determined prior to running the mixture. In previous studies [68,69,149,155], the additivity rule was observed: a monosaccharide residue in a PA-oligosaccharide makes an intrinsic contribution to the retention time of the PA-saccharide with a certain HPLC apparatus, column, column temperature, and mode of gradient elution. Fig. 3.1a shows that PA-β-lactose was eluted before some of the PA-monosaccharides, e.g. mannose and glucose.

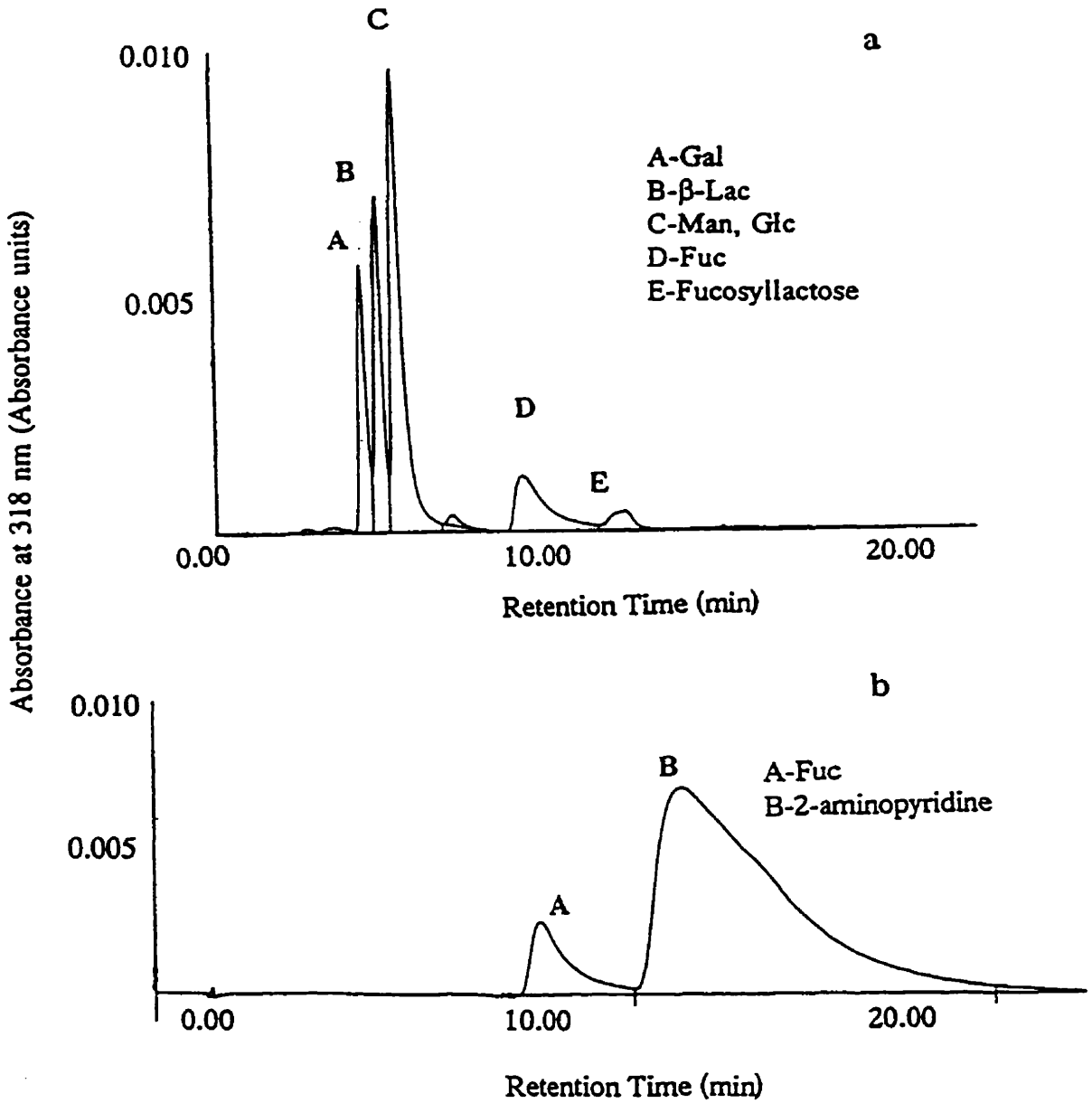

Fig. 3.1: a) Reversed phase HPLC-UV chromatogram of the PA derivatives of small sugars. b) Chromatogram showing the elution of 2-aminopyridine and PA-L(-)-fucose. Column:Vydac Protein & Peptide C_{18}, (25 x 0.46cm). Gradient: from 0.025% to 0.425% 1-butanol in 0.1M ammonium acetate over 50 min, 1mL/min. Detection: 318 nm. Gal = galactose, Lac = lactose, Man = mannose, Glc = glucose, Fuc = fucose. Sample concentration: 0.5-2.8 nmol/μL. Sample injected: 5μL of the mixture of PA-D(+)-mannose, D(+)-galactose, D(+)-glucose, L(-)-fucose, β-lactose (14 nmol each) and 2'-fucosyllactose (2.5 nmol).

The elution order observed here is similar to that reported by Takemoto and co-workers [156]. A longer retention time is observed for 2'-fucosyllactose, which is predictable according to its three-ring composition. Fucose, or 6-deoxy-galactose, is less polar than galactose, resulting in a longer retention time relative to that of galactose. The peaks corresponding to PA-mannose and PA-glucose are superimposed, but all other components were resolved. The broad 2-aminopyridine peak obtained using the same conditions (Fig. 3.1b) was absent from the chromatogram of the mixture (see Fig. 3.1a), demonstrating that extraction of the excess reagent with chloroform was quite efficient as reported earlier [149]. If 2-aminopyridine is not removed properly, it can interfere severely with PA-derivatives during HPLC analysis. Size exclusion chromatography was reported to be an efficient method to remove very small quantities of 2-aminopyridine from PA-derivatives [149]. However, in addition to being time-consuming, this procedure makes use of buffer salts which are not favorable for MALDI or ESI analysis. An attempt was made to adjust the pH of the buffer used in our HPLC experiments from 6 to 4, as adopted previously [63,65,68,155]. However, results showed even lower resolution than observed in Fig. 3.1a at pH 6.

3.1.2.2 Reversed-phase HPLC of PMP-Labeled Small Sugars

Fig. 3.2 shows the elution pattern of PMP-derivatives of small sugars. An aliquot containing the derivatives of D(+)-mannose, D(+)-galactose, D(+)-glucose, L(-)-fucose, β-lactose, D(+)-glucosamine, D(+)-galactosamine, D(+)-N-acetylglucosamine (27.5 nmol each), 2'-fucosyllactose (5 nmol) and sialyllactose (3.8 nmol) was injected to obtain this chromatogram. The PMP-labeled sugar peaks were all sharp and almost baseline-resolved.

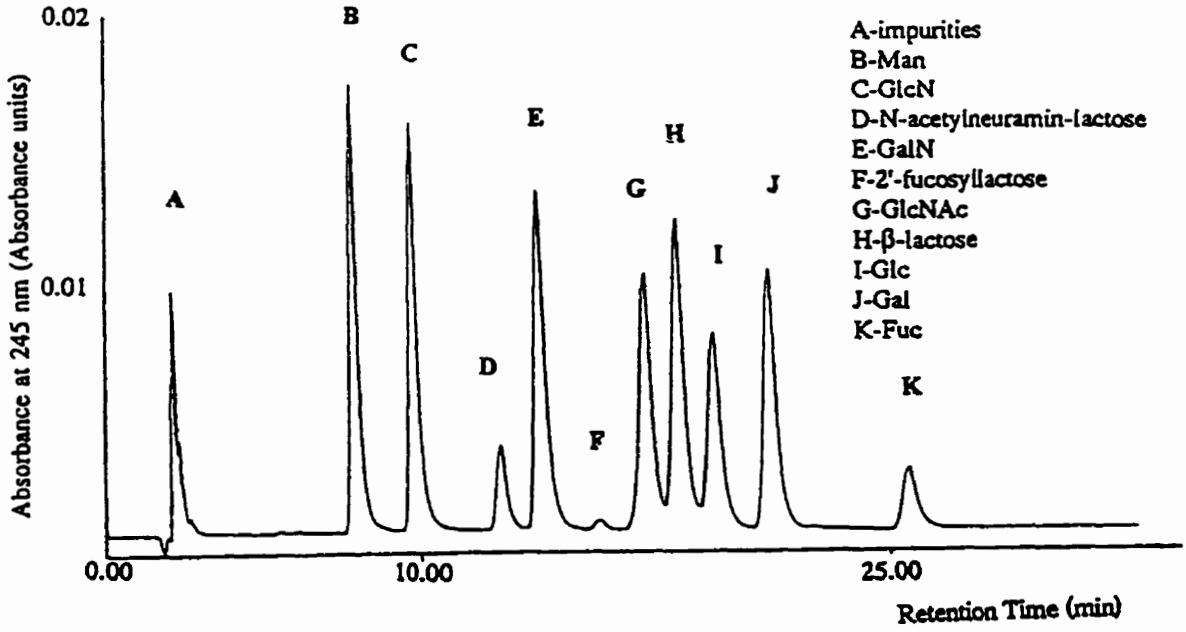

Fig. 3.2 Reversed-phase HPLC-UV chromatogram of the PMP-derivatives of small sugars. Column: Inertsil ODS (25cm x 0.46 cm). Gradient: from 16% to 25% acetonitrile in 0.1M ammonium acetate over 55 min, 1 mL/min. Detection: 245 nm. GlcN = glucosamine, GalN = galactosamine, GlcNAc = N-acetylglucosamine. Sample injected: the mixture of PMP-D(+)-mannose, D(+)-galactose, D(+)-glucose, L(-)-fucose, β-lactose, D(+)-glucosamine, D(+)-galactosamine, D(+)-N-acetylglucosamine (27 nmol each), 2'-fucosyllactose (5 nmol) and N-acetylneuramin-lactose (sialyllactose) (3.8 nmol).

A similar pattern had been reported by Fu and O'Neil [73]. The deoxy-hexose (fucose) eluted later than its parent compound galactose, as observed with PA-derivatives. The PMP-derivative of fucose produced a much smaller peak (labeled K in Figure 3.2) than the other monosaccharide derivatives, although equal amounts of all monosaccharides were used for derivatization.This may be caused by poor extraction recovery of PMP-fucose with chloroform, since it is more hydrophobic than the other derivatives, as reported by Fu and O'Neil [73]. The PMP reagent appears as a minor peak at a retention time of *ca.* 5.6 min, which indicates that PMP can be almost completely removed by the extraction procedure. Our results show that a low initial acetonitrile concentration and a shallow gradient can provide good quality separation of the reagent from PMP-labeled products as reported by Strydom [72]. The basic mode of separation in the present method appears to involves hydrophobic interactions, considering the generally observed shorter elution times with increasing acetonitrile concentration [71]. It has been found before that the structures eluted in order of decreasing molecular weight and polarity [134].

It has been reported that oligosacchrides derivatized with PA or PMP produce responses more than 10 times weaker than their parent oligosaccharides when using high pH anion exchange chromatography (HPAEC) [37]. Therefore, PA- or PMP-derivatives are not suitable for the HPAEC technique.

3.1.3 TLC Analyses of the PMP-Derivatives of Small Sugars

Following extraction with chloroform, the PMP-sugars were eluted on silica gel plates to ascertain efficiency of PMP removal. In addition, the R_f values of these individual PMP-derivatives can be used as reference data. In most cases, two spots could be

visualized under UV light, one due to the PMP-derivative and the other from a small amount of PMP. The R_f values measured for PMP-glucose and PMP itself are 0.43 and 0.90, respectively, and agree with the reported values [71]. The measured R_f data for PMP-derivatives of small sugars are given in Table 3.1. The relative standard deviations for the R_f values (n = 3) was within 3.6 % for all spots.

3.1.4 Mass Spectrometry of PA- and PMP-Derivatives of Small Sugars

The derivatives have been characterized using three ionization techniques: FAB, ESI and MALDI. The purposes of this investigation were first to determine the molecular masses of derivatization products, secondly to determine how much material was required to produce informative spectra, and thirdly to assess the relevance of the information obtained with each technique, for both types of derivatives.

3.1.4.1 Mass Spectrometry of PA-Derivatives of Small Sugars

1) FAB-MS of PA-Derivatives

The PA-monosaccharides produced $[M+H]^+$ ions at *m/z* 259 for PA-mannose, glucose (Figure 3.3a), galactose and at *m/z* 243 for PA-fucose. Glycerol produced multiple peaks (labeled with an asterisk). The secondary amine in the aminopyridine portion of each PA-derivative provides a favourable site for protonation and thus promotes the formation of $[M+H]^+$ ions [42,67,129,130,133]. The resulting sensitivity enhancement obtained with these derivatives relative to underivatized sugars was around one order of magnitude. Honda, and Kakehi et al. claimed a 100-fold sensitivity improvement over free maltooligosaccharides [133], whereas recently Okamoto, and

Table 3.1. Thin- layer chromatography R_f values measured for the PMP-derivatives of small sugars

PMP-derivative of...	**R_f***
D(+)-Galactose	0.39
D(+)-Glucose	0.43
D(+)-Mannose	0.41
L(-)-Fucose	0.56
D(+)-Galactosamine	0.17
D(+)-Glucosamine	0.20
D(+)-N-Acetylglucosamine	0.035
β-Lactose	0.13
2'-Fucosyllactose	0.08
Sialyllactose	0.00

*Relative standard deviation within 3.6% on 3 measurements

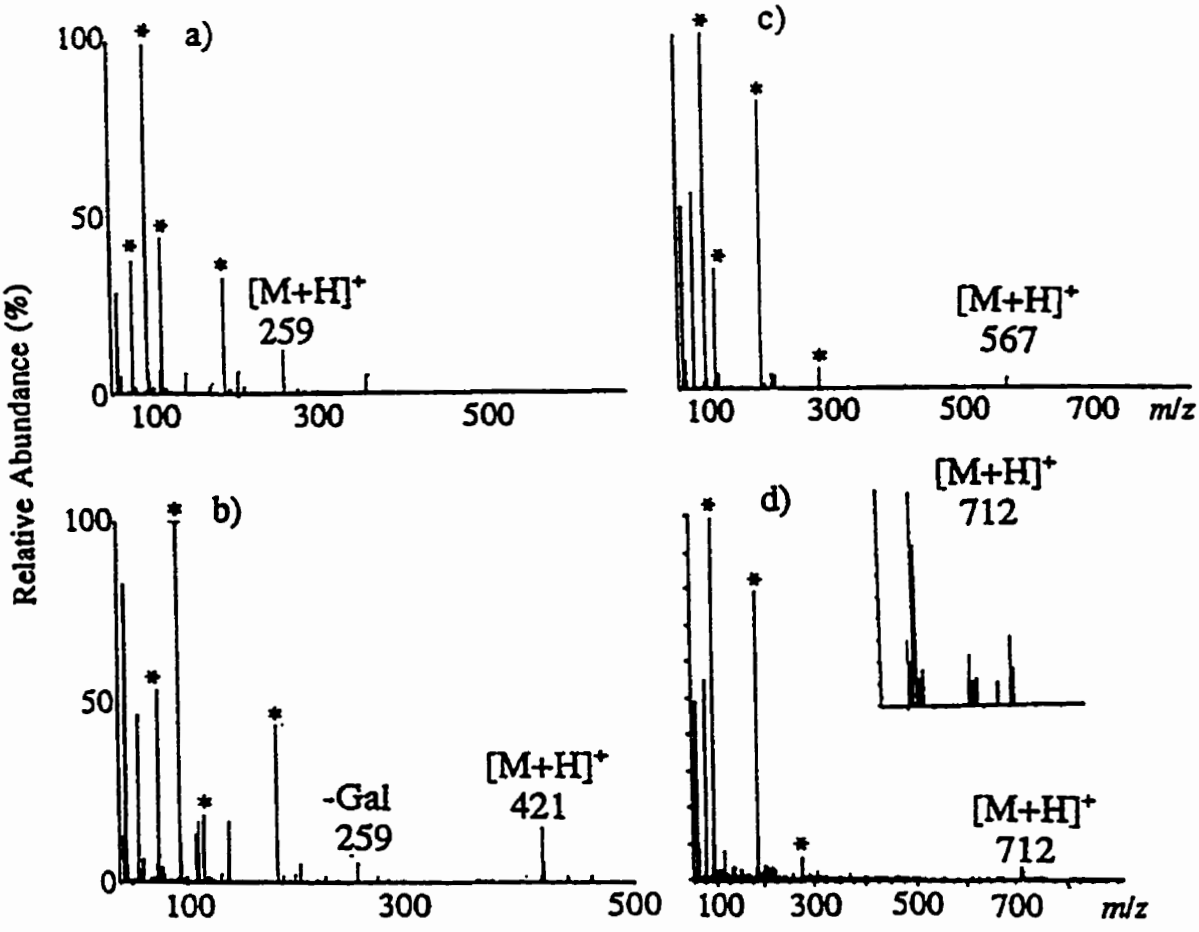

Fig.3.3 Positive mode FAB mass spectra of the PA-derivatives of small sugars: a) PA-glucose, b) PA-β-lactose, c) PA-2'-fucosyllactose, d) PA-sialyllactose. Details on conditions are given in Section 2.7.1.

Takahashi et al. reported an only three-fold sensitivity improvement in the positive ion mode [42]. Figure 3.3b shows the FAB spectrum of PA-β-lactose, which contains characteristic $[M+H]^+$ ions at *m/z* 421. Ions at *m/z* 259 indicate the loss of the galactose residue (Y-type cleavage [91]). Typically, the loss of a hexose residue is indicated by a peak 162 mass units below the parent ion. This is believed to result from cleavage of the glycosidic bond (away from the charged site) followed by hydrogen transfer to the glycosidic oxygen [127]. While molecular ions of PA-derivatives were relatively abundant, very few fragment ions with low abundance were present, as reported previously [129]]. PA-2'-fucosyllactose and PA-sialyllactose produced $[M+H]^+$ ions at *m/z* 567 and 712, respectively, as shown in Figure 3.3c and 3.3d. Especially in 3.3d, the fragment ions are obscured by background signals from the liquid matrix, making the spectrum nearly uninterpretable. Many of the peaks in FAB mass spectra are attributed to the matrix (glycerol in this case). This matrix-related chemical background can mask sample fragment peaks, making structural assignments difficult [127, 133]. Carr and Reinhold have pointed out that experimental factors such as mode of ionization, choice of liquid matrix, amount of compound analyzed and the presence of salts may also dramatically influence the ratio of molecular to sequence-related ions [129]. Also, it was reported that PA-derivatives gave little or no information in the negative ion mode [157].

With such lack of sensitivity, and specificity especially for larger oligosaccharides, it was decided that PA-derivatives of sugars larger than trisaccharides would be characterized by ESI and/or MALDI.

2) ESI-MS of PA-Derivatives of Small Sugars

The full-scan ESI spectra of a PA-derivative mixture recorded with a cone voltage 30 V and 50 V, are shown in Fig. 3.4a and 3.4b, respectively. This mixture is the same as that used to produce Fig. 3.1a but was diluted two times with 1:1 acetonitrile-water (the concentration of PA-derivatives was ca. 0.3 to 1.4 nmol/μL), however, the amounts injected were the same as used in Fig. 3.1a. Originally, alternate scans at low and high cone voltages were acquired in order to generate both the molecular ions and some fragmentation. However, these two spectra display no significant difference, and major peaks appear at m/z 243, 259, 421, 567 corresponding to the protonated molecular ions of PA-fucose, PA-hexose (mannose and glucose), β-lactose, and PA-2'-fucosyllactose; no sequence-related ions are apparent in either spectrum, even at high cone voltage (50 V). Sequence information may be obtained by selecting the appropriate protonated parent ion, inducing fragmentation by CID and analyzing the daughter ions produced. CID experiments were however not performed at this stage.

On-line HPLC/ESIMS of the same mixture was carried out using the same ESI conditions. Overlapping between the HPLC peaks made the interpretation of spectra rather difficult and these data will not be further discussed here. The overlapping was partly due to a lower ammonium acetate concentration than that used for HPLC-UV experiments in order to suit to ESI requirements. To summarize, ESI produced good quality spectra for each of the mono-, di-, and trisaccharides analyzed. Okamoto et al. [42] had made similar observations with ESI of PA-maltopentaose and had measured a 100-fold sensitivity improvement relative to ESI of the underivatized pentasaccharide in the positive ion mode. In the case of our mono-, di- and trisaccharides, the sensitivity

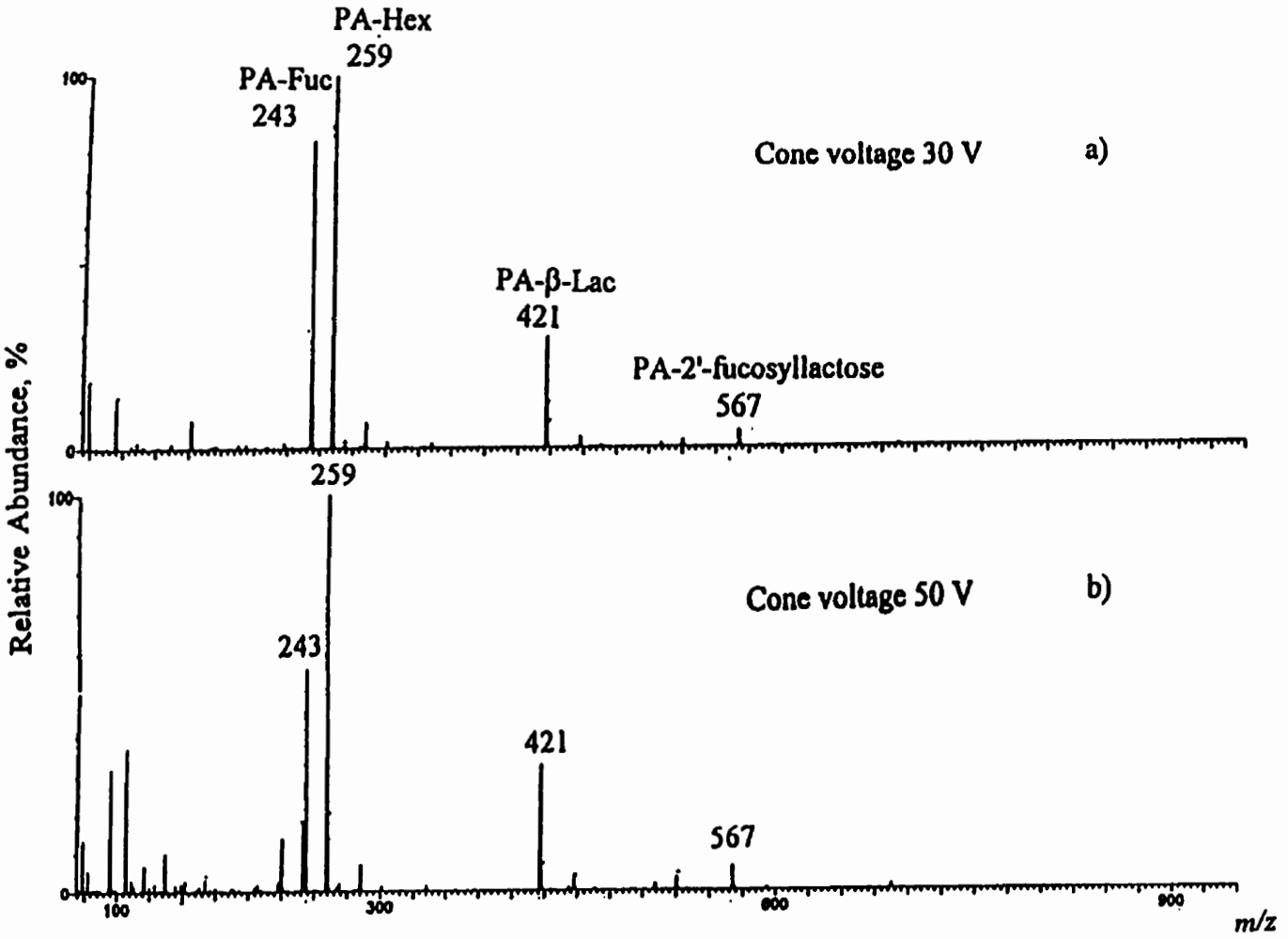

Fig. 3. 4 Positive mode ESI mass spectra of PA-derivative mixture of small sugars: a) at cone voltage 30 V, b) at cone voltage 50 V. The amount of sample injected was the same as that used in Fig. 3.1a. Details on conditions are given in Section 2.7.3.1.

improvement was approximately 50-fold.

3) MALDI-TOF-MS of PA-Derivatives of Small Sugars

In MALDI, the PA-derivatives produced predominant $[M+H]^+$ ions, with less abundant $[M+Na]^+$ species. For PA-monosaccharides, these ions appeared in the matrix-region of the spectra, i.e. where most background ions are present, making their assignments more difficult. The matrix used, α-cyano-4-hydroxy cinnamic acid (CHCA), has a molecular weight of 189.17 and produces $[M+H]^+$, $[M+Na]^+$ and other low mass ions which interfered with the peaks of the compounds of interest. In the case of di- and trisaccharides, the $[M+H]^+$ and $[M+Na]^+$ ions were easily recognized, although fragments were in turn obscured by the background in the matrix region. To summarize, MALDI signals for mono- and disaccharides were easily lost in the matrix background, making this technique more favorable to characterization of higher M_r PA-oligosaccharides. The sensitivity improvement observed was on the same order as in ESI.

3.1.4.2 Mass Spectrometry of PMP- Derivatives of Small Sugars

1) FAB-MS of PMP-Derivatives of Small Sugars

FAB mass spectra of PMP-derivatives are shown in Fig. 3.5 (PMP-fucose, galactose, N-acetylglucosamine) and Fig. 3.6 (PMP-β-lactose, 2'-fucosyllactose, and sialyllactose). The sensitivity enhancement obtained with these derivatives relative to underivatized sugars was of the order of 100. The PMP-derivatives produced abundant $[M+H]^+$ and $[M+Na]^+$ ions, and also fragment ions, although low in abundance. The $[M+Na]^+$ species predominated, as well as $[M-H+2Na]^+$ and $[M-2H+3Na]^+$ were present, due to excess sodium hydroxide used in the derivatization reaction. The loss of one PMP

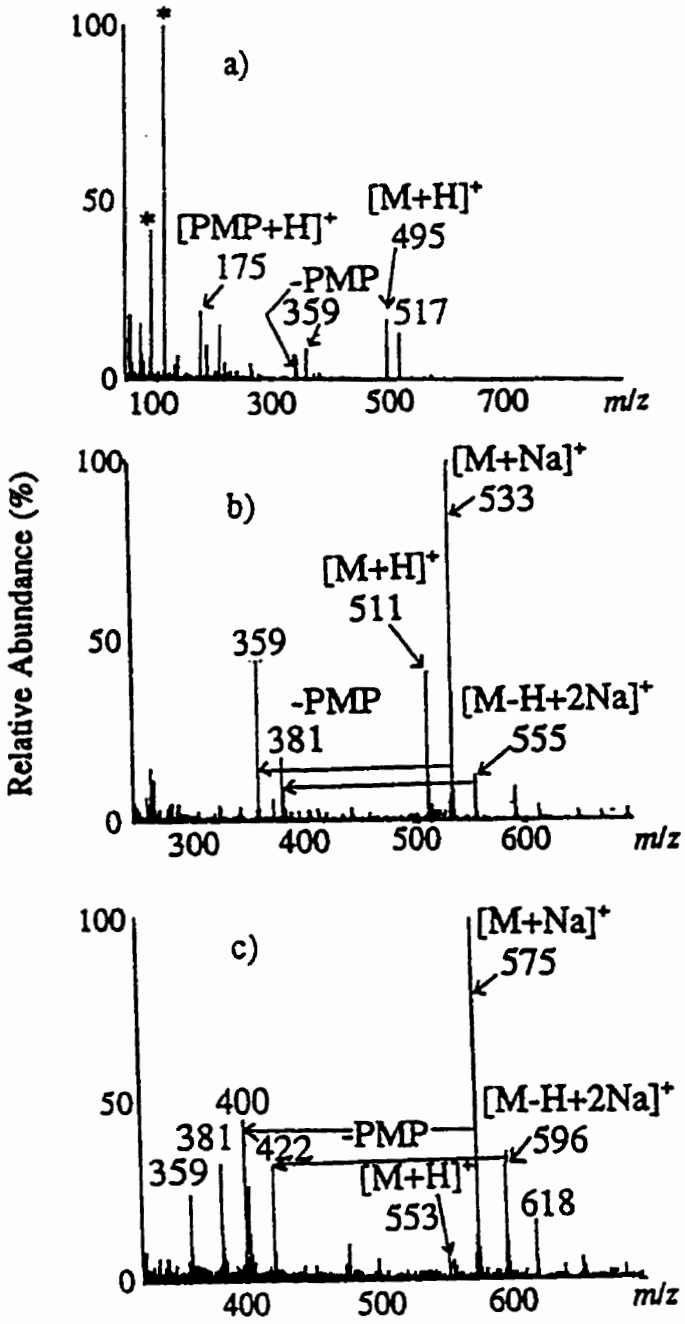

Fig. 3.5 Positive mode FAB mass spectra of the PMP-derivatives of monosaccharides: a) PMP-fucose, b) PMP-galactose, and c) PMP-N-acetylglucosamine. Details on conditions are given in Section 2.7.1.

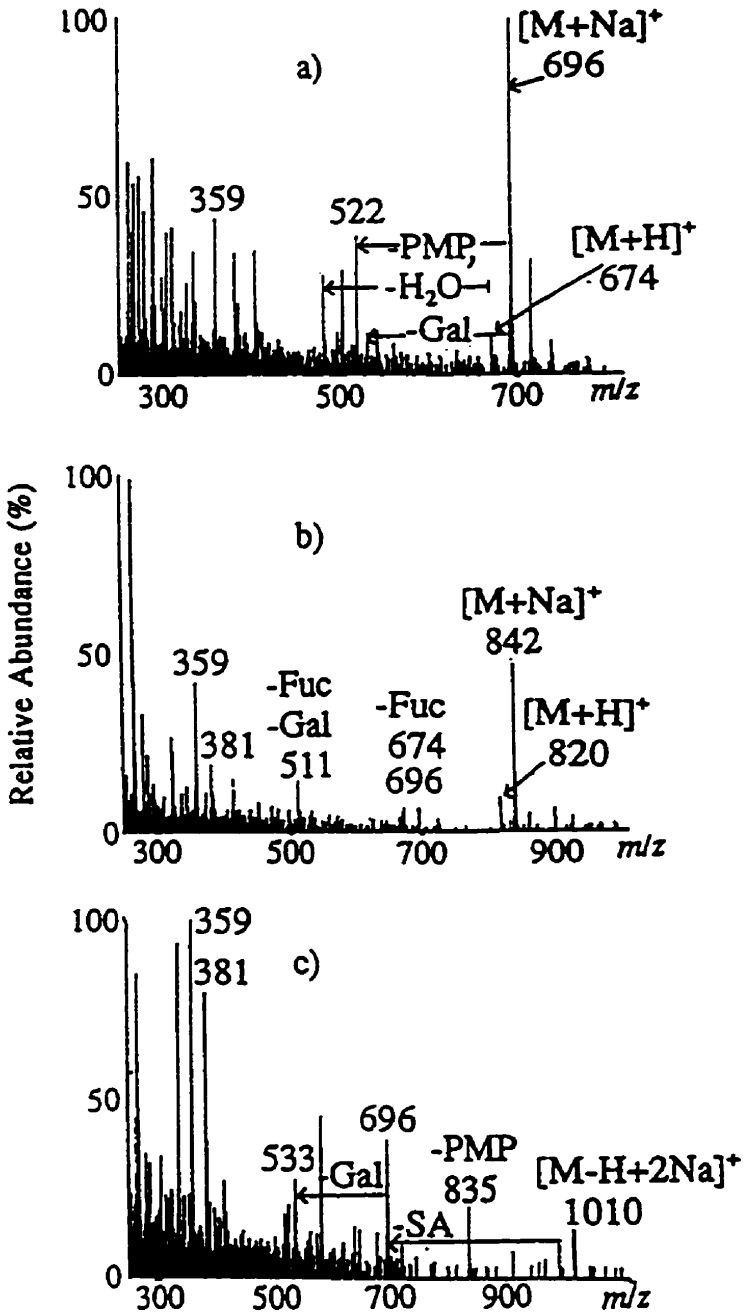

Fig. 3.6 Positive mode FAB mass spectra of the PMP-derivatives of di- and tri-saccharides: a) PMP-β-lactose, b) PMP-2'-fucosyllactose, c) PMP-sialyllactose. Details on conditions are given in Section 2.7.1.

residue from $[M+Na]^+$ ions produced abundant ions. The same loss from $[M+H]^+$ and $[M-H+2Na]^+$ ions produced fragment ions varying in abundance, depending on the overall sodium content of the sample. Figure 3.5c is a good example to illustrate these trends. In Fig. 3.6b, loss of the fucose residue from the non-reducing terminal of PMP-fucosyllactose produced abundant ions at *m/z* 674 and 696. Ions due to further loss of a galactose residue appear at *m/z* 511 and 533, respectively.

Fig. 3.6c shows the FAB mass spectrum of PMP-sialyllactose. The peaks at *m/z* 966, 988, and 1010 correspond to the $[M+H]^+$, $[M+Na]^+$ and $(M-H+2Na)^+$ ions, respectively. The abundant ions at *m/z* 696 and 533 result from sequential losses of sialic acid and galactose residues from the non-reducing end of the $[M+Na]^+$ ions. The high abundance of ions at *m/z* 696 is possibly due to increased lability of the sialyl linkage owing to substitution of H^+ by Na^+ as the counter ion to the carboxylate group [129]. The spectra of all PMP-sugars examined contained two high peaks at *m/z* 359 and 381 (Fig. 3.5 and 3.6). These signals were attributed to cleavage of Bond 1 of the terminal reducing end (between C1and C2), producing fragments bearing two PMP residues (without and with sodium attached). Also, for sugars with a hexose residue at their reducing end, ions at *m/z* 359 and 381 could be in part due to fragment ions corresponding to mono-PMP-hexose, with one and two sodium attached, respectively. Tables 3.2 and 3.3 list the major ions contained in the FAB spectra discussed above. These results show that PMP-labeling enhances sensitivity by almost an order of magnitude over PA-derivatization for the analysis of small sugars in FAB-MS. According to Suzuki et al. [57], PMP-labeled maltopentaose yielded two to three-fold enhanced relative intensity over its PA-derivative

Table 3.2. Molecular ions observed in the fast atom bombardment mass spectra of the PMP-derivatives of small sugars.

PMP-derivative of...	**Calculated molecular mass***	**Molecular ions, *m/z***			
		$(M+H)^+$	$(M+Na)^+$	$(M-H+2Na)^+$	$(M-2H+3Na)^+$
D(+)-Galactose, D(+)-Glucose, D(+)-Mannose	510.3	511	533	555	—
L(-)-Fucose	494.5	495	517	539	—
D(+)-GalN, D(+)-GlcN	509.4	510	532	554	575
N-GlcNAc	551.5	552	574	966	618
β-Lactose	672.6	674	696	718	740
2'-Fucosyllactose	818.7	820	842	864	—
3'- and 6'-Sialyllactose	963.9	966	988	1010	—

*Calculated using monoisotopic values

Table 3.3: Fragment ions observed in the fast atom bombardment mass spectra of the PMP-derivatives of small sugars.

PMP-derivatives of ...	Fragment ions, *m/z*							
	(M-PMP) $+H^+, +Na^+, -H^+ +2Na^+$	(M-PMP-H_2O) $+H^+, +Na^+$	(*bis*PMP+CH) $+H^+, +Na^+$	(M-Gal) $+Na^+$	(M-Fuc) $+H^+, +Na^+$	(M-Fuc-Gal) $+H^+, +Na^+$	(M-SA*) $+Na^+$	(M-SA-Gal) $+Na^+$
Gal,Glc,Man	337, 359, —		359, 381					
Fuc	321, 343, —		359, 381					
GalN, GlcN	336, 358, —		359, 381					
GlcNAc	—, 400, 422		359, 381					
β-Lactose	—, 521, 543	483, 505	359, 381	533				
2'-Fucosyllactose	—, 667, —		359, 381		674, 696	511, 533		
3' and 6'-Sialyllactose	—, 813, 835		359, 381				696	533

*SA = Sialic acid

in a glycerol matrix in the positive ion mode. PMP-labeling produces sugars with a more hydrophobic tail than the PA method, and thus enhances surface activity of the analytes during FAB experiments. Poulter and co-workers [125] reported the same phenomenon with the labeling of sugars using n-alkyl p-aminobenzoates for liquid secondary ion mass spectrometry (LSIMS). Our results also show that all types of small saccharides (hexoses, fucose, aminohexoses, acetoaminohexoses, fucosylated and sialyllated lactose) can be labeled with PMP to form bis-PMP-derivatives. The extensive loss of one PMP residue observed in the mass spectra may indicate instability of bis-PMP-derivatives and relatively higher stability of mono-PMP-derivatives, as indicated previously for PMPMP-compounds [70]. Overall, the PMP-derivatives were more readily fragmented than PA-derivatives under FAB conditions. Also, for PMP-di- and trisaccharides, more information on the sugar sequence was obtained than with PA-derivatives, which provided mainly M_r information.

Because of the limited mass range and sensitivity available with the FAB technique, no informative spectra could be obtained for PMP-sugar derivatives with M_r above 800. The use of ESI- and MALDI-MS was thus investigated for characterization of PMP-sugars.

2) ESI-MS of PMP-Derivatives of Small Sugars

Suzuki and co-workers [57] have previously reported that PMP-derivatives of maltopentaose gave the highest ESI sensitivities among other types of derivatives investigated, such as PA-, ABEE-, 2-aminoethanethiol (AET)- and 2-aminobenzenethiol (ABT)-derivatives.

The ESI spectra of PMP-β-lactose and 2'-fucosyllactose are shown in Fig. 3.7a and 3.7b. The full-scan ESI spectrum of β-lactose (not shown) contained many unknown ions due to impurities and thus an ESI-MS/MS spectrum of the $[M+H]^+$ ions at m/z 674 was recorded instead (Fig. 3.7a). The peaks at *m/z* 511 and 337 correspond to successive losses of a galactosyl residue and of one PMP group. The peak at *m/z* 373 has been interpreted as a X_0 ion originating from cleavage of the C2-C3 bond followed by proton transfer and loss of H_2O. Fig. 3.7b shows the full-scan ESI spectrum of PMP-fucosyllactose. The ionic pattern somehow differs from that of Fig. 3.6b (FAB). For example, the peak observed at *m/z* 696 in the FAB spectrum and corresponding to loss of a fucosyl residue from $[M+Na]^+$ ions is small in the ESI spectrum and dominated by an ion peak at *m/z* 667, which indicates the preferential loss of a PMP residue from $[M+Na]^+$. The ESI spectrum of Fig. 3.7b, obtained at relatively high cone voltage (100 V), required 100 times less material (50 pmol) than the FAB spectrum, and the absence of matrix ions in ESI yielded a much cleaner spectrum. Fig. 3.7a and 3.7b show that Y-type cleavages from $[M+H]^+$ are readily produced by ESI, in the specific cone conditions used here. At a low cone voltage (40 V), $[M+H]^+$ ions dominated the spectra of all sugars investigated in this study, whereas higher values (100 V) favored the $[M+Na]^+$ ions. The additional ions created by increasing the cone voltage are mostly due to fragmentation of $[M+H]^+$, as suggested by MS/MS experiments on the latter (not shown here). Full-scan ESI mass spectra of a mixture of PMP-derivatives recorded at a cone voltage 45 V is shown in Fig. 3.8. The $[M+H]^+$ and $[M+Na]^+$ ions of PMP-derivatives labeled as such in Fig. 3.8 dominated the spectrum, and two abundant fragment ions at m/z 175 and 359 are

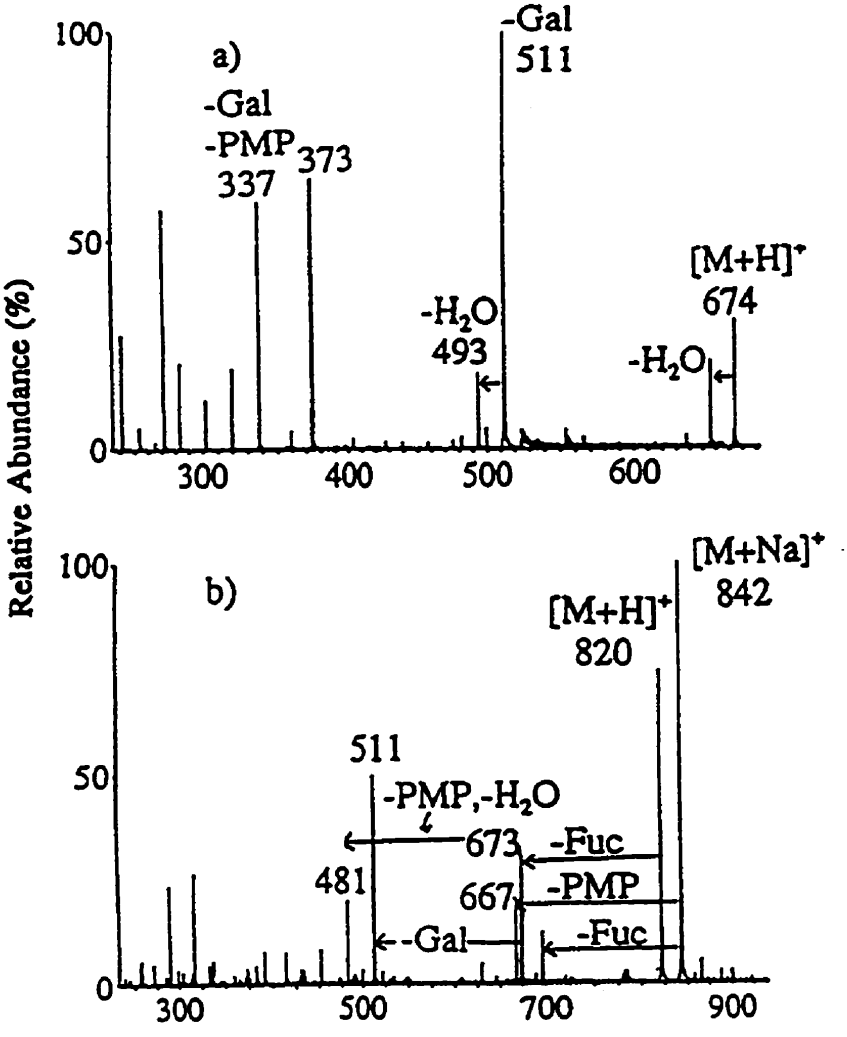

Fig. 3.7 a) Positive ESI-MS/MS spectrum of the $[M+H]^+$ ions of PMP-β-lactose. b) Full-scan ESI-MS spectrum of 2'-fucosyllactose. Details on conditions are given in Section 2.7.3.1.

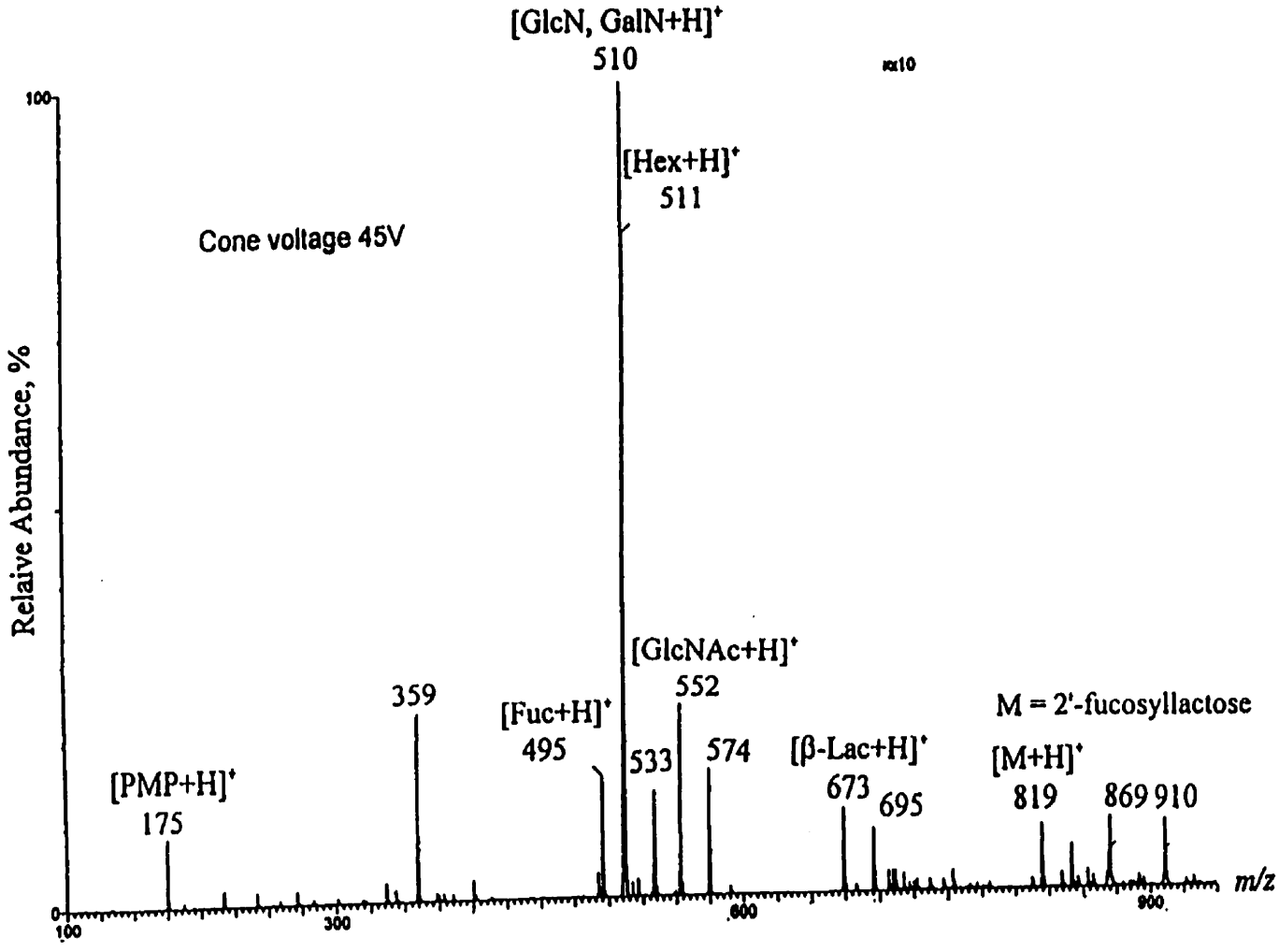

Fig. 3.8 Positive ESI mass spectrum of PMP-derivative mixture of small sugars at cone voltage 45 V. The amount of sample injected was one tenth of that used in Fig. 3.2.

observed. The former was attributed to protonated PMP, and the latter, which was also predominant in the FAB mass spectra shown in Fig. 3.5 and 3.6, has been explained in the text above. The peaks at m/z 510 (base peak) and 511 are present in high intensities since they were caused by superimposition of isomers of PMP-GlcN and GalN (*m/z* 510), and by the superimpostion of PMP-Man, Glc, and Gal (*m/z* 511). The peaks at m/z 869 and 910 could not be assigned here and might be fragment ions from PMP-sialyllactose. $[M+H]^+$ and $[M+Na]^+$ of PMP-sialyllactose are supposed to appear at m/z 966 and 988, respectively, but were not detected there.

Overall, sensitivity improvement of one order of magnitude was obtained by performing ESI-MS of PMP-derivatives rather than PA-derivatives. The signal to noise ratios observed with ESI were in general higher than those observed with FAB, although only 1% of the sample amount used for FAB was injected into the ESI source.

3) MALDI-MS of PMP-Derivatives of Small Sugars

The MALDI spectra of PMP-2'-fucosyllactose and sialyllactose are shown in Fig. 3.9a and 3.9b. These spectra show simpler patterns than FAB- and ESI spectra. For instance, two high peaks are observed at *m/z* 673 and 511 (Figure 3.9a) and correspond to the sequential losses of fucosyl and galactosyl residues from the non-reducing end of fucosyllactose. The ions due to loss of one PMP residue from either molecular or fragment ions are predominant in the MALDI (and ESI) spectra of the derivatives. The peak at *m/z* 568 (Fig. 3.9b) originates from trimers of the matrix. The ions at *m/z* 359 and 381 observed with FAB were mostly absent from MALDI spectra. The signal-to-noise ratios observed with MALDI were also higher than those obtained by FAB with the same

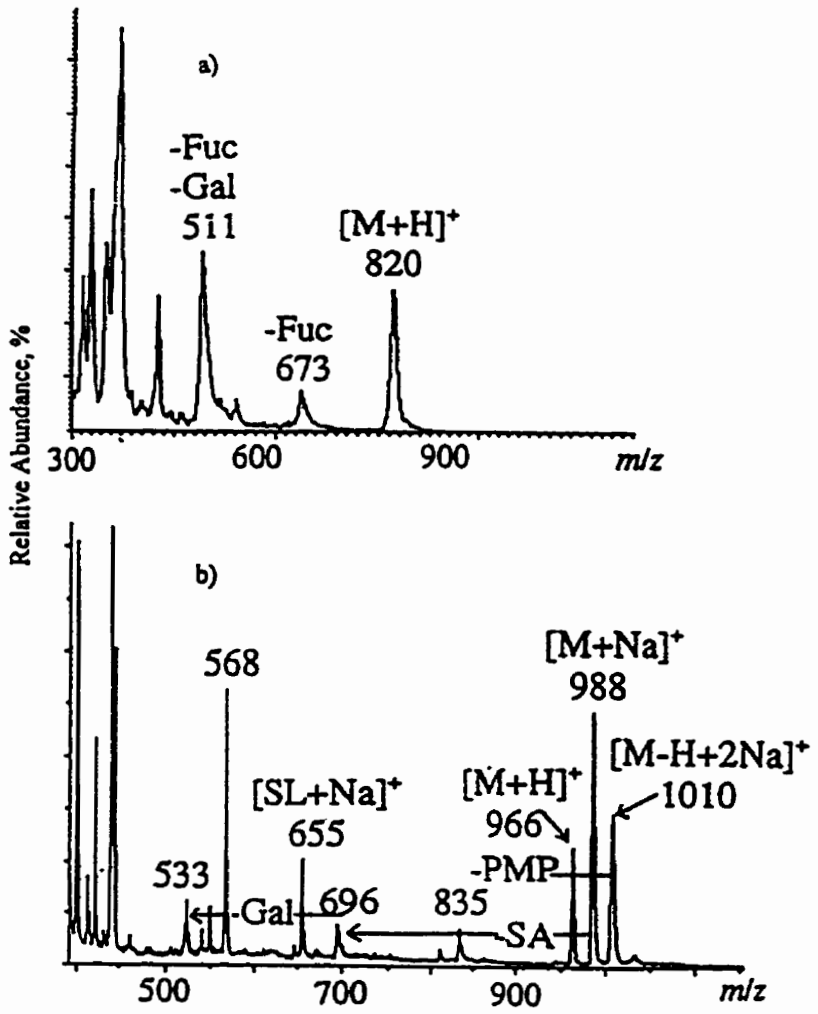

Fig. 3.9 Linear mode MALDI-TOF mass spectra of a) PMP-2'-fucosyllactose, b) PMP-sialyllactose. Details on conditions are given in Section 2.7.2.

amount of sample as used for ESI. The MALDI spectrum of PMP-fucosyllactose contains $[M+H]^+$ ions, and that of PMP-sialyllactose shows both $[M+H]^+$ and $[M+Na]^+$. This could be attributed to the affinity of the carboxyl group (in sialic acid residues) for sodium ions. Also, Lemoine and co-workers [45] showed that the extent of ionization by either protonation or addition of a sodium ion depends on which region of the sample spot, prepared with the dried-droplet method [92], is irradiated. Irradiation of the crystalline region at the edges of the sample spot tends to produce $[M+H]^+$ species, whereas desorption from the center of the spot (less crystalline, sometimes amorphous), yields $[M+Na]^+$ ions. Application of a more sophisticated sample preparation method may circumvent this discrimination [147,158].

Overall, a sensitivity improvement of one order of magnitude in MALDI was obtained by using the PMP-labeling method rather than preparing the PA-derivatives.

4) On-Line HPLC/ESI-MS of PMP-Derivatives of Small Sugars

On-line HPLC/ESI-MS experiments performed on a mixture of PMP-labeled small sugars produced better quality chromatograms and mass spectra than the on-line work achieved with the PA-mixture. Good chromatographic separation (similar to that obtained in Fig. 3.2) provided for almost unambiguous ESI spectra, with characteristics similar to those discussed above (e.g. Fig. 3.7 and 3.8).

The UV absorbance chromatogram and total ion current (TIC) chromatograms of 20 µL of PMP-derivative mixture (0.02 to 0.14 nmol/µL) are shown in Fig. 3.10. The correspondence of the UV chromatogram (Fig. 3.10a) to the TIC chromatograms (Fig. 3.10b and 3.10c) (the mass spectrometer's analog to the UV absorbance trace) was quite

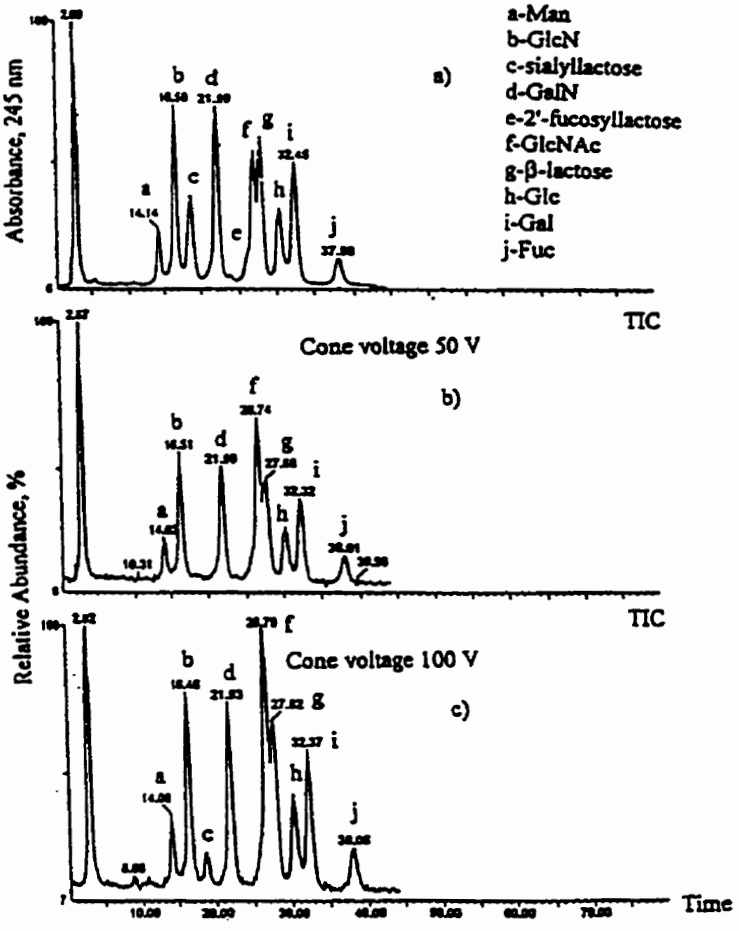

Fig. 3.10 a) Simultaneous UV absorbance chromatogram, b) TIC chromatogram at cone voltage 50 V, and c) TIC chromatogram at cone voltage 100 V of a mixture of PMP-derivatives observed during LC/ESI-MS. Approximately 20 µL of the sample was injected containing 0.14 nmol/µL each of PMP-D(+)-mannose, D(+)-galactose, D(+)-glucose, L(-)-fucose, β-lactose, D(+)-glucosamine, D(+)-galactosamine, (D+)-N-acetylglucosamine, 0.03 nmol/µL of 2'-fucosyllactose and 0.02 nmol/µL of sialyllactose using LC/ESI-MS mobile phase A and B as given in Section 2.7.3.2. HPLC gradient elution was performed as follows: 27 to 60% B over 55 min, then linearly to 100% over 25 min. Details on conditions are given in Section 2.7.3.2.

good, allowing reliable correlation of retention times with mass spectra. However, the peak appearing at a retention time of 18.54 min (which has been identified as PMP-sialyllactose) in the UV absorbance chromatogram is not observed in the TIC chromatogram recorded at a cone voltage of 50 V (Fig. 3.10b), and it appears very weakly in the TIC chromatogram recorded at a cone voltage of 100 V (Fig. 3.10c). These differences may be attributed to low ionization efficiency of this component: the presence of a sialic acid residue makes it more efficiently ionized in the negative ion mode because of deprotonation of the carboxyl group in sialic acid. At 100 V, it appears that a sufficient amount of $[M+Na]^+$ is formed, and allows observation of a chromatographic peak. The small differences in signal intensities between UV detection and TIC traces (Fig. 3.10) can be attributed to the specificity of each of the two detectors. The UV detector is sensitive to the number of chromophores present in the compounds while the mass spectrometer is sensitive to ionization efficiencies [159]. The mass spectral data were evaluated by correlating all UV peaks to mass spectral scan times in order not to miss any component which may produce a weak TIC response (the mass spectral data were acquired over a m/z 100-2000 range). Mass spectra were thus obtained by averaging all scans belonging to each individual PMP-compound on the TIC chromatogram. It was possible to obtain a mass spectrum for each individual component of the mixture except for PMP-2'-fucosyllactose and sialyllactose, due to incomplete resolution or low ionization efficiency. Also, compared with the other PMP-derivatives in the mixture, the initial concentrations of these two derivatives were lower. The spectra of PMP-β-lactose and PMP-Glc obtained from these HPLC/ESI-MS data are shown in Fig. 3.11 and 3.12. Both spectra

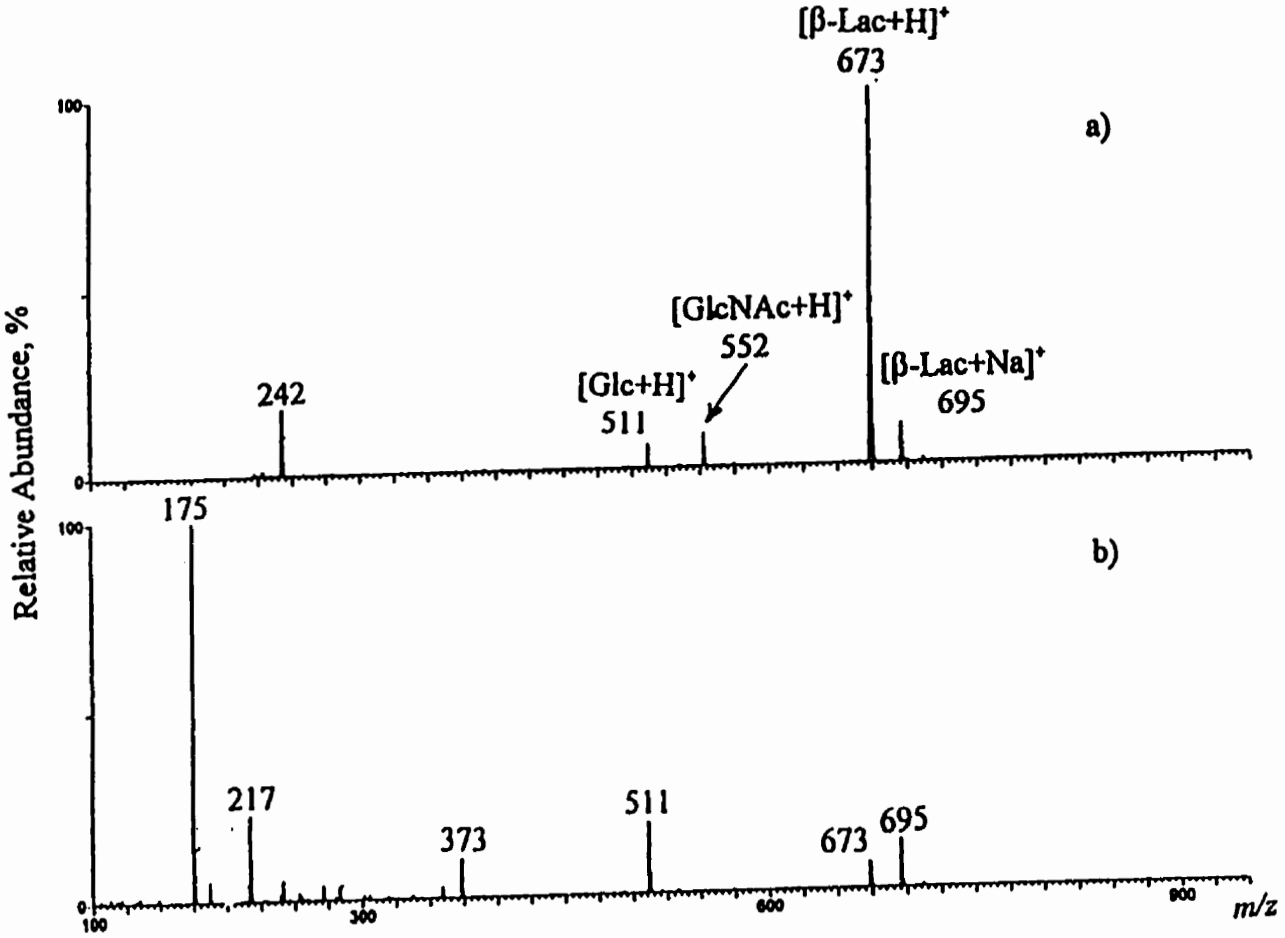

Fig. 3.11 Partial ESI mass spectrum of PMP-β-lactose: a) at cone voltage 50 V, b) at cone voltage 100 V. Spectrum is the average of scans 267-272 of the LC/ESI-MS shown in Fig. 3.10. See Fig. 10 for experimental details.

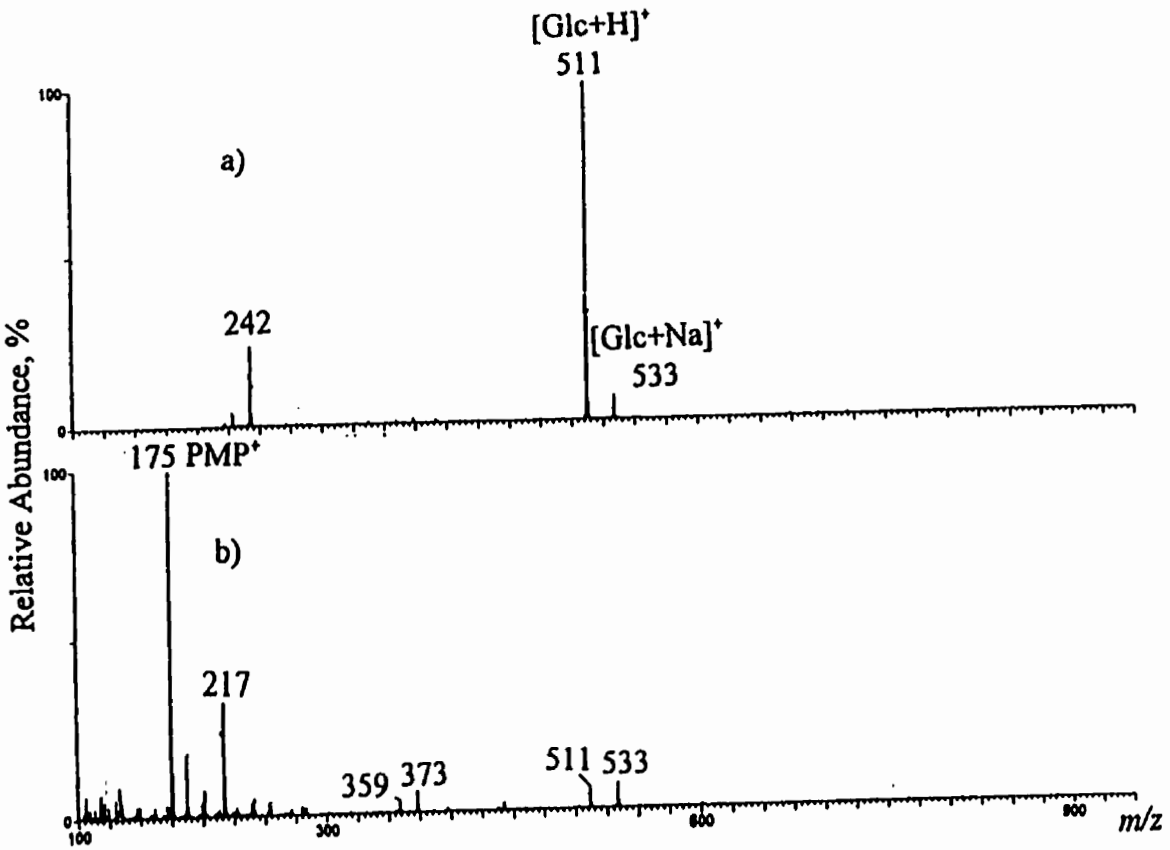

Fig. 3.12 Partial ESI mass spectrum of PMP-Glc: a) at cone voltage 50 V, b) at cone voltage 100 V. Spectrum is the average of scans 290-297 of the LC/ESI-MS shown in Fig. 3.10. See Fig. 3.10 for experimental details.

were obtained by averaging the scans acquired over their respective peaks. Fig. 3.11a shows the ESI mass spectra of PMP-β-lactose at cone voltage 50 V (a) and 100 V (b). The spectra are the sums of scans 267 to 272, corresponding to the peak labeled g in the TIC trace shown in Fig. 3.10. Fig. 3.12 shows the ESI mass spectra of PMP-Glc at cone voltage 50 V (a) and 100 (b), which are the sums of scans 290 to 297, corresponding to the peak labeled h in the TIC trace shown in Fig. 3.10. These data easily indicated which peaks in the TIC trace corresponded to the *m/z* values of expected structures. However, at this stage, this technique can not distinguish between the isobaric components such as PMP-Glc, Man, and Gal or PMP-GlcN and GalN. Therefore the assignments of these isomers was possible only from a study of their retention times (re: Fig. 3.2).

Comparing Fig. 3.11a with 3.11b and Fig. 3.12a with Fig. 3.12b, it can be seen that at low cone voltage (50V), the predominant ions are $[M+H]^+$, for example the peak at m/z 673 for PMP-β-lactose and 511 for PMP-Glc. Some fragment ions due to glycosidic cleavage (Y-ions) are also present, such as the peak at m/z 511 in Fig. 3.11a. At high cone voltage (100 V), $[M+H]^+$ ions were more dissociated and more abundant fragment ions were present, with the peak at m/z 175 as the base peak corresponding to protonated PMP. On the other hand, the sodiated molecular ions dominated the spectra without noticeble fragmentation (3.11b and 3.12b). This indicates that protonated molecular ions of PMP-derivatives are not stable at high cone voltage, and therefore fragment easily, whereas the sodiated molecular ions are more stable at high cone voltage and are not readily fragmented. This difference is highlighted by comparing the abundance of m/z 695 ions in Fig. 3.11b and Fig. 3.11a, or by comparing the abundance of *m/z* 533 ions in

Fig. 3.12b and Fig. 3.12a.

Our results indicate that on-line coupling of HPLC with MS is rapid and simple. A key advantage of this method is that it provides instantaneous identification of coeluting components. Even if the separation is incomplete, the MS can identify and quantify the compounds of interest. The molecular mass of each component in the mixture can be measured and the further study on structure of each compound can be carried out by MS/MS. This method is especially useful for analyzing a mixture, for example, that of glycans cleaved from a glycoprotein. HPLC and MS complement each other, i.e., if it is difficult to separate the mixture by HPLC and coelution occurs, LC/MS and/or LC-MS/MS can help overcome the problem and make it possible to determine the structures of the coeluting components.

3.2 ESI-MS of Native and PMP-Tetraglucose: Sensitivity Study as a Benchmark for Other Native and PMP-Oligosaccharides

Aqueous solutions of native and PMP-tetraglucose of different concentrations (10^{-3}, 10^{-5}, 10^{-6}, 10^{-7}, and 10^{-8} M) were prepared. Tetraglucose was used as a model compound to assess the ESI-MS sensitivity toward native and PMP-oligosaccharides. Also, it was of interest to study the behaviour and fragmentation of these compounds under ESI-MS and CID-MS/MS conditions. Fig. 3.13 shows the structure of PMP-tetraglucose and indicates some fragmentation pathways characteristic of PMP-oligosaccharides.

3.2.1 Conventional Full-Scan ESI-MS of Native and PMP-Tetraglucose

The full-scan positive and negative ion mass spectra of PMP-tetraglucose are

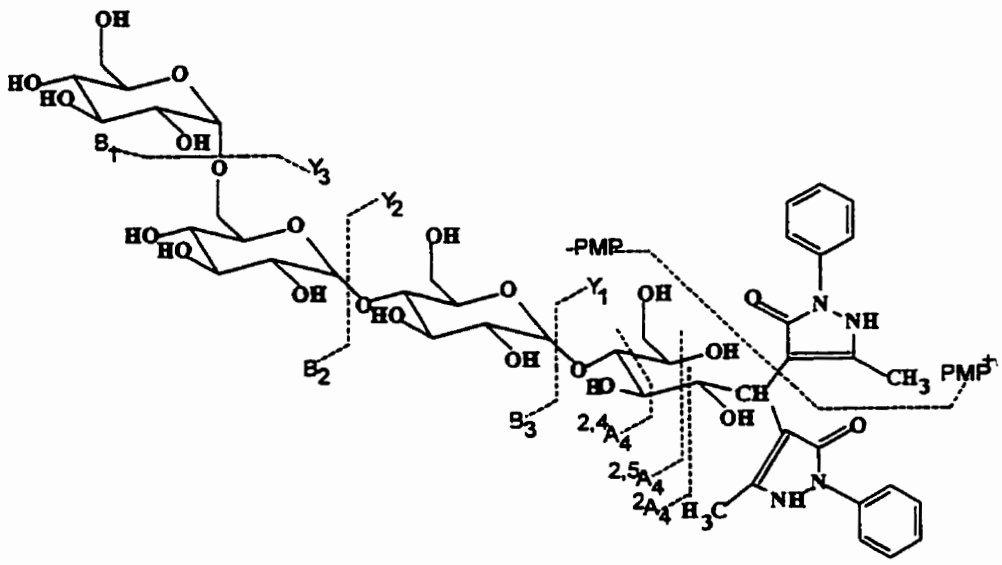

Fig. 3.13 Structure of the PMP derivative of tetraglucose.

shown in Fig. 3.14, displaying different characteristics. In each case, 20 μL of a 10^{-5} M solution were injected (200 pmol), and 20 scans were averaged. The 20 μL injections and averaging of 20 scans remained consistent throughout the study. In the positive ion spectrum (Fig. 3.14a), the base peak at *m/z* 997 comes from $[M+H]^+$, whereas corresponding $[M+Na]^+$ ions appear at *m/z* 1019 with lower abundance. Abundant ions at *m/z* 823 and 845 are attributed to the loss of one PMP from the $[M+H]^+$ and $[M+Na]^+$ ions. Other fragment ions are of the Y-types, such as at *m/z* 835, 673, and 511 coming from $[M+H]^+$ ions, as well as 857, 695, and 533, from $[M+Na]^+$ with lower abundance. This sequential loss of 162 u was expected, since the structure of tetraglucose is linear and consists of four glucose units. All fragments contain the reducing end of tetraglucose and gradually decrease in abundance from low to high mass. A noticeable peak at *m/z* 689 corresponds to the $[M+Na]^+$ ions of native tetraglucose. The presence of native sugar will be discussed further in the text.

The negative ion spectrum (Fig. 3.14b) is dominated with $[M-H]^-$ ions at *m/z* 995 and the ions resulting from loss of one PMP residue (base peak) at *m/z* 821. In contrast to the positive ion spectrum, several fragment ions containing the non-reducing end are observed as reported earlier by Honda and co-workers [57]. The peak at *m/z* 701 is attributed to a chloride adduct, $[B_4+H_2O+Cl]^-$. It could also be due in part to adduction of chloride on native tetraglucose $[M+Cl]^-$. The signal appearing at *m/z* 503 corresponds to C_3 fragments. In addition, a few fragment ions from cross-ring cleavages are observed. The peaks at *m/z* 545, 587, and 605 have been attributed to $^{2,4}A_4$, $^{2,5}A_4$ and $^{0,2}A_4$ fragments, respectively. The observation of these ions suggests that the opening of the reducing

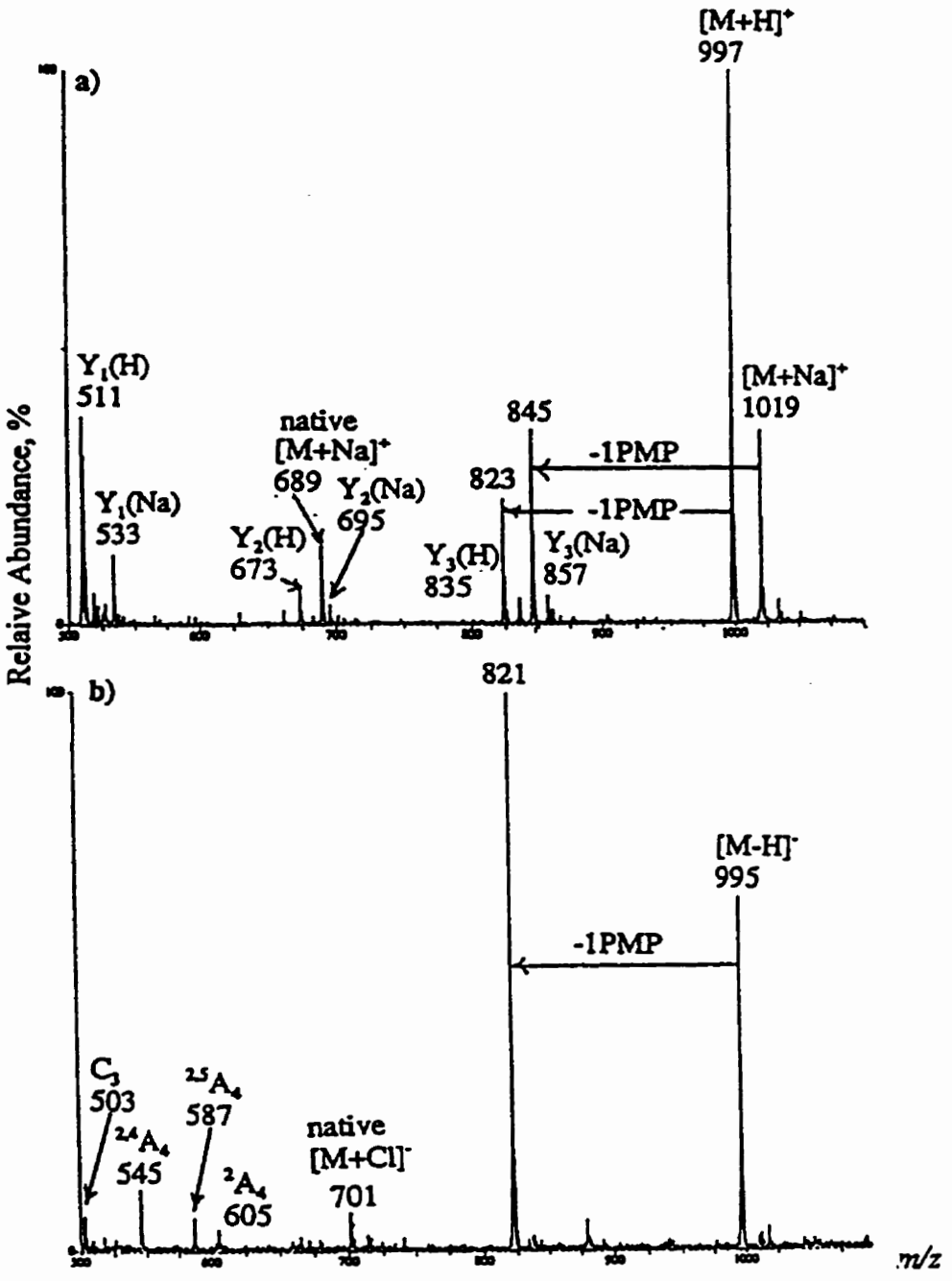

Fig. 3.14 Full-scan ESI mass spectra of PMP-tetroglucose: a) positive ion mode, b) negative ion mode.

glucose through tagging enhances its fragmentation in the negative mode. Even if the spectrum of Fig.3.14a provides more interpretable sequence information than its negative analog, both ionization modes complement each other, as very different types of ions are obtained from one spectrum to the other.

In both Figures 3.14a and b, there are peaks associated with native tetraglucose. The presence of native material indicates that much precaution must be taken when derivatizing sugars, since in this case a portion of the material has not been transformed into the PMP compound. This phenomenon was not observed for the small sugars, which could indicate that the yield of PMP-derivatives is higher for small sugars than for larger oligosaccharides. We have estimated a 10-fold increase in sensitivity of molecular ion signal with PMP- vs. native sugars, and therefore the sample used to generate Fig. 3.14a may have contained equal amounts of derivatized and underivatized material. Out of many cases of preparing PMP-labeled carbohydrates, very rare are the cases where native material was left unreacted.

For comparison, the positive and negative full-scan ion spectra of native tetraglucose are shown in Fig. 3.15. The positive ion spectrum (Fig. 3.15a) shows abundant $[M+Na]^+$ and $[M+K]^+$ ions, whereas sequence-related ions are generally absent, except for C_2 (or Y_2) species at *m/z* 365, which result from loss of two glucose units from $[M+Na]^+$. It has been reported that sugar chains in the positive ion mode are often ionized by formation of sodium or potassium adducts rather than by protonation [89]. The signal at *m/z* 161 could result from B_1 cleavage followed by loss of H_2, and the peaks at *m/z* 517 and 230 can not be assigned.

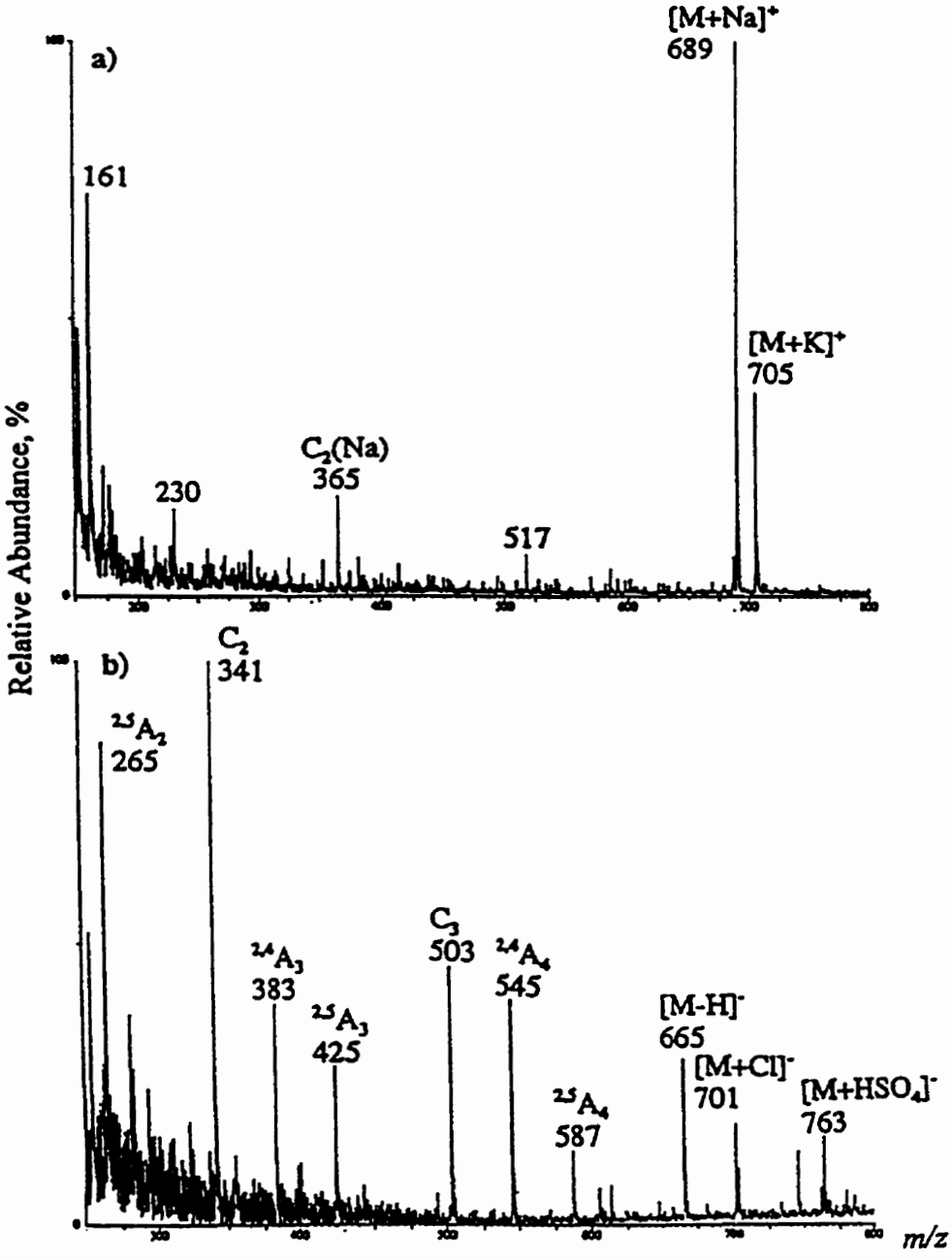

Fig. 3.15 Full-scan ESI mass spectra of native tetraglucose: a) positive ion mode, b) negative ion mode.

Unlike the positive ion spectrum, the negative ion spectrum of native tetraglucose (Fig.3.15b) not only gives molecular ions, but also sequence-related fragment ions. The $[M-H]^-$ ions at *m/z* 665 are accompanied by $[M+Cl]^-$, $[M+HSO_4-H_2O]^-$ and $[M+HSO_4]^-$ ions at *m/z* 701, 745 and 763, respectively, due to contamination. Signals at *m/z* 503 and 341 arise from the sequential loss of one and two glucose units from $[M-H]^-$ due to glycosidic cleavages. They could correspond to either C_3, C_2 (as assigned) or Y_3, Y_2. The peaks at m/z 587, 545, 425, 383 and 265 are non-reducing end fragment ions and are assigned to $^{2,5}A_4$, $^{2,4}A_4$, $^{2,5}A_3$, $^{2,4}A_3$ and $^{2,5}A_2$ due to cross-ring cleavages. Here again, each spectrum is complementary to the other. With this particular sample, molecular mass information is better obtained in the positive mode, whereas the negative mode provides more structural information.

The sensitivity of positive and negative ion full-scan ESI-MS toward native and PMP-tetraglucose was investigated next. Solutions with concentrations ranging from 10^{-3} to 10^{-7} M, starting with 10^{-3} M solutions were injected into the mass spectrometer. Fig. 3.16a and 3.16b show the results obtained for 10^{-6} M solutions of both PMP- and native tetraglucose. In the positve mode, the detection limit for PMP-tetraglucose was 2 pmol: A 20 µL of a 10^{-7} M solution yielded a 5.5/1 S/N ratio for $[M+H]^+$ ions. However, at 10^{-7} M, only $[M+H]^+$ ions were identifiable and no structural information was available (not shown). For native tetraglucose, the detection limit is 20 pmol under the same conditions (Fig. 3.16b): 20 µL of a 10^{-6} M solution produced a 4/1 S/N ratio for $[M+Na]^+$ ions.

In the negative ion mode, 20 pmol (20 µL of a 10^{-6} M solution) was the lowest

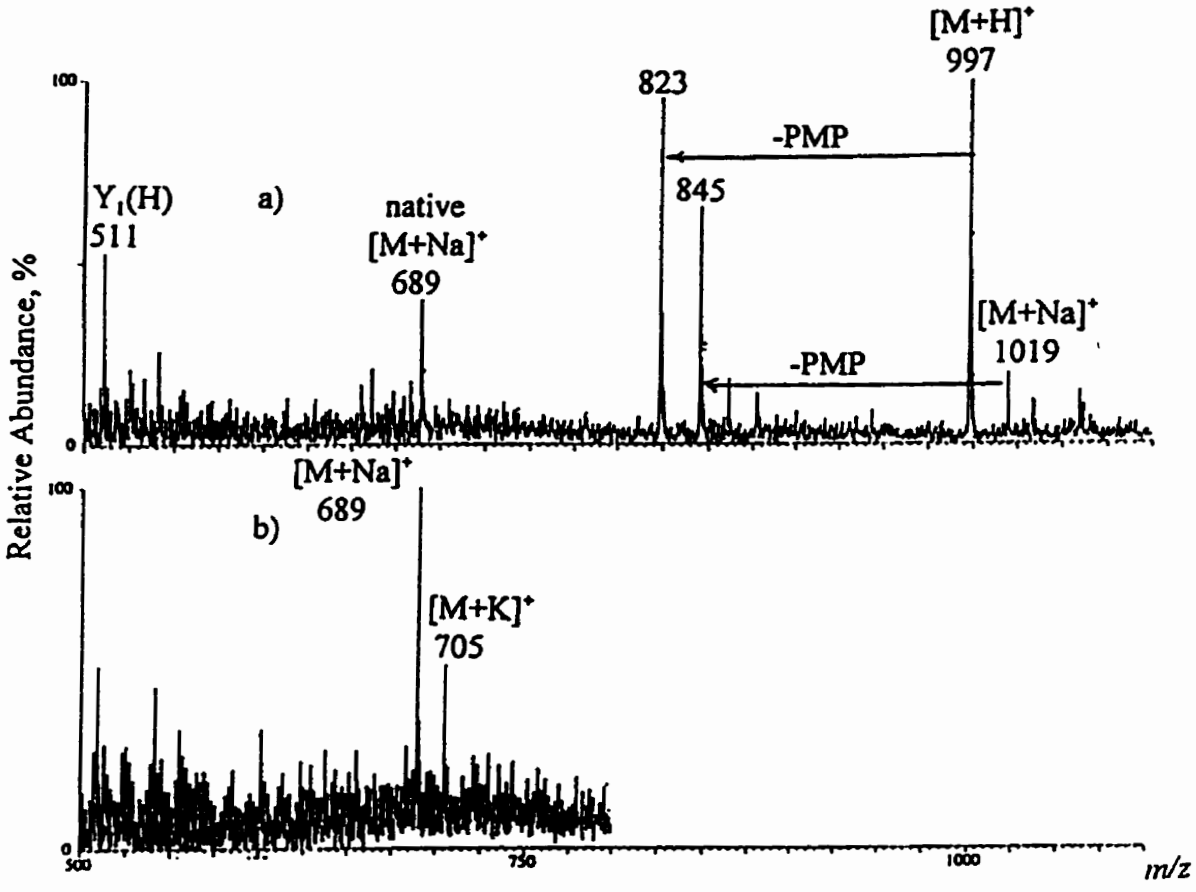

Fig. 3.16 Sensitivity of positive ion ESI for a) PMP-tetraglucose and b) native tetraglucose. Spectra obtained with 10^{-6} M solutions. For each spectrum, 20 scans were accumulated.

quantity detectable for both PMP- and native tetraglucose as shown in Fig. 3.17a and b. However, at this concentration level, the PMP-derivative yields a S/N ratio of 16/1 for $[M-H]^-$ ions, while the native compound yields a S/N ratio of only 2/1 for $[M-H]^-$ ions.

These results indicate that positive mode ESI of PMP- derivatives should be used to enhance sensitivity. As well, Fig. 3.14 shows that these derivatives are able to produce information on the sugar sequence, which is useful in situations where MS/MS is not available.

The positive and negative spectra obtained for PMP-tetraglucose all showed abundant ions corresponding to the molecular species having lost one PMP-moiety. As it became unclear whether the PMP unit was lost as a result of fragmentation in the ion source or occurred prior to mass spectral analysis, the origin of the $[M+H-PMP]^+$ and $[M-H-PMP]^-$ ions was investigated by varying the cone voltage. If the loss of PMP becomes more extensive at higher cone voltages, it is a good indication that the loss occurs in the ion source. Fig. 3.18 and 3.19 show the effect of varying the cone voltage on the abundances of molecular and fragment ions. By increasing the cone voltage from 50 V to 80 V in the positive ion mode (Fig. 3.18), the abundance ratio of the $[M+H]^+$ ion peak (at *m/z* 997) to the $[M+H-PMP]^+$ fragment ion peak (at *m/z* 823) is almost unchanged, and the same is observed for the corresponding sodiated ions (the peaks at *m/z* 1019 and 845, respectively). In contrast, in the negative ion mode (Fig. 3.19), by changing the cone voltage from 15 V to 90 V, the ratio of the abundances of $[M-H]^-$ to $[M-PMP-H]^-$ decreases from 5.0 to 0.35. These results indicate that higher cone voltages favour fragmentation of molecular ions by loss of one PMP unit in the negative ion mode only,

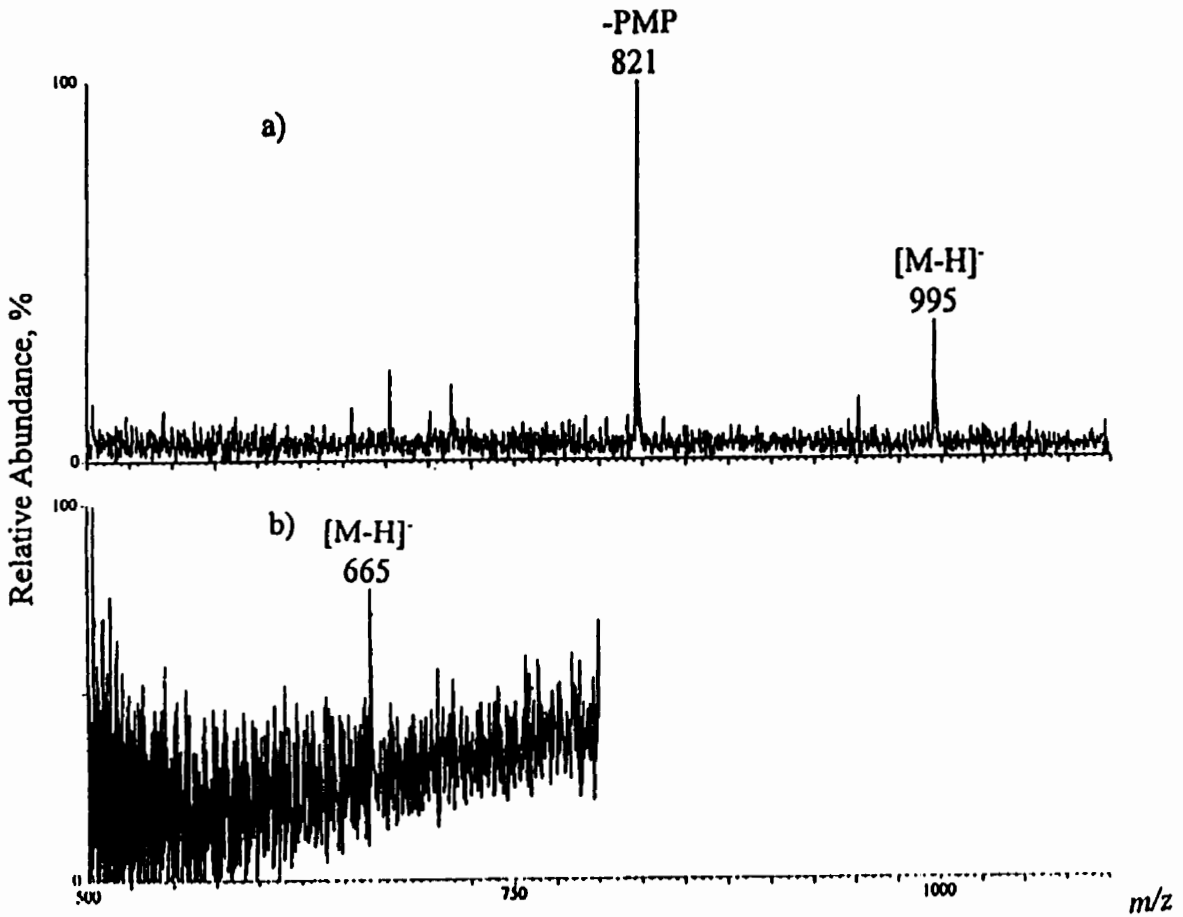

Fig. 3.17 Sensitivity of negative ion ESI for a) PMP-tetraglucose and b) native tetraglucose. Spectrum obtained with 10^{-6} M solutions.

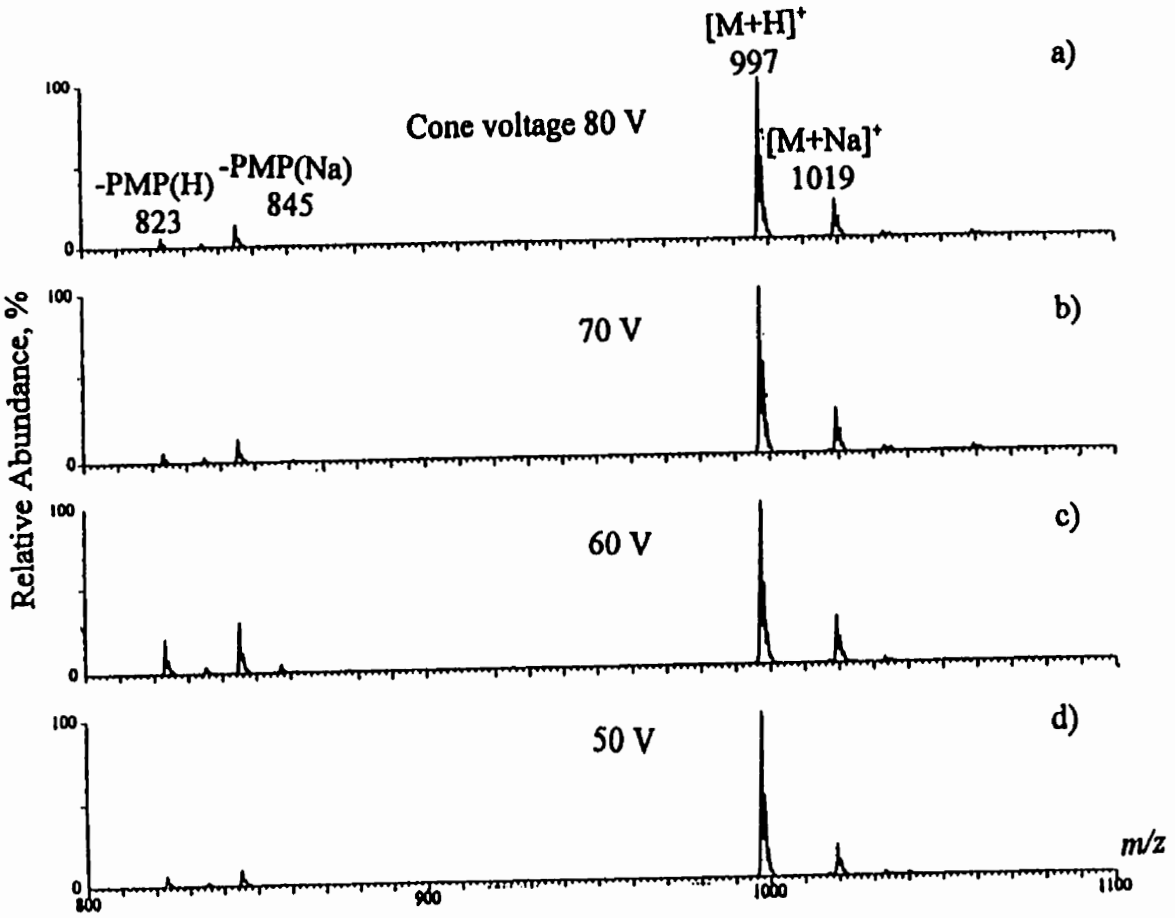

Fig. 3.18 Effect of changing the cone voltage on the dissociation of PMP-tetraglucose in the positive ion mode: a) at cone voltage 80 V, b) 70 V, c) 60 V, d) 50 V.

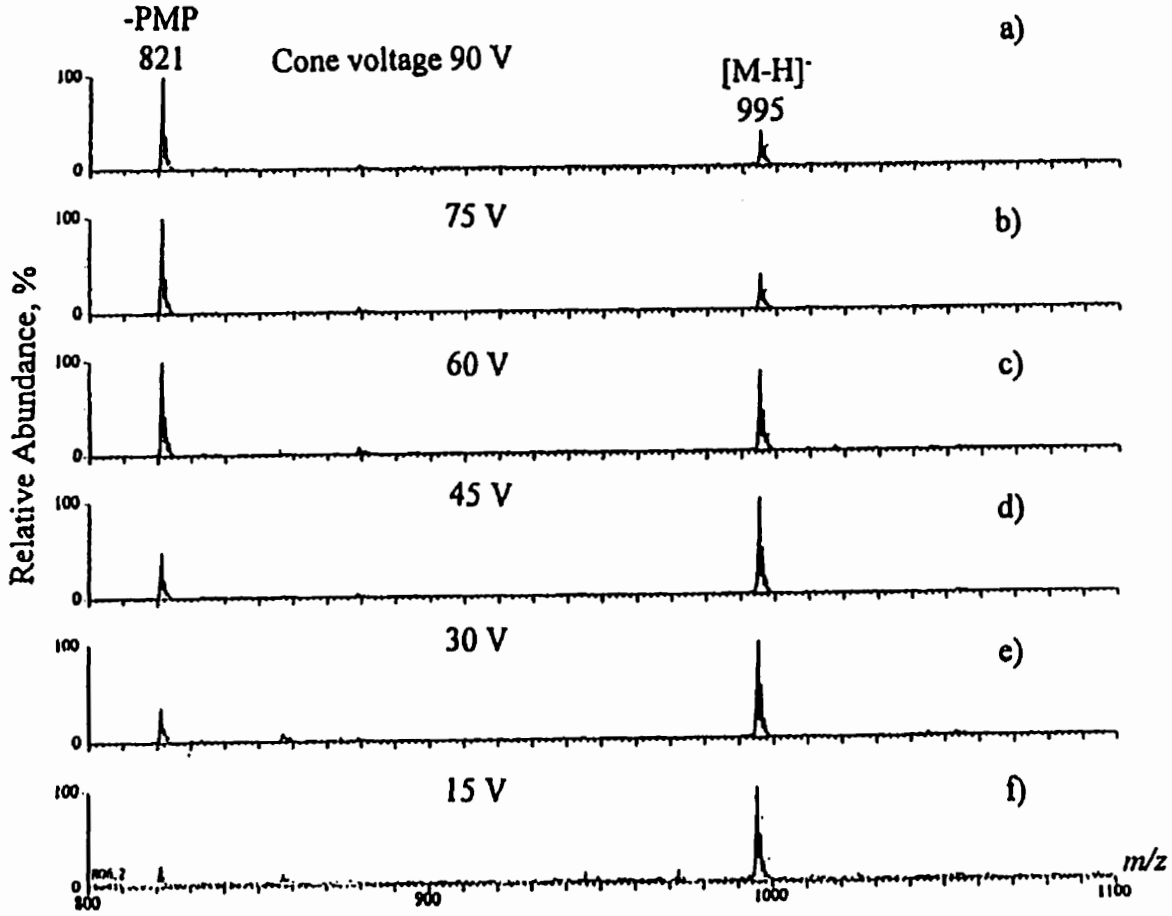

Fig. 3.19 Effect of changing the cone voltage on the dissociation of PMP-tetraglucose in the negative ion mode: a) at cone voltage 90 V, b) 75 V, c) 60 V, d) 45 V, e) 30 V, f) 15 V.

whereas they have no effect at all on the positive ion spectra. The variation of the relative ionic abundances between $[M-H]^-$ and $[M-H-PMP]^-$ seems to indicate in-source fragmentation by loss of one PMP. However, results obtained in the positive ion mode do not show this trend and rather indicate that loss of PMP had already occurred prior to mass spectral analysis. It is safe to assume that PMP loss is partly due to in-source fragmentation, and partly due to degradation prior to analysis.

3.2.2 ESI-CID-MS/MS of Native and PMP-Tetraglucose

In order to evaluate the usefulness of sequence information obtained by CID-MS/MS, the protonated and deprotonated molecular ions of PMP-tetraglucose at *m/z* 997 and 995 were selected as the precursor ions for positive and negative ion ESI-CID-MS/MS, respectively.

The daughter ion spectrum of the $[M+H]^+$ ions of PMP-tetraglucose (Fig. 3.20a) is much like that of the $[M+H]^+$ ions of β-lactose (Fig. 3.7a). Mainly Y-type sequence ions are observed due to cleavages of glycosidic bonds. Fragment ions at *m/z* 835, 673, and 511 were consistent with the successive loss of glucose units from the molecule, the positive charge always being retained at the reducing end. The ions at *m/z* 337 correspond to loss of a PMP residue from those at *m/z* 511. The signal at *m/z* 823 is due to the loss of one PMP from the precursor ions. The peak at *m/z* 217 could be due to further fragmentation of the ions at *m/z* 337 by a loss of 120 u. The absence of B_4 fragment ions from the CID-MS/MS spectrum confirms that the peak at *m/z* 689 in Fig. 3.14a is due to native tetraglucose left unreacted during derivatization.

In comparison, the product ion spectrum of the $[M-H]^-$ ion of PMP-tetraglucose

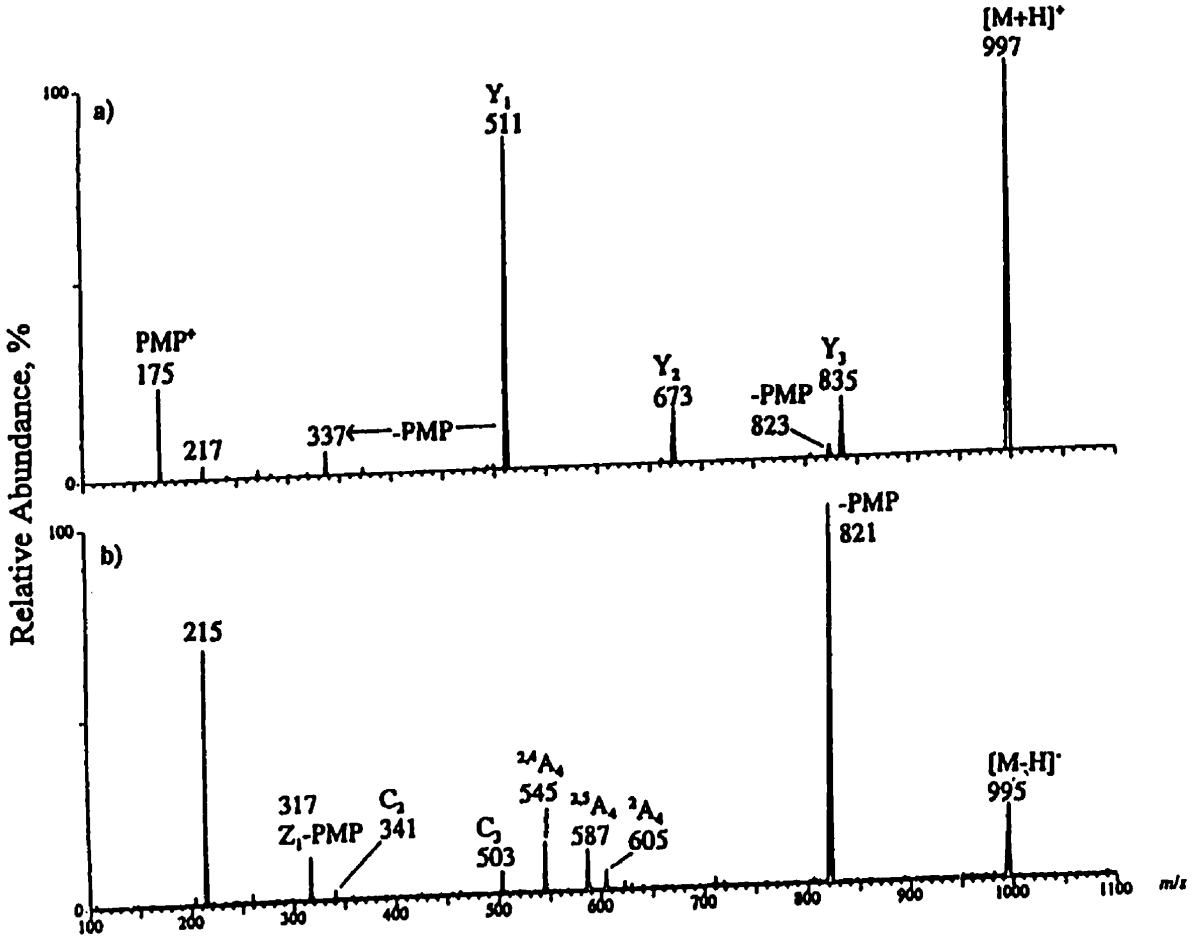

Fig. 3.20 ESI-CID-MS/MS spectra of molecular ions of PMP-tetraglucose: a) $[M+H]^+$ at *m/z* 997, b) $[M-H]^-$ at *m/z* 995.

(Fig. 3.20b) contains very little information related to the sugar sequence. Ions related to cleavage of the open sugar ring next to the PMP groups (A-type) are observed, as well as C_2 and C_3 ions. The spectra of Fig. 3.20 are qualitatively very similar to those of Fig. 3.14 indicating that in-source fragmentation in the full-scan mode may yield as much information as MS/MS, given that clean samples of individual sugars are available. The full-scan and MS/MS results on PMP-tetraglucose show that positive mode ESI will yield M_r and sequence information quickly, whereas negative mode ESI can be used to confirm a proposed structure or to obtain more details regarding linkage positions, owing to observation of A-type ions.

The daughter ion spectra of the $[M+Na]^+$ ions (*m/z* 689) of native tetraglucose are shown in Fig. 3.21. In contrast to full-scan positive ion ESI-MS, there are here abundant sequence-related fragments. The spectrum (Fig. 3.21a), obtained using 20 nmol of material, is dominated by Y- and Z-type ions spaced by increments of one hexose residue. Each of these ions contains sodium, and could also be fragments containing the non-reducing end of the sugar (B- and C-types). The low abundance ions originating from a ring cleavage are present at *m/z* 629, 467, and 305 arising from a loss of 60 u from $[M+Na]^+$ and Y-ions [160]. In contrast, Duffin et al. [43] reported that CID-MS/MS product ion spectra of $[M+Na]^+$ ions of oligosaccharides lacked the presence of structurally-significant fragment ions. In their case, even at high collision energies relative to ours (100 eV vs. 60 eV), the abundances of product ions were low relative to the parent ions, resulting in poor signal-to-noise ratio.

The daughter-ion spectra of the $[M-H]^-$ ions of the native tetraglucose (Fig. 3.22)

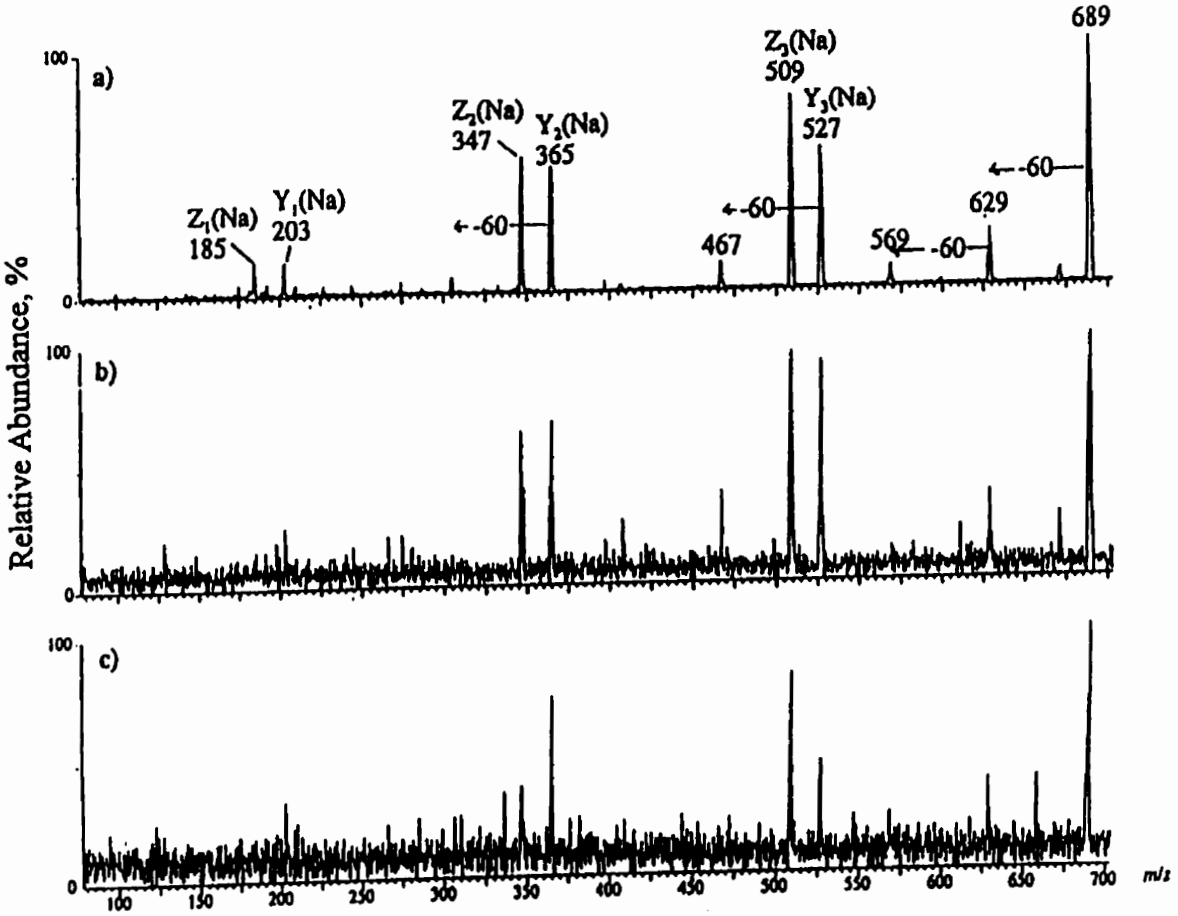

Fig. 3.21 ESI-CID-MS/MS spectra of $[M+Na]^+$ ions of native tetraglucose, at *m/z* 689: at concentrations of a) 10^{-3} M, b) 10^{-5} M, c) 10^{-6} M.

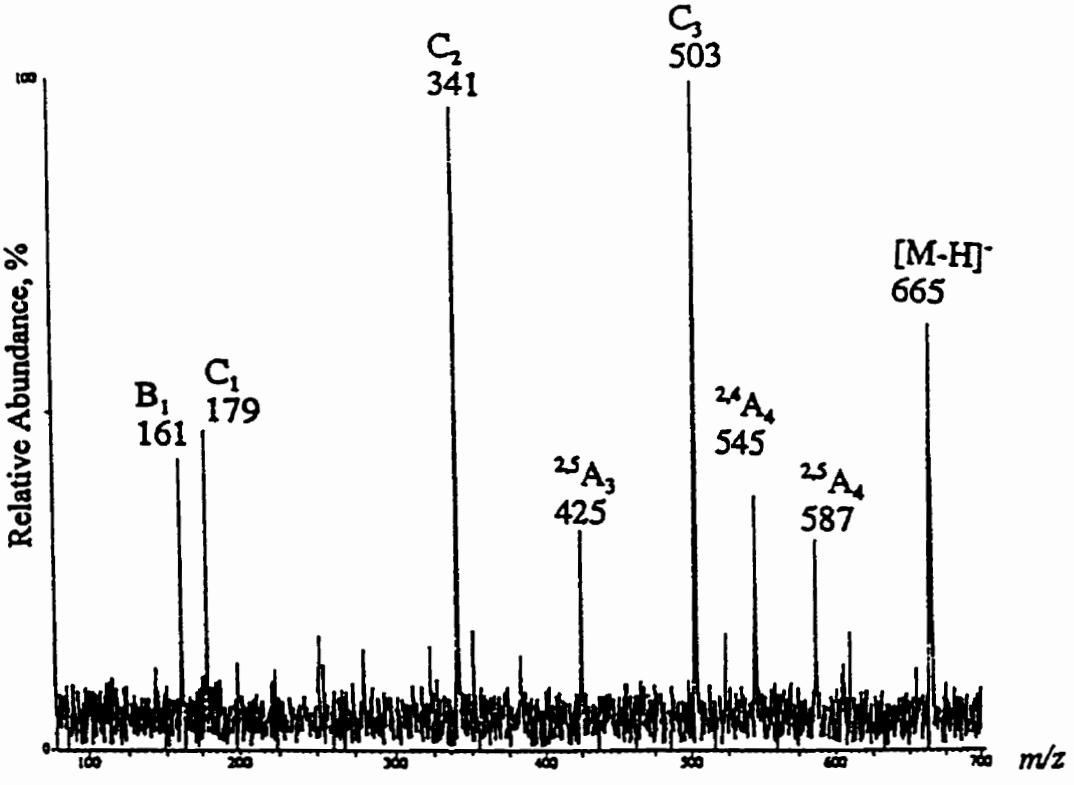

Fig. 3.22 ESI-CID-MS/MS spectrum of $[M-H]^-$ ions of native tetraglucose, at *m/z* 665, recorded at a concentration of 10^{-3} M.

is similar to the full-scan spectrum shown in Fig. 3.15b, except for $[M+Cl]^-$, $[M+HSO_4-H_2O]^-$, and $[M+HSO4]^-$ ions, which are absent from the MS/MS spectrum. In the negative ion mode, Fig. 3.14b, 3.15b, 3.20b and 3.22 show that more easily interpretable structural information can be obtained from the spectra of the native compound than those of the PMP-derivative.

Experiments were carried out next to determine the minimum amounts of native and PMP-tetraglucose required to obtain informative sequence ions in positive ion ESI-CID-MS/MS. Minimal amounts of 200 pmol and 20 pmol, respectively, were required for native and PMP-tetraglucose to obtain diagnostic sequence information as shown in Fig. 3.21b and Fig. 3.23c.

The results obtained for native and PMP-tetraglucose constitute a good basis for studying neutral sugars, i.e., sensitivity and amount of information obtained from ESI-MS and ESI-CID-MS/MS analysis would probably be similar for other neutral oligosaccharides. Overall, positive mode ESI of the PMP-derivative produced the best results, from both qualitative and quantitative points of view. However, sugars containing GlcNAc or GalNAc would be expected to have lower detection limits in the positive mode and higher detection limits in the negative mode than their neutral analogs. Also, the presence of acetylamino groups is known to promote B-type fragmentations in the positive mode, while mainly Y-type species are formed with PMP-tetraglucose. On the other hand, sialylated oligosaccharides in their native form are expected to be better suited for negative ion analysis than neutral sugars.

3.3 Application to Larger Oligosaccharides

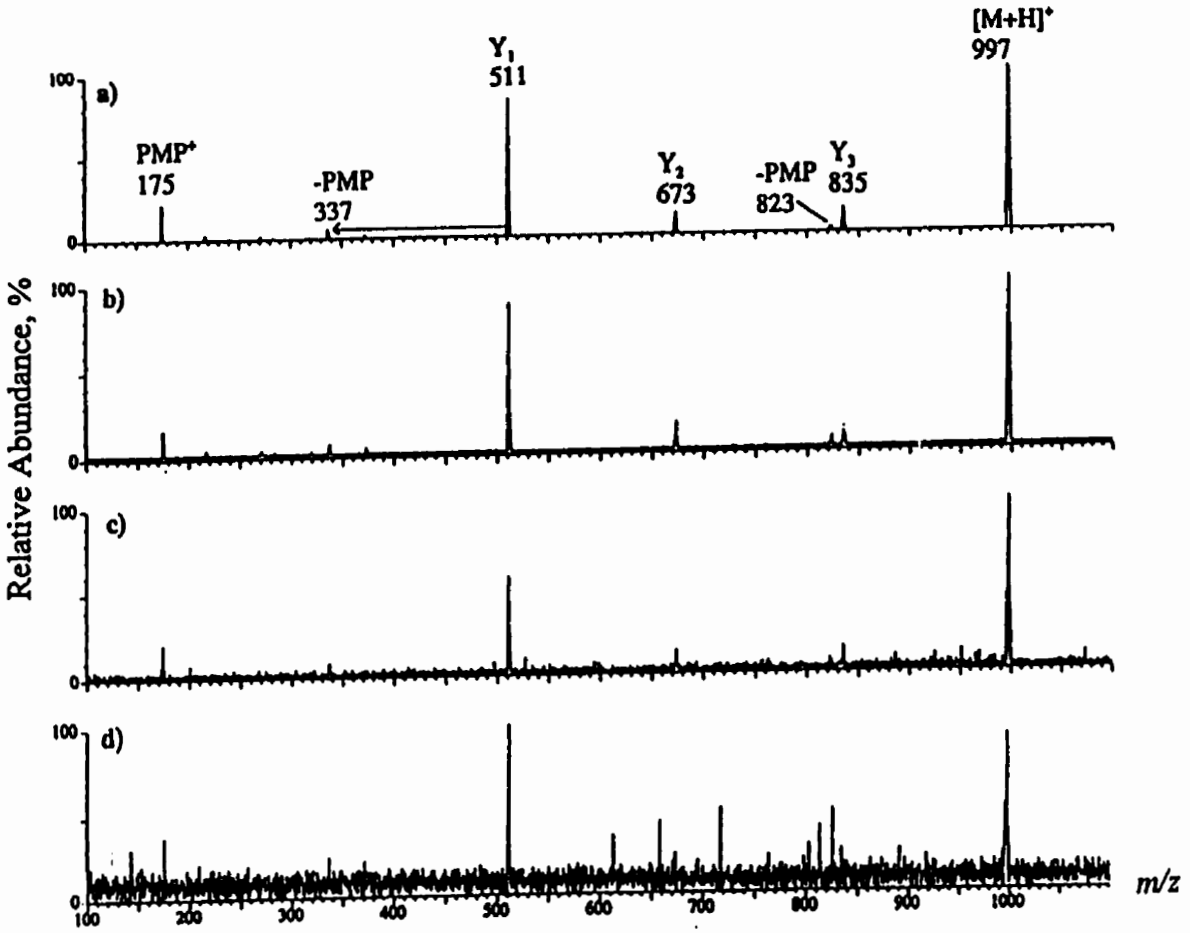

Fig. 3.23 ESI-CID-MS/MS spectra of $[M+H]^+$ ions of PMP-tetraglucose, at *m/z* 997: at concentrations of a) 10^{-3} M, b) 10^{-5} M, c) at 10^{-6} M, d) at 10^{-7} M.

So far, our results have indicated that: i) PMP-derivatives are more readily separable by HPLC than PA-compounds; ii) our FAB-MS system does not offer sufficient sensitivity for analysis of nanomolar quantities of sugars with $M_r > 800$; iii) MALDI or ESI are more suitable than FAB for higher M_r oligosaccharides on smaller amounts of material; iv) the PMP-derivatives yield an at least 10-fold sensitivity improvement over PA-compounds under ESI and MALDI conditions; and v) easily interpreted sequence information is available from the positive ion ESI-MS spectra of PMP-tetragucose, either with or without using CID. Prior to examining the derivatized mixture of glycans cleaved from ovalbumin, the present study was extended to well-characterized N-linked oligosaccharides obtained commercially, since they are more representative of glycans from glycoproteins than tetraglucose.

Three oligosaccharide standards, M3N2, NGA3, and NGA4, were thus labeled with PA and PMP. The structures of these three sugars are shown in Fig. 3.24. The PA-derivatives were centrifuge-evaporated several times after addition of 0.5 mL of distilled water in order to remove ammonium acetate, which was used to neutralize acetic acid after the derivatization step. Vacuum centrifugation spins the tubes under vacuum to evaporate solvent while continuously forcing the remaining solution to stay at the bottom of the tube. This method has the advantage of concentrating the sample to a small area at the bottom of the tube rather than drying it over a larger surface area, as occurs with evaporation under a stream of inert gas. It also eliminates "bumping " during evaporation [99]. Ammonium acetate is volatile enough to be partly removed in this way [48]. The presence of the salt would otherwise yield unsatisfactory results for MS analysis, as

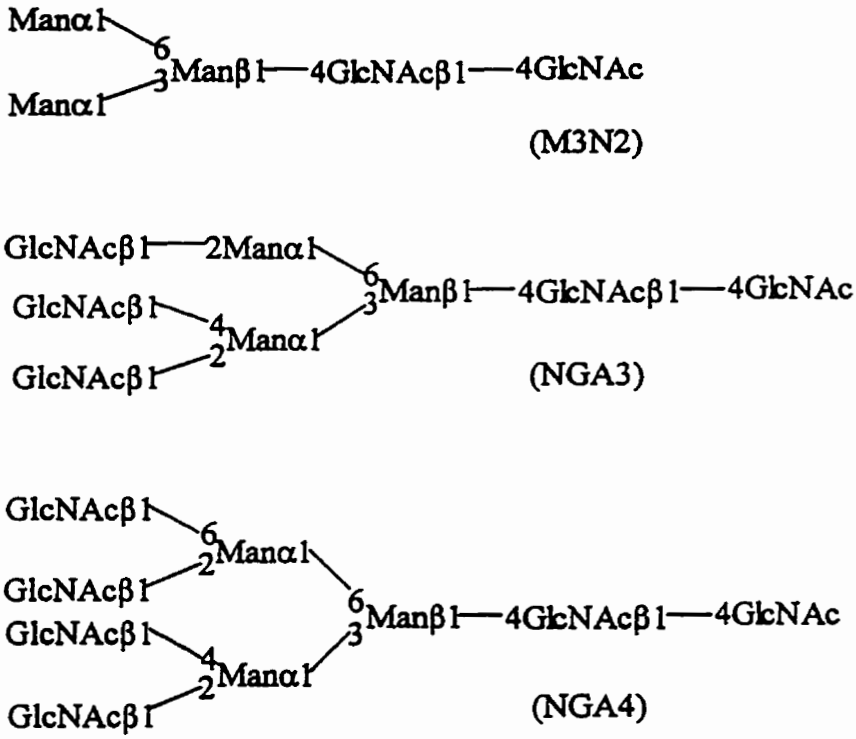

Fig. 3.24 Structures of standard oligosaccharides obtained commercially. The carbohydrate structures are drawn to reproduce the structures supplied with these commercial oligosaccharide standards.

explained below. It has been reported that addition of salts, including ammonium acetate, can significantly enhance the positive-ion sensitivity for native oligosaccharides [43]. However, the present study has demonstrated that the presence of ammonium acetate had an adverse effect. This may be due to much higher concentrations of ammonium acetate in our sample than that mentioned in that report (0.1 mM) [43]. On the other hand, the presence of salts is not as suitable for MS of PA-derivatives as much as it is for native sugars.

3.3.1 PA-Derivatives of Larger Oligosaccharides by ESI-MS

After evaporation, the PA-derivatives were reconstituted and subjected to ESI-MS. The positive ion ESI mass spectra of PA-M3N2 and NGA3 are shown in Fig. 3.25a and b. In the case of PA-M3N2 (Fig. 25a), prominent $[M+H]^+$ ions at *m/z* 990 are observed, and the $[M+Na]^+$ ions appear as an intense signal at *m/z* 1012. Losses of one, two, and three mannose residues from $[M+H]^+$ ions produce Y-type fragment ions of low abundance at *m/z* 827, 665, and 506. The low intensity of the signal at *m/z* 665 may be attributed to the requirement of cleaving two glycosidic bonds to produce these ions. The next prominent signal, appearing at *m/z* 447, (59 u below the signal at *m/z* 506), may result from the further loss of an acetylamino group from the GlcNAc residue. The peak of high intensity at *m/z* 690 is attributed to fragment ions from the non-reducing terminus containing three Man and one GlcNAc units.

Figure 3.25b shows the ESI mass spectrum of PA-NGA3, where the $[M+H]^+$ ions appear as at *m/z* 1600. The fragment ions due to losses of one, two, three, four and five monosaccharide residues are noticeable, but obscured by background noise. The signals at

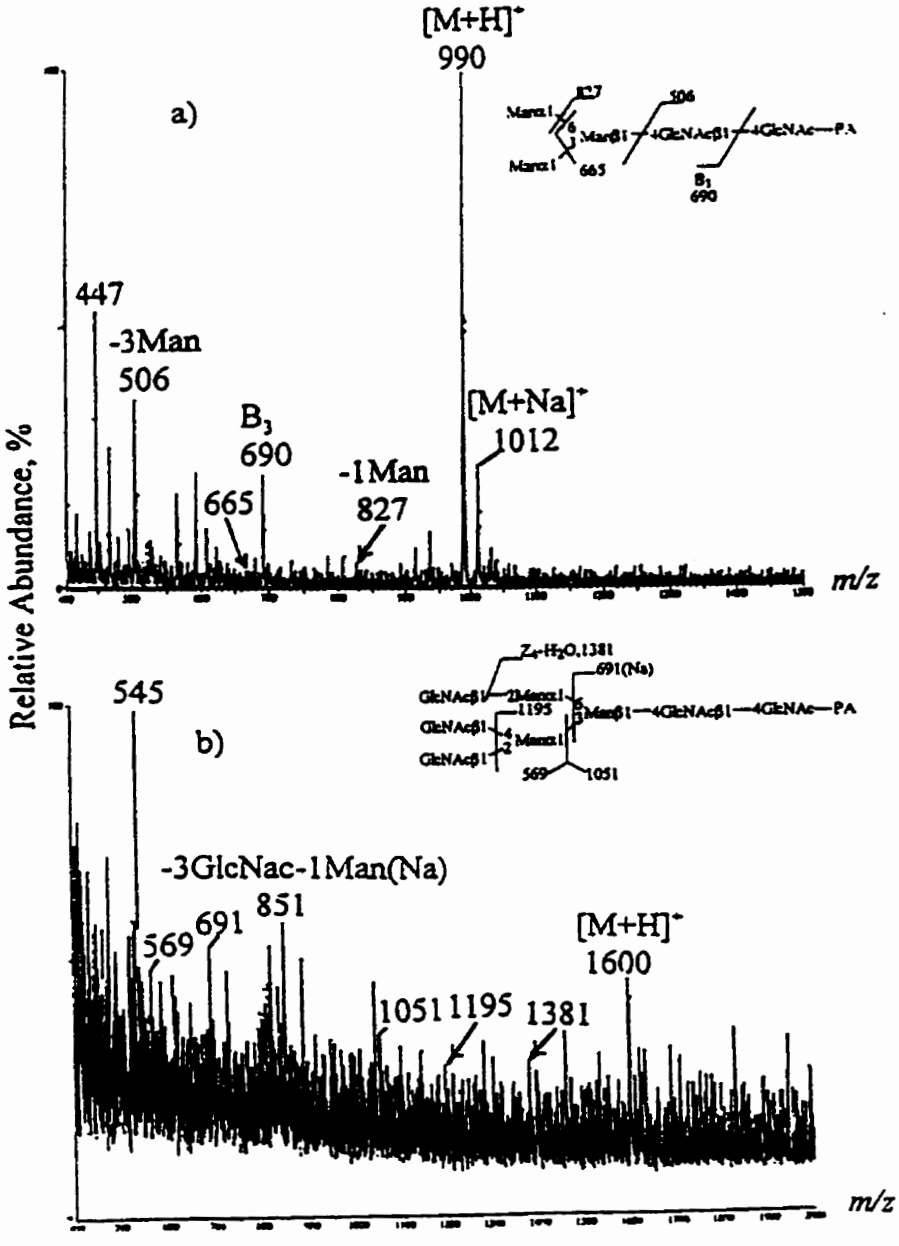

Fig. 3.25 ESI mass spectra of PA-oligosaccharides: a) PA-M3N2, b) PA-NGA3. The sample injected was 50 pmol and the cone voltage was set at 60 V.

m/z 851, 691 due to losses of four and five residues are sodium adducts of the fragments. The peak at *m/z* 569 results from fragment ions from the non-reducing terminus. While positive ion ESI-MS yielded high intensity $[M+H]^+$ signals for PA-derivatives, the relative abundance of fragments was generally too low to give diagnostic sequence information. However, it has been clearly demonstrated that most fragment ions observed retain the charge at the reducing end of a given oligosaccharide.

The three preparations of PMP-derivatives (M3N2, NGA3, and NGA4) were each divided into three portions. Two portions were directly subjected to MALDI- and ESI-MS, and/or ESI-MS/MS analysis. The third portion was separated by RP-HPLC first and the fractions collected were concentrated and characterized by ESI-MS in order to compare with direct ESI-MS without HPLC. Also, the RP-HPLC retention times for these PMP-derivatives were obtained during these experiments.

3.3.2 PMP-Derivatives of N-linked Oligosaccharides by MALDI-MS

PMP-derivatives were first characterized by linear mode MALDI-TOFMS in order to ascertain observation of molecular ions at the low nanomole and picomole level. Figure 3.26 shows the resulting mass spectra of PMP-M3N2 and NGA4, both obtained with 10 pmol of material. Mainly $[M+Na]^+$ and/or $[M+H]^+$ ions appeared and no fragment ions were observed. The measured and calculated *m/z* values for the $[M+Na]^+$ ions of the three sugars are given in Table 3.4. There is a good agreement between measured and calculated masses, and the error lies within ± 0.2 %.

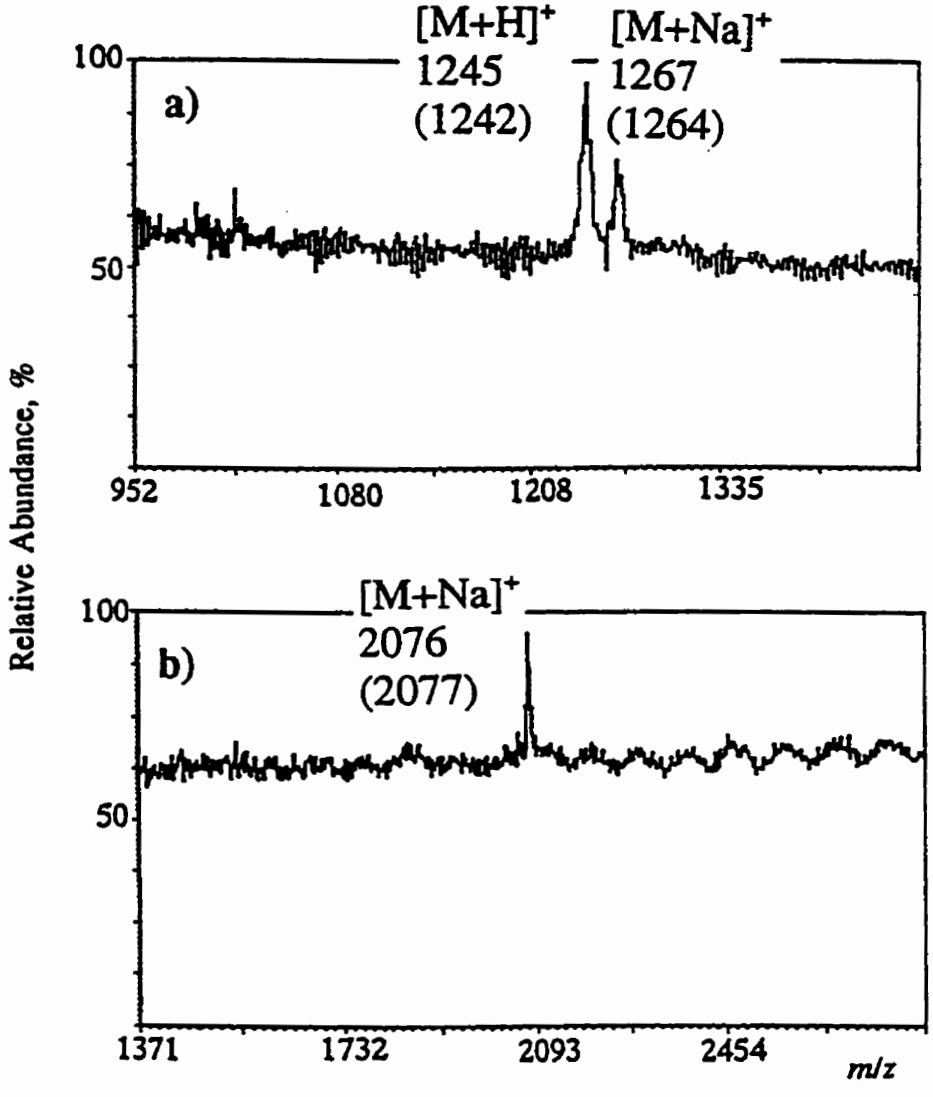

Fig. 3.26 Linear mode MALDI-TOF mass spectra of PMP N-linked oligosaccharide standards: a) PMP-M3N2, b) PMP-NGA4, showing experimental and calculated masses (in parentheses). MALDI-TOFMS conditions are given in Section 2.7.2.

Table 3.4: MALDI-TOFMS molecular mass measurements on the PMP-derivatives of three oligosaccharide standards.

PMP-derivatives of ...*	**Observed *m/z*, $(M+Na)^+$**	**Calculated *m/z*†, $(M+Na)^+$**
M3N2	1267	1264.2
NGA3	1875	1873.8
NGA4	2076	2077.0

*Structures of the oligosaccharides given in Fig. 3.24.

†Calculated using average values.

3.3.3 PMP-Derivatives of N-linked Oligosaccharides by off-line HPLC/ESI-MS.

The PMP-standards (2 to 3 nmol of each, in total) were then eluted on a RP-HPLC C_{18} column for salt removal. Separation of the PMP-derivatives from contaminants was carried out using a water-acetonitrile system containing 0.01 M of TFA, instead of ammonium acetate as suggested in the literature [73] and used here for smaller sugars. Our early experience had indicated that the presence of ammonium acetate in the collected fractions gave unsatisfactory MALDI results, since salts in the samples caused a wide distribution of adduct ions and disabled accurate M_r measurements. Although it has been reported that MALDI is tolerant to the presence of low mM concentrations of salts in protein samples, buffer concentrations of more than a fivefold molar excess over the analyte concentration have been known to suppress the ionization of oligosaccharide samples [142].The HPLC procedure with use of TFA allowed for preparation of samples devoid of the salt, i.e. NaCl, which was eluted shortly after the injection peak. TFA is readily removed from fractions by centrifuge-evaporation. The removal of TFA is in general much more complete than that of ammonium acetate.

In order to isolate fractions without overloading the column, the derivatized sugars were injected several times in a row, with only 50-µL aliquots containing ca. 100 pmol of PMP-derivative each time. Fig. 3.27 shows the RP-HPLC-UV chromatogram obtained for PMP-M3N2. The peak appearing at a retention time of 11.3 min is PMP-M3N2, which was identified afterwards by ESI-MS. The PMP reagent had been completely removed and was not detected, and if present, would produce a broad peak at ca.16 min. The other two minor components at 9.3 and 22.9 min are unidentified impurities or side-products.

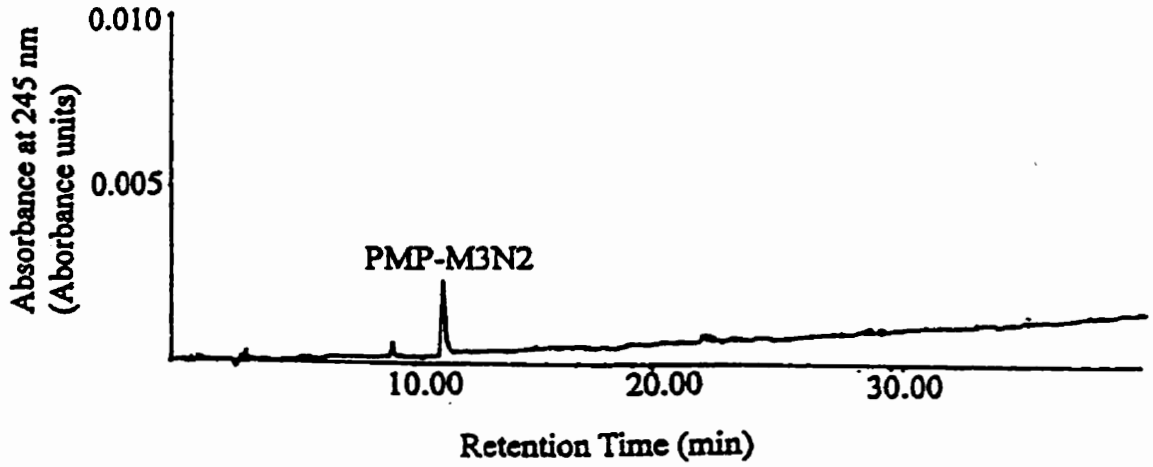

Fig. 3.27 Reversed-phase HPLC-UV chromatogram of PMP-M3N2. Column: SUPELCOSIL™ LC-18 column (25 × 0.46 cm). Gradient: from 20% to 100 % acetonitrile containing 0.01 M TFA over 70 min, 1 mL/min. An aliquot containing ca. 100 pmol PMP-M3N2 was injected.

Fractions collected from several runs were combined and concentrated to obtain 10 µL of solution. An aliquot of this solution was diluted five times with 1:1 acetonitrile-water containing 1% acetic acid and 20 µL was injected for ESI-MS. The resulting ESI spectra displayed weak $[M+H]^+$ signals sufficient for the purposes of identification by M_r as shown in Fig. 3.28, but not enough for MS/MS experiments to be performed. The estimated quantity of each PMP derivative used for these ESI runs was 50 pmol. Unlike the samples subjected directly to ESI-MS, which produced $[M+Na]^+$ ions, off-line HPLC-cleaned PMP-derivatives produced $[M+H]^+$ ions, as with on-line HPLC/MS discussed below. The off-line coupling of HPLC with ESI-MS was therefore a convenient way to determine the retention times of PMP-derivatives, even in the presence of impurities. Since the impurities also exhibit absorbance at 245 nm, the retention times of PMP-derivatives could not be obtained by HPLC alone.

3.3.4 Native and PMP-NGA3 by ESI-MS, ESI-MS/MS, and on-line HPLC/ESI-MS

The N-linked oligosaccharide, NGA3, was first characterized by ESI-MS in the native form. Fig. 3.29 shows full-scan positive ESI mass spectra acquired with 1 nmol of material in 49:49:2 water-methanol-formic acid. The spectrum in Fig. 3.29a was recorded at a cone voltage of 60 V, and that in Fig. 3.29b with a voltage of 30 V. Interestingly, the cone voltage had a strong impact on the nature of ions observed in the spectra, which was not the case in our hands with native tetraglucose. At 30 V (Fig. 3.29b), the spectrum was dominated by $[M+2H]^{2+}$ ions, whereas at 60 V (Fig. 3.29a), an informative in-source CID spectrum was obtained. Fig. 3.29a shows $[M+H]^+$ ions (*m/z* 1521) and also significant sequence-related fragment ions. The spectrum is dominated with B- and C-type ions, as

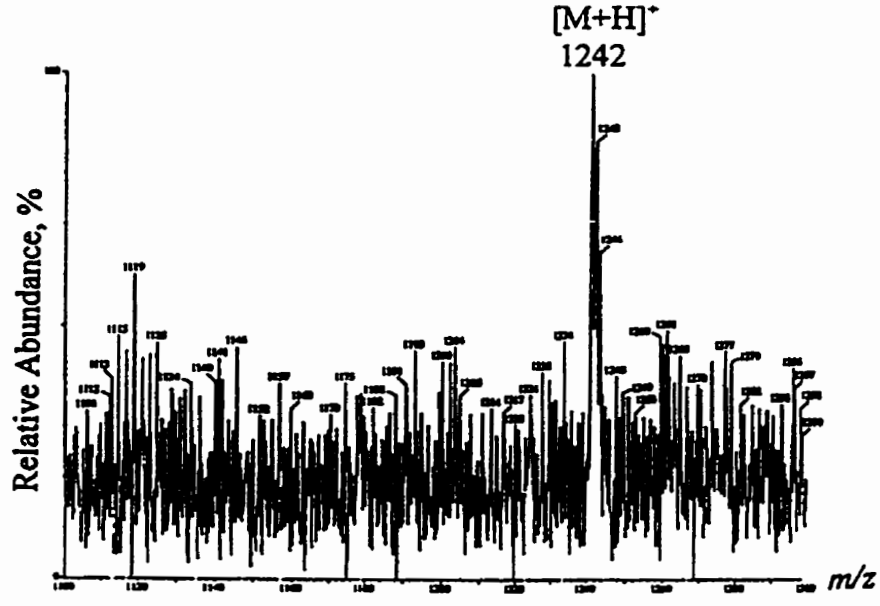

Fig. 3.28 ESI mass spectrum of PA-M3N2 collected from the HPLC fraction at 11.3 min in Fig. 3.27. The sample injected was 50 pmol and the cone voltage was set at 60 V.

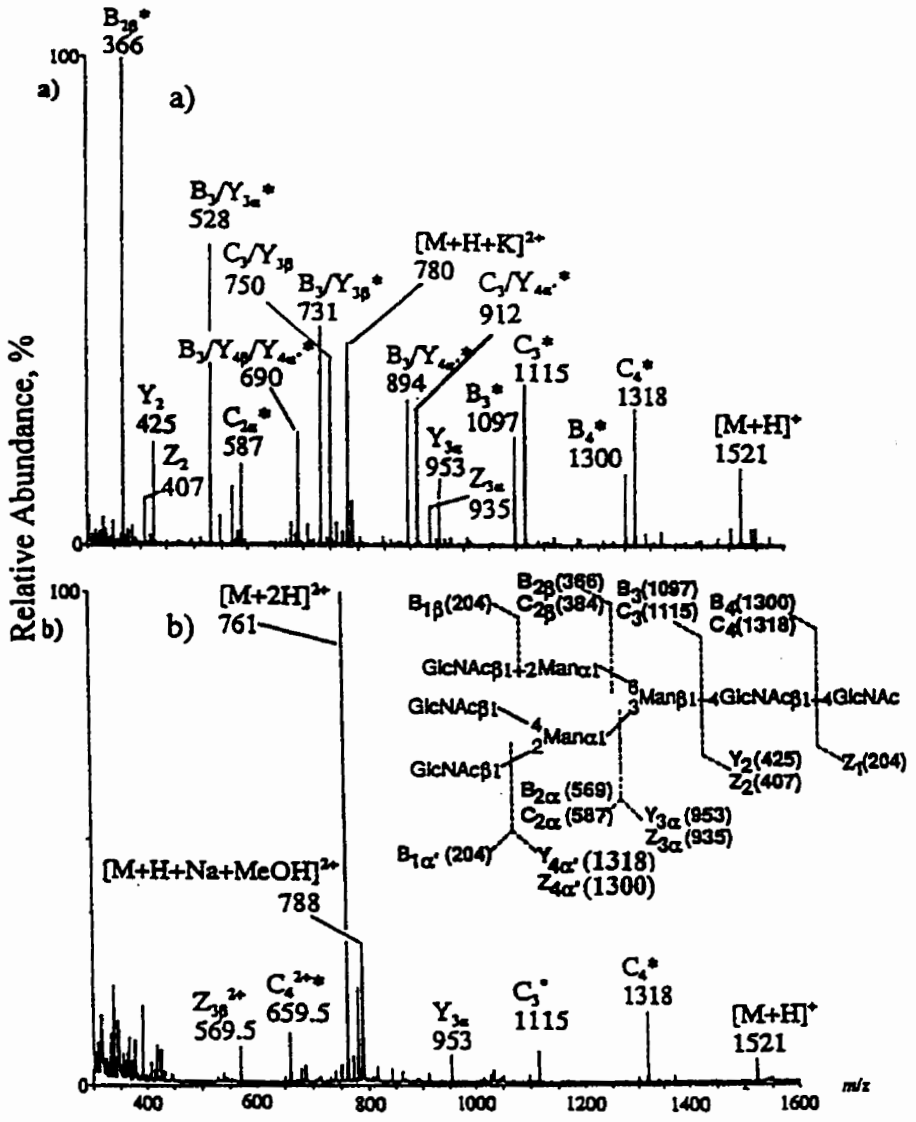

Fig. 3.29 ESI-MS spectra of native N-linked standard NGA3: a) cone voltage 60 V, b) 30 V. Possible fragmentation pathways are shown with the structure of the compound. Ion labels including a star (*) indicate that more than one fragmention pathway may lead to ions with the same *m/z* value.

well as the second-generation fragment ions including $C_3/Y_{4\alpha'}$, $C_3/Y_{3\beta}$, $B_3/Y_{4\alpha'}$, $B_3/Y_{3\beta}$, $B_3/Y_{3\alpha}$. A few Y- and Z-type ions, e.g. $Y_{3\alpha}$, $Z_{3\alpha}$, Y_2, and Z_2 exist at relatively high abundances at *m/z* 953, 935, 425, and 407, respectively. In addition, even the third-generation fragment ions can be observed at high abundance such as $B_3/Y_{4\beta}/Y_{4\alpha}$ at *m/z* 690. The peak with high intensity appearing at *m/z* 780 is attributed to a doubly charged monopotassium adduct, $[M+H+K]^{2+}$. The CID MS/MS spectrum of the $[M+2H]^{2+}$ ions was also recorded, at 40 eV collison energy. The ions observed in this spectrum (not shown) were similar to those of Fig. 3.29b. The amount of NGA3 used was the same as that used for the spectra in Fig.3.29.

PMP-NGA3 was also analyzed by full-scan ESI-MS. Since the derivatization step introduced large quantities of salts in the sample, an appropriate workup procedure had to be applied prior to the ESI-MS analysis. Sep-Pak C_{18} cartridges were tested first to purify the PMP-derivative, but no useful ESI mass spectra could be acquired due to significant loss of the desired PMP-derivative during the cleanup step. This loss might have occurred during the loading of the sample onto the Sep-Pak cartridge because of residual chloroform used to extract the excess PMP reagent, since the aqueous phase was saturated with chloroform after extraction, which might have resulted in elution of some PMP-derivative within the void volume. As RP-HPLC is well-known not only to provide good separation but also to remove salts efficiently, it has been used here instead of the Sep-Pak procedure. On-line HPLC/ESI-MS was thus used in order to acquire good quality spectra. The presence of a low quantity of TFA helped protonation of the molecular ions. The resultant spectrum of PMP-NGA3 in the positive ion mode is shown

in Fig. 3.30a and was acquired at a cone voltage of 60 V with 5 nmol of material. The same amount of information could still be obtained with 1 nmol, but not with smaller quantities. The spectrum is dominated by Y-type ions and their second-generation fragments. The ions resulting from Y-type cleavages include $Y_{4\beta}$, $Y_{3\beta}$, $Y_{3\alpha}$, Y_2 and Y_1, appearing at *m/z* 1648, 1485, 1283, 755, and 552. Second-generation fragments such as $Y_{4\alpha}/Y_{4\beta}$, $Y_{3\alpha}/Y_{4\beta}$, and $Y_{3\alpha}/Y_{3\beta}$ are registered at *m/z* 1445, 1080, and 918. B-type ions, e.g. $B_{2\beta}$ and B_3 at *m/z* 366 and 1096, as well as their second-generation fragments ($B_3/Y_{3\beta}$ at *m/z* 731 and $B_3/Y_{4\beta}$ at *m/z* 893) are also observed with relatively high abundance. It should be mentioned that $B_3/Y_{3\beta}$ and $B_3/Y_{4\beta}$ could also be possibly second-generation fragments arising from Y-types ions. Interestingly, the PMP-derivative did not favor glycosidic cleavages next to GlcNAc groups. For example, B_4 ions were not observed, and Y_2 ions were not prominent in the spectrum. Y_1 ions appear as the base peak, presumably due to protonation taking place on the double PMP moiety.

Compared with the spectrum of Fig. 3.29a, that of Fig. 3.30a contains peaks that can be assigned more easily with more certainty. The peaks marked with an asterisk in Fig. 3.29a have more than one possible origin. For example, in Fig. 29a, the signal marked as B_3 (*m/z* 1097) could be also assigned as $Y_{4\beta}/Z_{4\alpha'}$, $Y_{4\beta}/Z_{4\alpha''}$, $Y_{4\alpha'}/Z_{4\alpha''}$, $Y_{4\alpha'}/Z_{4\beta}$, $Y_{4\alpha''}/Z_{4\alpha'}$, and $Y_{4\alpha''}/Z_{4\beta}$, whereas in Fig. 3.30a, B_3 is the only possible assignment for this signal. Both spectra contain informative sequence-related fragment ions and are complementary to each other. For example, the ESI mass spectra of native oligosaccharides can be used as fingerprints for qualitative comparison, whereas the spectra of PMP-derivatives can be used to provide sequence information, especially for unknown compounds since they are

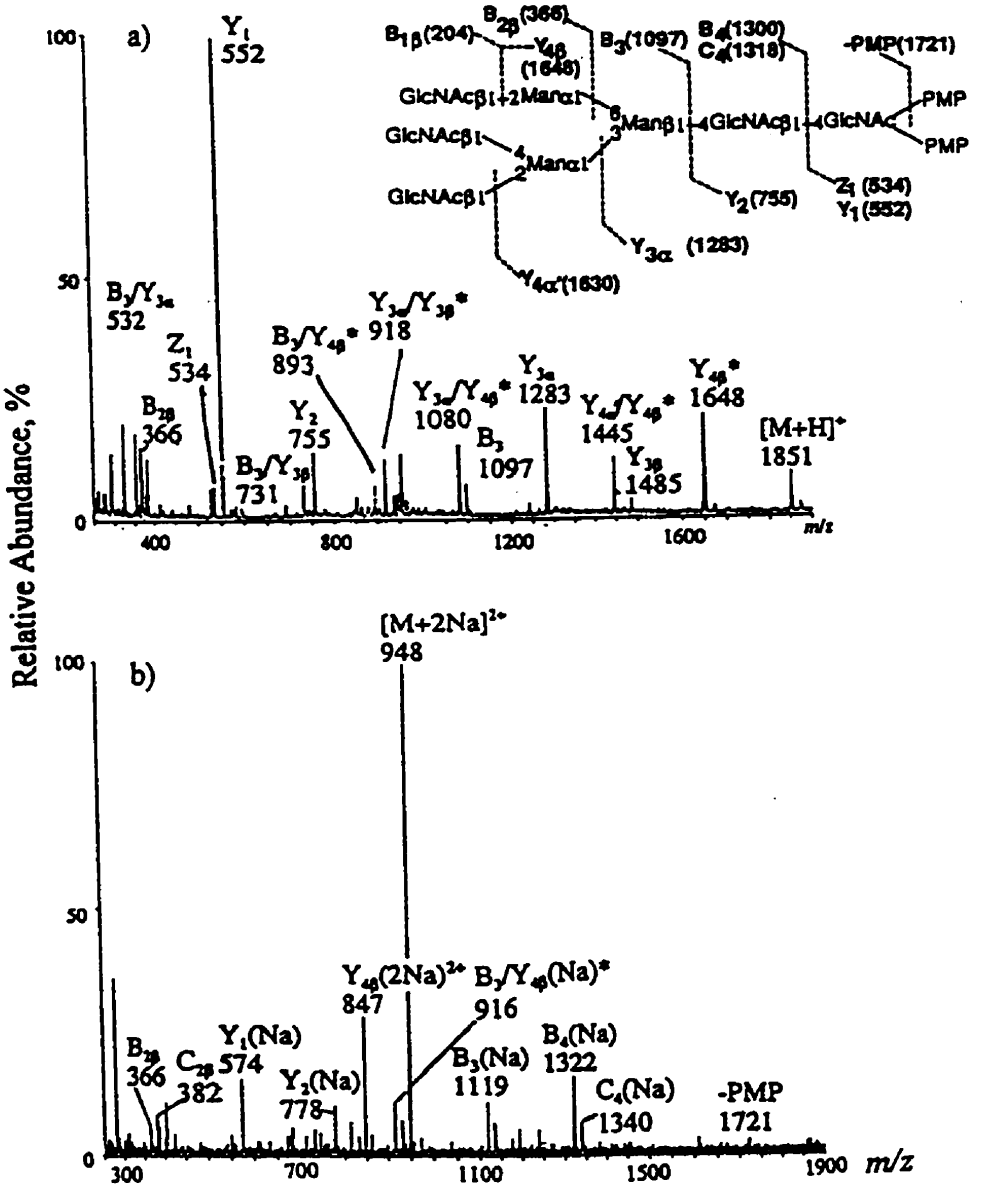

Fig. 3.30 a) Full-scan in-source CID spectrum of PMP-NGA3, desalted by on-line HPLC and b) ESI-CID-MS/MS spectrum of the $[M+2Na]^{2+}$ ions of PMP-NGA3, at *m/z* 948.5, before desalting. Ion labels including a star (*) indicate that more than one fragmentation pathway may lead to ions with the same *m/z* value. Conditions are given in Section 2.7.3.4 and 2.7.3.5.

much easier to interpret, due to observation of reducing end-containing fragments in majority.

The molecular ions of PMP-NGA3 were then analyzed by ESI-MS/MS. The full-scan positive ESI mass spectra of the PMP-NGA3 contained predominantly $[M+2Na]^{2+}$ ions. Therefore, only $[M+2Na]^{2+}$ ions could be selected as the precursor ions rather than $[M+H]^{+}$ ions, since the samples were not desalted after derivatization. As mentioned above, the Sep-Pak C_{18} cartridges cleanup procedure failed to enable us acquire ESI-MS and/or ESI-MS/MS spectra because of sample loss and limited amount of material. In addition, HPLC/ESI-MS/MS is still not readily available on our instrument at this stage. Therefore, sodiated molecular ions appeared as the predominant peaks under these conditions. The ESI-MS/MS spectrum of the $[M+2Na]^{2+}$ ions of PMP-NGA3 at *m/z* 948 (Fig. 3.30b) demonstrates that $[M+2Na]^{2+}$ ions are not easily fragmented under the CID conditions employed here (50 eV), which agrees with Duffin's observation that sodium-adducted oligosaccharide ions were more difficult to break down than their protonated analogs [43]. It is very interesting to notice that unlike the full-scan ESI-MS spectrum of PMP-NGA3, its MS/MS spectrum is quite similar to the full-scan spectrum of native NGA3. Fig. 3.30b is dominated by sodiated B- and C-type ions, the former with higher abundance (C_4, B_4, C_3, B_3, and $C_{2\beta}$ and $B_{2\beta}$). A second-generation fragment is also observed, i.e. $B_3/Y_{4\beta}$ (Na) at *m/z* 916. Some sodiated Y-type ions, e.g. $Y_{4\beta}$ (2Na), Y_2(Na), and Y_1(Na) appear with high abundance as well. Even though significant peaks could be assigned, less diagnostic sequence information was obtained by ESI-CID-MS/MS than by full-scan in-source CID ESI. The presence of two Na^{+} moieties on the precursor and

therefore fragment ions with zero, one or two Na^+ attached make peak assignment much more difficult than that if only protonated species were present, which emphasizes the importance of a desalting step when using PMP derivatization.

To summarize, no gain of sensitivity was obtained by derivatizing NGA3 with PMP. However, more specific fragmentation pathways were achieved for the derivative than for native compound, i.e. formation of reducing end-containing fragments with PMP attached was favored. For both native and PMP-NGA3, in-source-CID with 60 V cone voltage was sufficient to obtain informative fragmentation patterns, i.e. it was unnecessary to use ESI-CID-MS/MS. At low cone voltage values (e.g. 30 V), both native and PMP-NGA3 produced mainly $[M+2H]^{2+}$ ions. Thus, for a mixture of PMP-N-linked oligosaccharides, low cone voltage values seem preferable to high values in order to obtain mainly molecular ions rather than fragments which make spectra interpretation more complex.

As a general observation, the PMP-oligosaccharides yielded better sensitivity in MALDI than in ESI, but more accurate M_r measurements were achieved with ESI. The measured *m/z* values of the $[M+H]^+$ or $[M+Na]^+$ ions with ESI were within 0.05% of the predicted monoisotopic values. The MALDI results indicate that the PMP-derivatives of N-linked oligosaccharides are stable and do not fragment readily under the MALDI-MS conditions employed. MALDI- and ESI-MS data on large oligosaccharide standards can not only verify the masses of the derivatives but also give some insight into the nature of possible adduct species which could be formed with unknown sugars from glycoproteins. These data also display the preferred fragmentation pathways of the derivatives.

3.4 Application to Ovalbumin

3.4.1 Mass Spectrometry of Intact Ovalbumin: Background

ESI and MALDI were used to obtain information on the molecular mass and degree of heterogeneity of intact ovalbumin. ESI was useful in showing site specific carbohydrate heterogeneity, whereas MALDI allowed for rapid and simple determination of the average molecular mass of all glycoforms. Both methods can provide information with pmol to fmol sensitivity [161].

3.4.1.1 Intact Ovalbumin by MALDI-TOFMS

MALDI, which is capable of low picomole sensitivity, speed (5 min per sample) and accuracy (< 0.1% error) [95], has been adopted as an invaluable technique to determine molecular masses of biomolecules [162].The MALDI mass spectra of ovalbumin are shown in Fig. 3.31a and b, using sinapinic acid (SA) and CHCA as a matrix, respectively. An acetonitrile-water solution (1:1) containing 0.1% TFA and saturated with SA or CHCA was used to dispense the matrix. The instrument was calibrated with an external standard, horse skeletal muscle myoglobin. In contrast to the results reported by Sottani and Fiorentino, et al. [161], where only singly charged molecular ions were observed, the present results show multiply charged molecular ions without fragmentation. Fig. 3.31a shows the presence of singly and doubly charged protonated molecular species, as well as a singly protonated dimer of ovalbumin with SA as the matrix. The peaks in Fig. 3.31b correspond to singly, doubly, triply, quadruply, and even multiply charged ($[M+6H]^{6+}$) molecular ions obtained with CHCA as the matrix. This multiple charging phenomenon could be attributed to the lower pH of the matrix solutions

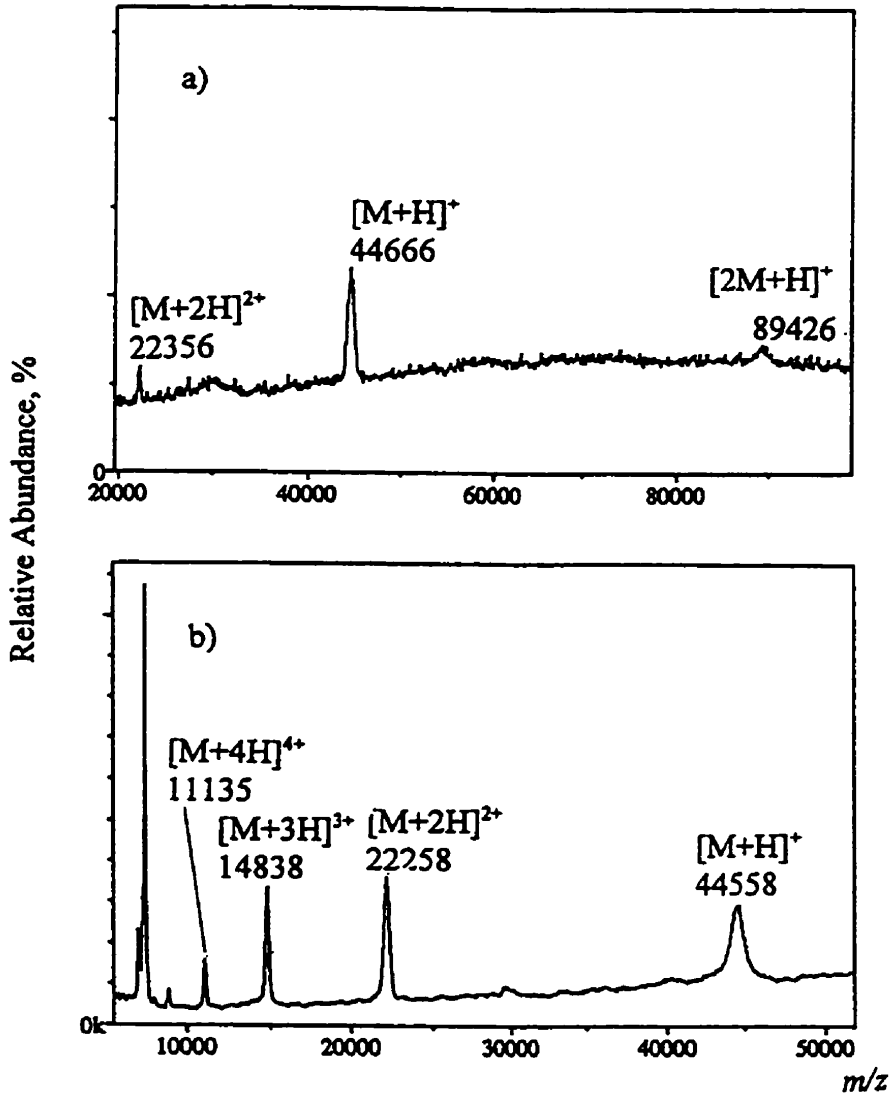

Fig. 3.31 Linear mode MALDI-TOF mass spectra of intact ovalbumin obtained with different matrices: a) sinapinic acid (SA), b) α-cyano-4-hydroxy-cinnamic acid (CHCA). Horse skeletal muscle myoglobin was used as an external calibrant. Conditions are given in Section 2.7.2.

prior to drying. Due to operation of the Manitoba II instrument in the linear TOF mode, it was not possible to resolve the individual glycoforms of this highly heterogeneous glycoprotein, with either of these two matrices. However, broad unresolved molecular ion peaks as shown in Fig. 3.31a and b provided an average molecular mass of 44688 ± 0.05% with SA as a matrix, and 44584 ± 0.2% with CHCA, and these values are quite close to that of 44287 previously reported [135,136], with an accuracy of 0.8%. The width of the peaks gives a measure of the amount of heterogeneity in the compound [44]. The amount of ovalbumin loaded to obtain each of the spectra was only 1 pmol, and a high signal-to-noise ratio was observed for multiply charged molecular ion peaks. As already indicated, the limitations of MALDI-TOFMS in this study are the lack of resolution and mass accuracy, the latter being typically of the order of 0.5% [134]. The values reported here result from an average of all charged states and the errors represent the precision, not the accuracy. They are consistently higher than the predicted value, which may be due on one hand to the use of external (rather than internal) calibration and on the other hand to matrix adducts onto the molecular ions [163]. However, it has been indicated that if an appropriate matrix is selected and sample-matrix preparation, pH and instrumentation conditions are optimized, resolution of glycoforms could also be achieved [161].

3.4.1.2 Intact Ovalbumin by ESI-MS

ESI-MS can be used to measure the masses of glycoproteins accurately and to resolve oligosaccharide heterogeneity on these biomolecules [43]. Reinhold and co-workers also indicated that a mass profile of all glycoforms as obtained by ESI-MS can be very informative and serve in the first step of structure inquiry, akin to carbohydrate

composition analysis [164].

Intact ovalbumin was thus analyzed by ESI-MS, according to a procedure reported previously [43]. The preparation of an ovalbumin solution was as follows: the glycoprotein had to be dissolved in water first, acetonitrile and formic acid were then added sequentially until a concentration of 100 pmol/μL in 2:1 H_2O-CH_3CN was reached. If ovalbumin was mixed with water, acetonitrile and formic acid simultaneously, it failed to dissolve. The same happened if a H_2O-CH_3CN mixture was first prepared, followed by addition of formic acid. Acetonitrile is likely too hydrophobic for the hydrophilic glycoprotein, and the solute-solvent pair is incompatible. The full-scan mass spectrum of ovalbumin (Fig. 3.32) was acquired by scanning from 500 to 2500 u over 7 s and averaging 20 scans. The amount of sample injected was 2 nmol. Fig. 3.32 displays multiply charged ions formed by attachment of different numbers of protons to the molecule. Within each charge state, several glycoforms of ovalbumin can be resolved, as indicated by the inset in Fig. 3.32, which shows the $[M+24H]^{24+}$ and $[M+25H]^{25+}$ *m/z* region. The molecular masses corresponding to the individual glycoforms can be calculated and displayed by deconvolution using an algorithm which extracts molecular mass information from the peaks displayed in Fig. 3.32. The resulting deconvoluted spectrum is shown in Fig. 3.33. This spectrum clearly displays, within ± 4 u, the 162 and 203 u mass increments corresponding to Hex and HexNAc residues. The masses of the different oligosaccharides attached to the glycosylation site of ovalbumin can be determined by subtracting the average M_r of 42859 u which represents non-carbohydrate moiety [160 (phosphate part) + 42699 (peptide molecular mass)] [135,136] from the masses of individual glycoforms

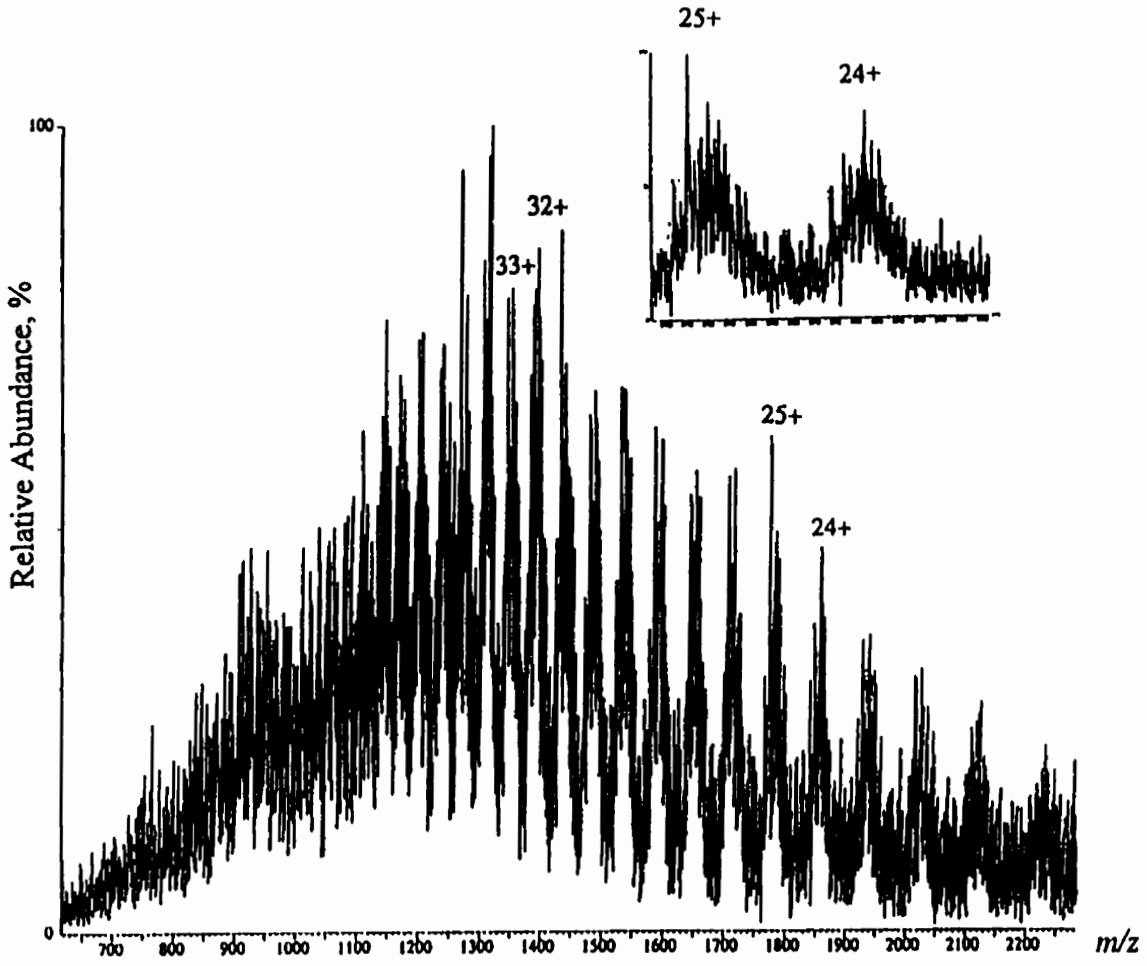

Fig. 3.32 Positive full-scan ESI mass spectrum of intact ovalbumin. ESI condtions are given in Section 2.7.3.6.

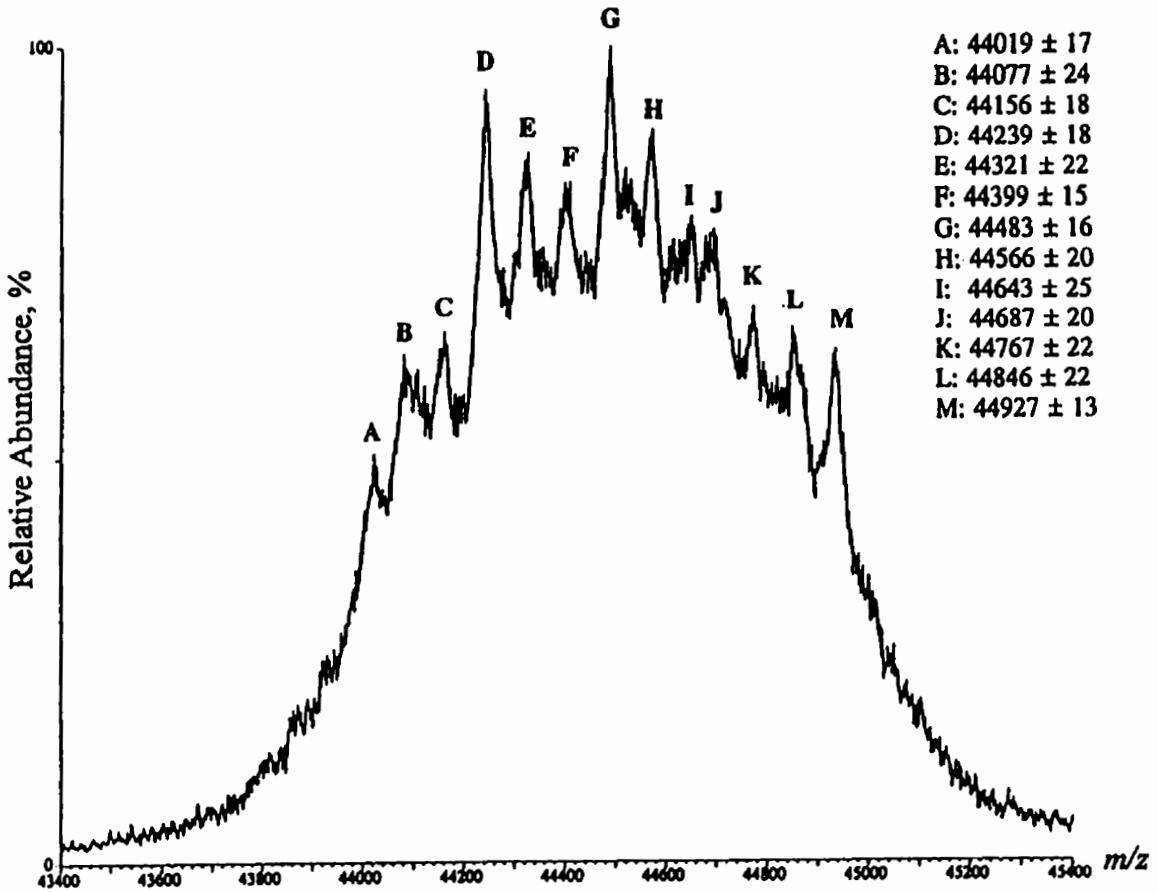

Fig. 3.33 Transformed mass spectrum of intact ovalbumin, obtained from the spectrum in Fig. 3.32 by deconvolution.

detected in Fig. 3.33 [43]. These glycoforms are listed in Table 3.5. Here we need to take into consideration the loss of water upon formation of the asparagine-carbohydrate bond, therefore, 18 u must be added to the subtracted value when calculating the masses of glycans. This procedure allowed differentiation of 12 oligosaccharides with different molecular masses, and provided tentative compositions for these glycans since data from the Complex Carbohydrate Database indicated that there were very few mass degenerations which could give rise to ambiguities of composition [95], suggesting that this glycosylation site possesses a variety of non-sialylated oligosaccharide structures. The two most abundant glycoforms observed in the deconvoluted spectrum of Fig. 3.33 were assigned with the compositions, $Hex_6GlcNAc_2$ and $Hex_5GlcNAc_4$, which are in good agreement with data reported previouly [43]. Although all 12 compositions listed in Table 3.5 have already been reported, it is the first time that so many different glycoforms can be detected by only performing full-scan ESI-MS of intact ovalbumin, i.e. without detaching the glycans [43,134,136-147]. Reinhold and co-workers have indicated that, although not always experimentally possible, intact profiles would best represent glycan heterogeneity, uncompromised by selective enzymatic and isolation techniques, while deglycosylation may be discriminating or incomplete and chromatography could enrich or exclude particular subforms [33].

3.4.2 PMP-Derivatized Glycans from Ovalbumin by ESI-MS and off-line HPLC/MALDI-TOFMS

To verify and validate the results on the oligosaccharide content of ovalbumin, the glycans were chemically cleaved by hydrazinolysis and isolated from the peptide backbone.

Table 3.5. Summary of the information obtained from Fig. 3.33, listing the M_r values of different glycoforms of ovalbumin as detected by ESI-MS. The corresponding M_r and compositions of oligosaccharides are also given.

Re: Fig. 3.31	[a]Deconvoluted M_rs of ovalbumin	M_rs of corresponding oligosaccharides[b]	Composition + calculated M_rs of oligosaccharides[c]
1 B	44077	1236	$Hex_5HexNAc_2$ (1234)
2 C	44156	1315	$Hex_3HexNAc_4$ (1316)
3 D	*44239	1398	$Hex_6HexNAc_2$ (1396)
4 E	44321	1480	$Hex_4HexNAc_4$ (1478)
5 F	44399	1558	$Hex_7HexNAc_2$ (1558)
6 G	*44483	1642	$Hex_5HexNAc_4$ (1640)
7 H	44566	1725	$Hex_3HexNAc_6$ (1722)
8 I	44643	1802	$Hex_6HexNAc_4$ (1802)
9 J	44687	1846	$Hex_5HexNAc_5$ (1843)
10 K	44767	1926	$Hex_3HexNAc_7$ (1925)
11 L	44846	2005	$Hex_6HexNAc_5$ (2005)
12 M	44927	2086	$Hex_4HexNAc_7$ (2087)

[a] * Most abundant glycoforms detected in the ESI mass spectrum of Fig. 3.33.

[b] Obtained by subtracting 42859 u, which represents the non-carbohydrate moiety [135, 136]

[c] Hex = hexose; HexNAc = N-acetylhexosamine; the data in parentheses are calculated monoisotopic M_r for oligosaccharides.

The oligosaccharide mixture was subjected to PMP-derivatization on a small scale. The PMP-glycan mixture thus obtained was either subjected directly to ESI-MS and ESI/MS/MS, or characterized by off-line coupling of HPLC with MALDI-TOFMS. The results were compared to those obtained from ESI-MS experiments on intact ovalbumin.

3.4.2.1 Analysis of PMP-Glycans from Ovalbumin by ESI-MS and ESI-MS/MS

The methodology developed for analysis of small sugars and larger oligosaccharide standards was applied to the PMP-derivatized glycan mixture. Since the earlier experience showed that the presence of significant amounts of salts caused problems in ESI-MS analyses of PMP-oligosaccharides, the sample was desalted with a Sep-Pak C_{18} cartridge prior to ESI-MS. The ionization conditions were optimized with PMP-tetraglucose first in order to minimize fragmentation and observe mainly molecular ions, otherwise it would make interpretation of the spectra too difficult and yield a distortion of the indigenous glycan structures. Fig. 3.34 shows the ESI mass spectrum obtained for the mixture of PMP-derivatized glycans, i.e. the N-linked oligosaccharide profile of ovalbumin. With a cone voltage of 30 V, and after desalting on a Sep-Pak C_{18} cartridge, $[M+H]^+$ and $[M+2H]^{2+}$ ions are observed. The charge states of the ions of PMP-derivatives were deduced by examining the *m/z* differences within an isotopic cluster. For example, a *m/z* difference of 0.5 among isotopes indicates a doubly charged PMP-oligosaccharide ion, whereas a mass-to-charge difference of one belongs to a singly charged ion state. The signals corresponding to different PMP-oligosaccharide compositions were observed reproducibly over four independent analyses and are presented in Table 3.6. The two intense signals at *m/z* 529 and 599 observed in Fig. 3.34 remain unexplained and may

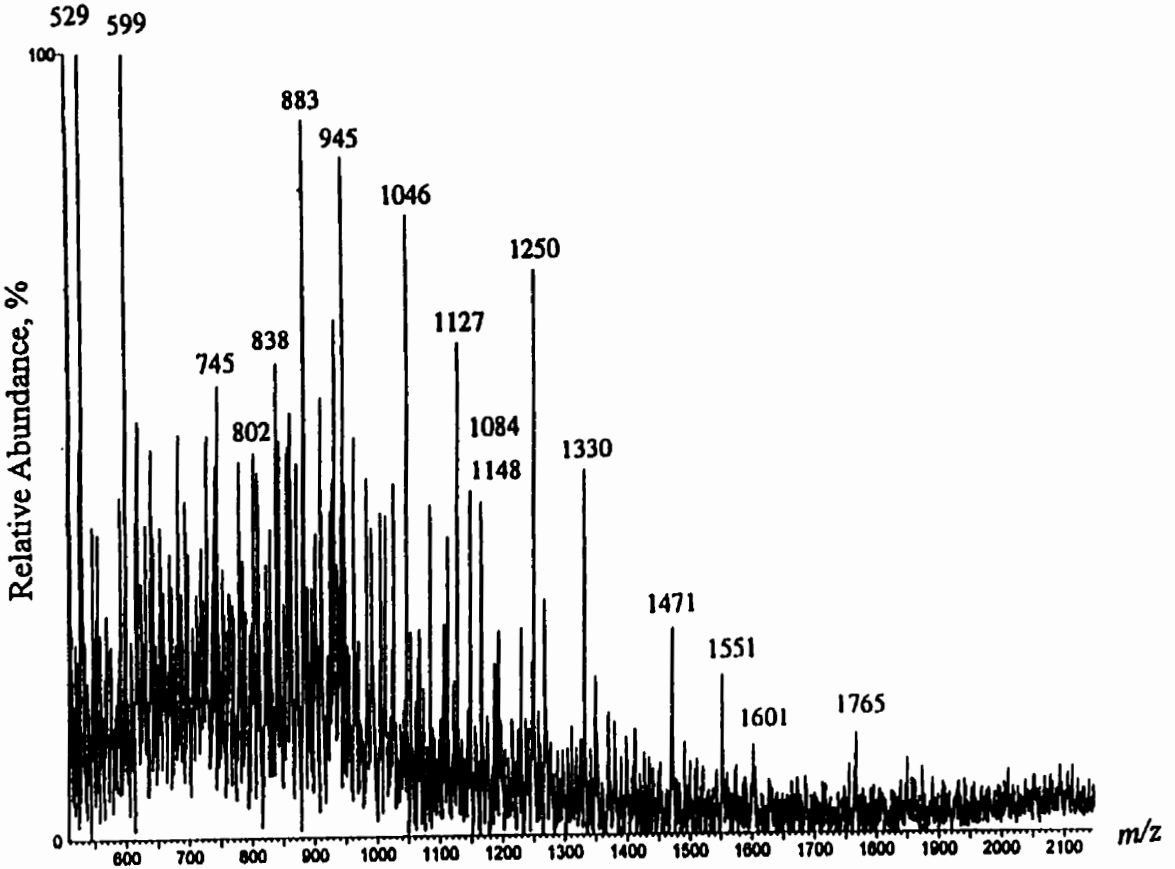

Fig. 3.34 Positive full-scan ESI mass spectrum of the mixture of PMP-derivatized glycans cleaved from ovalbumin by hydrazinolysis. ESI conditions are given in Section 2.7.3.7.

Table 3.6. Summary of the information obtained from Fig. 3.34, listing the M_r and compositions of oligosaccharides cleaved from ovalbumin and derivatized with PMP, values deduced from the *m/z* values of the molecular ions of PMP-derivatives.

No[a]	Observed *m/z* data of PMP-oligosaccharides[b]	M_rs of oligosaccharides from experiments [c]	Composition with calculated M_rs of oligosaccharides
13 *	745 (2+)	1158	$Hex_2HexNAc_4$ (1154)
14	† 883 (2+)	1434	$Hex_5HexNAc_3$ (1437)
5	† 945 (2+)	1558	$Hex_7HexNAc_2$ (1558)
15 *	1046 (2+)	1760	$Hex_7HexNAc_3$ (1761)
10	1127 (2+)	1922	$Hex_3HexNAc_7$ (1925)
16 *	1148 (2+)	1964	$Hex_7HexNAc_4$ (1964)
17 *	1250 (2+)	2168	$Hex_7HexNAc_5$ (2167)
18 *	1330 (2+)	2328	$Hex_8HexNAc_5$ (2329)
19 *	1471(2+)	2610	$Hex_{11}HexNAc_4$ (2612)
20 *	1551(2+)	2770	$Hex_{12}HexNAc_4$ (2774)
21	1601(1+)	1270	$Hex_4HexNAc_3$ (1275)
14	1765 (1+)	1434	$Hex_5HexNAc_3$ (1437)

[a] * Not reported in the literature.

[b] 1+ singly charged ion, 2+ doubly charged ion, † possibly truncated

[c] These data were obtained by subtracting the mass of the PMP portion (330.4) from the observed M_rs of PMP-derivatives.

be non-sugar contaminants. The molecular masses and sugar compositions of these oligosaccharides were obtained by subtracting the mass of the PMP portion from M_rs calculated from the observed *m/z* values of $[M+H]^+$ and $[M+2H]^{2+}$ ions of the PMP-derivatives. Here it was assumed that the glycans have $[(Hex)_x(HexNAc)_y(Fuc)_z]$ structures. Since a limited amount of sample was available, priority was put on tuning up the instrument for high sensitivity, which resulted in decreased resolution. The low resolution yielded poor definition of the isotopic clusters and thus there is some uncertainty about the charge states assigned to the ions in Table 3.6.

In order to obtain more structural oligosaccharide information, three doubly charged ions of PMP-oligosaccharides with high abundances at *m/z* 883, 945, and 1047, (see Fig. 3.34) were selected as the precursor ions and characterized by ESI-CID-MS/MS. Fig. 3.35a, b, and c show the ESI-MS/MS spectra of $[M+2H]^{2+}$ for these three PMP-oligosaccharides. The spectrum in Fig. 3.35a was obtained for the parent ions at *m/z* 883, and accordingly, the composition suggested for these parent ions is $Hex_5HexNAc_3$. The peak at *m/z* 1746 is attributed to loss of water from the$[M+H]^+$ ion. Fragment ions due to losses of one, two, and three GlcNAc units are observable at *m/z* 1542, 1338, and 1137, respectively. The peak at *m/z* 782 arises from loss of a GlcNAc residue from the doubly charged precursors. The peak at *m/z* 204 is characteristic of all N-linked oligosaccharides, since it arises from a GlcNAc residue. This oligosaccharide with $Hex_5HexNAc_3$ composition was not found by ESI-MS analysis of intact ovalbumin (Fig. 3. 33 and Table 3.5). The sequential loss of three GlcNAc from the parent ions would be possible only if these three GlcNAc were peripheral residues at the non-reducing end, since the fragment

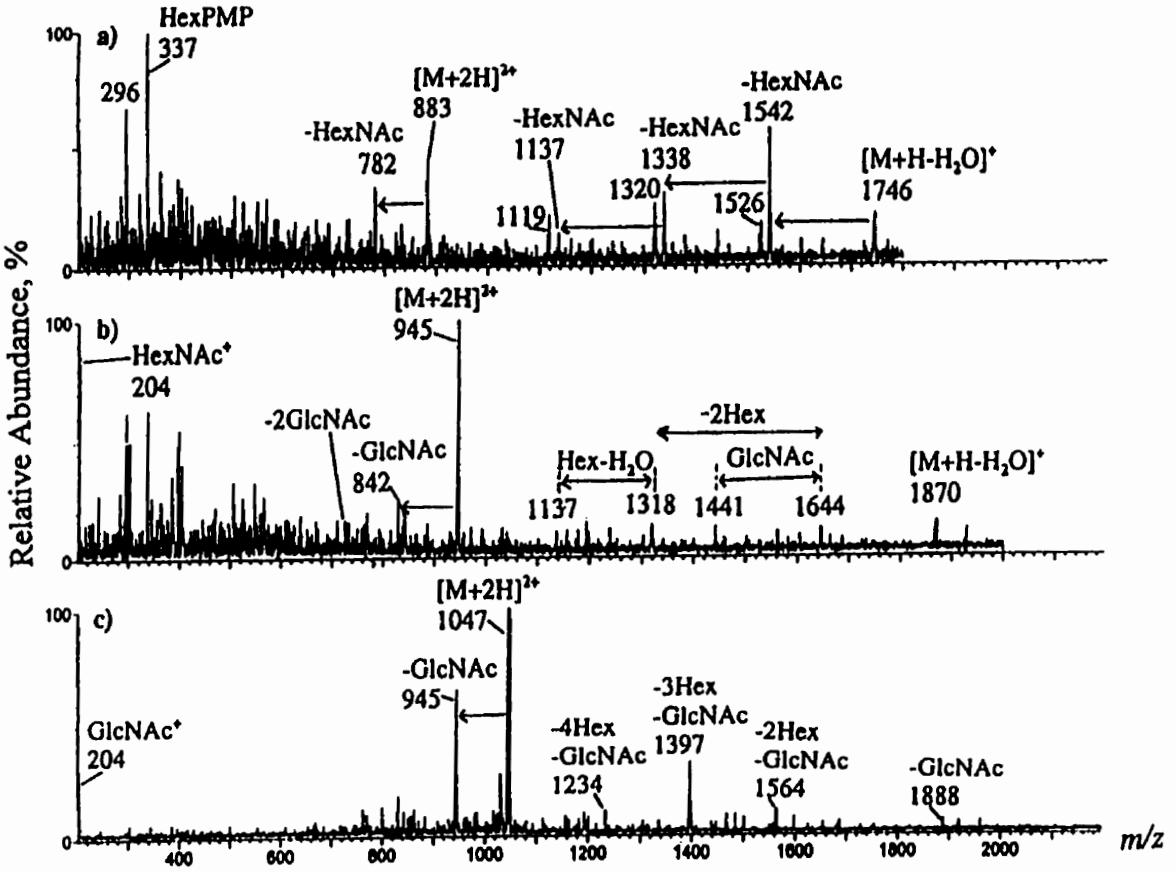

Fig. 3.35 ESI-CID-MS/MS spectra of three $[M+2H]^{2+}$ ions of PMP-derivatives of oligosaccharides cleaved from ovalbumin. Precursors at (a) *m/z* 883, (b) *m/z* 945, and (c) *m/z* 1047. Conditions are given in Section 2.7.3.7.

ions appearing at *m/z* 1542, 1338, and 1137 still contain the PMP portion. Also, ions appearing at *m/z* 337 most probably correspond to $[Hex+1PMP-H_2O]^+$, which suggests that the reducing end is Man instead of GlcNAc as in the common core of all N-linked oligosaccharides, i.e. Manα1-6(Manα1-3)Manβ1-4GlcNAcβ1-4GlcNAc. The losses of these GlcNAc residues can not therefore originate from this core. According to the fragmentation pathways observed for PMP-derivatives of tetraglucose and N-linked standards, losses of non-reducing end residues should be prominent in the positive ion mode. The loss of the three GlcNAc residues thus probably originates from peripheral branches. If two GlcNAc units in the core are also taken into consideration, there should originally be five GlcNAc residues contained in this oligosaccharide (i.e., $Hex_5HexNAc_5$). However, the precursor ion has been already described to contain only three GlcNAc residues. The conclusion which can be drawn from the spectrum of Fig. 3.35a could be that the oligosaccharide with the composition $Hex_5HexNAc_3$ may have been truncated either during hydrazinolysis of ovalbumin or as a result of the workup procedure. The remaining sugar would therefore not comprise the entire common core. Dell has reported that FAB data showed that hydrazinolysis had effected a partial fission of the chitobiose core [81]. Two structures have been reported for oligosaccharides with $Hex_5GlcNAc_5$ composition and are shown in Fig. 3.36 [139,142]. Structure I in Fig. 3.36 is likely to correspond to that of the precursor ion in Fig. 3.35a, although two GlcNAc units are missing from the reducing end.

The precursor ions at *m/z* 945 (Fig. 3.35b) have been assigned the composition $Hex_7GlcNAc_2$. A corresponding structure has been reported by a few research groups

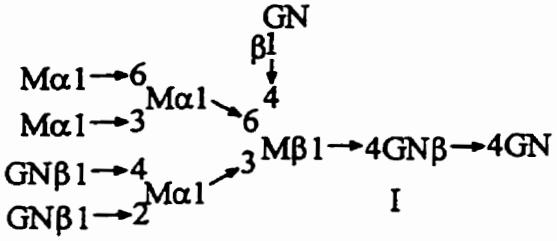

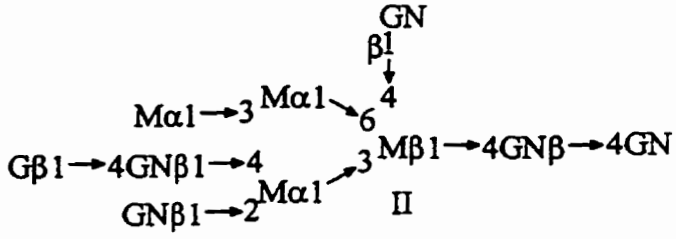

Fig. 3.36 Two oligosaccharide structures from ovalbumin reported previously having the composition $Hex_5GlcNAc_5$. M, Man; GN, GlcNAc; G, Gal [139].

[139,141,142]. As in the spectrum in Fig. 3.35a, the peak appearing at *m/z* 1870 in Fig. 3.35b is due to the singly charged molecular ion $[M+H]^+$ having lost one water molecule. Ions at *m/z* 1644 arise from loss of 60 u from a Y fragment formed by loss of a hexose residue, whereas the signal at *m/z* 1441 is attributed to a further loss of GlcNAc from the *m/z* 1644 ion. The signals at *m/z* 1318 and 1137 resulted from the losses of two and three Hex residues from the ion at *m/z* 1644. The ions at *m/z* 842 and 733 are doubly charged Y-fragments due to losses of one and two GlcNAc residues from the precursor. Again, in this case, truncation of the trimannosyl core must have occurred, and the original structure of the oligosaccharide was possibly $Hex_7GlcNAc_3$, or $Hex_7glcNAc_4$. Observation of ions at *m/z* 337 as described above supports these two suggested compositions.

Fig. 3.35c shows the CID-MS/MS spectrum of $[M+2H]^{2+}$ ions at *m/z* 1047, whose composition has been tentatively assigned as $Hex_7GlcNAc_3$. A few fragment ions are observed, and labeled in Fig. 3.35c. The oligosaccharide with the composition $Hex_7GlcNAc_3$ and the six other oligosaccharides labeled with an asterisk in Table 3.6 have not been reported elsewhere so far. This oligosaccharide produced molecular ions losing only one GlcNAc residue (*at m/z* 1888, and 945 ions) and no ions at *m/z* 337, suggesting that no truncation of the trimannosyl core occurred. However, since there is some uncertainty as to the charge states assigned to the oligosaccharides in Table 3.6, (especially for 19#, and 20#), there is also a doubt as to the compositions suggested for these two oligosaccharides.

The ESI-MS/MS results obtained here can not give complete structural information, however, they are useful to confirm some of the sugar compositions

previously suggested by full-scan ESI-MS measurements on intact ovalbumin as well as detached and derivatized sugars. The fragments resulting from losses of Hex and HexNAc residues provide strong evidence that the three signals appearing in Fig. 3.34 (*m/z* 883, 945, and 1047) definitely belong to PMP-derivatized glycans. In addition, these results indicate that the charge states assigned to these three PMP-derivatives are correct, since some daughter ions have higher *m/z* values than the selected precursor ions. Unfortunately, the preliminary experiments with PMP-tetraglucose and PMP-N-linked standards never consisted of fragmenting $[M+2H]^{2+}$ ions. Thus the direct comparisons between the spectra of unknowns and those of the standards were not possible. As a reminder, the PMP-tetraglucose and especially PMP-N-linked standards used for full-scan ESI-MS, available in very low quantities and costly, had not been desalted in order to avoid loss of material, and thus protonated molecular ions were substituted by $[M+Na]^{+}$ or $[M+2Na]^{2+}$ species. Furthermore, the derivatized pool of glycans from ovalbumin without desalting resulted in an ESI spectrum completely uninterpretable.

3.4.2.2 Analysis of PMP-Glycans from Ovalbumin by off-line Combination of HPLC with MALDI-TOFMS

The PMP-derivatized glycans cleaved from different lots of ovalbumin were eluted on an Hypersil ODS column, using the same conditions as for the PMP-derivatives of larger standards.The gradient had been previously optimized with the PMP-derivatives of small sugars. Figure 3.37 shows the HPLC-UV profile obtained for the PMP-oligosaccharides from ovalbumin. The PMP-sugar chains were separated according to their chemical structures and compositions. The broad peak appearing at retention time

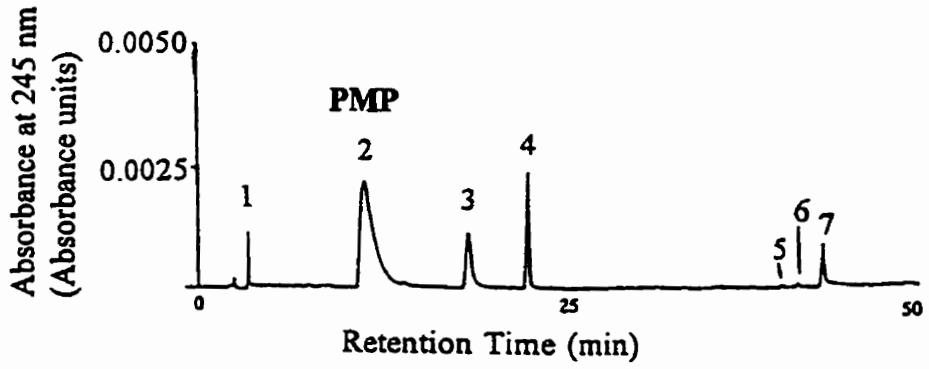

Fig. 3.37 Reversed phase HPLC-UV chromatogram of the glycans from ovalbumin, PMP-derivatized. Column: Hypersil ODS column (25 cm X 0.46 cm); Gradient: from 20% to 100 % acetonitrile in 0.01 M aqueous TFA over 70 min; flow rate 1 mL/min; wavelength 245 nm. The peaks are labeled 1-7 and correspond to different collected fractions.

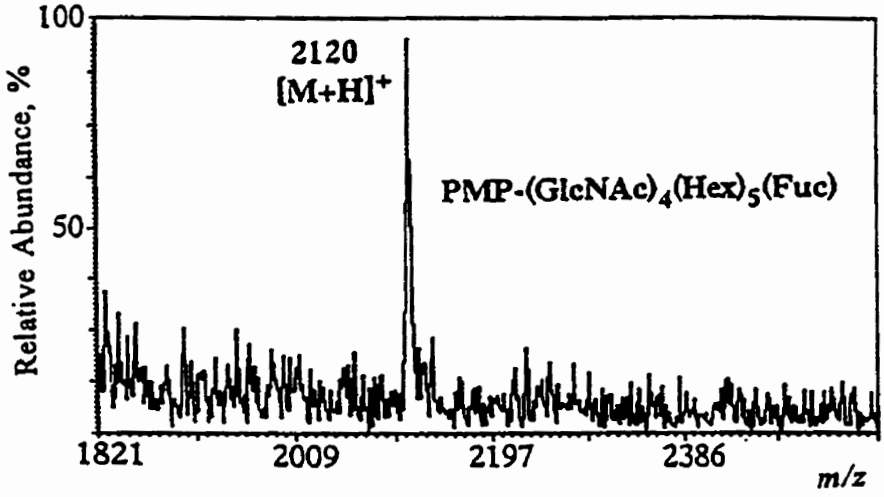

Fig. 3.38 Linear mode MALDI-TOF mass spectrum of one of the PMP-glycans from ovalbumin following RP-HPLC separation (fraction 4).

9.8 min is due to a large amount of PMP reagent, left behind even after cleanup. The results obtained from RP-HPLC indicated that PMP-glycans from ovalbumin had similar chromatographic behaviours to those of PMP-derivatives of larger standards.

In order to isolate fractions more efficiently without overloading the column, the derivatized glycan mixture was injected several times in a row, with only 50-100-μL aliquots (0.044-0.088 mg of glycans) each time. Fractions corresponding to each of the peaks shown in Fig. 3.37 was collected manually, and fractions from several runs were combined, then evaporated by Speed Vac. The repetitive runs yielded quite reproducible chromatograms. It has been reported that, typically, a modest recovery of 50% is experienced in isolating N-linked oligosaccharides from silica RP-HPLC columns, presumably due to irreversible interaction of the carbohydrate with the column support [see Ref.141 and the references therein]. The same report also pointed out that this loss can be overcome by using polymer RP-HPLC columns, which can provide 90% recovery of carbohydrates, at the expense of greatly reduced resolution.

The Speed Vac-dried combined fractions were reconstituted in 10 μL of water and subjected to MALDI-TOFMS. Aliquots (1 μL) of these solutions were used as samples for MALDI. Prior to characterizing the cleaved glycan mixture obtained from ovalbumin, three PMP-derivatized oligosaccharide standards were examined by MALDI-MS as described above. This confirmed the character of the derivatized oligosaccharides through obtaining their M_rs, but also gave an indication of the nature of adduct species that could be expected [134]. An example of a MALDI spectrum obtained for one of the PMP-glycans collected from peak 4 in Fig. 3.37 is presented in Figure 3.38. Since most

sodium ions had been removed by RP-HPLC, mainly protonated molecular species $[M+H]^+$ were observed with MALDI-MS. Table 3.7 gives a list of some suggested glycan compositions, deduced from their observed M_r. The calculation method used for the results from ESI-MS analyses of PMP-glycans has been applied here to the MALDI results. As indicated by Harvey and co-workers [147], the essential absence of any ions other than the molecular ions ensured that MALDI spectra are ideal for the examination of mixtures as each peak in the spectrum could be assigned with confidence to have been produced by a different oligosaccharide. However, it cannot be ruled out that individual peaks could be produced by two or more isobaric sugars. Except for two, i.e. $(Hex)_5(GlcNAc)_4(Fuc)$ and $(Hex)_1(GlcNAc)_2$, the compositions suggested in Table 3.7 had been reported previously [43,66,134,136-147]. Two structures observed here, i.e.$(Hex)_1(HexNAc)_2$, and $(Hex)_2(HexNAc)_2$, may result from fragmentation due to cleanup or the MALDI process. The $(GlcNAc)_4(Hex)_5(Fuc)$ structure suggested by our study was not reported elsewhere and the other possible composition corresponding to this molecular mass might be $(Hex)_6(GlcNAc)_4$-H_2O. The oligosaccharide with the compositon of $(Hex)_6(GlcNAc)_4$ was also detected by ESI-MS of intact ovalbumin, as shown in Table 3.5. It has also been pointed out by Harvey and co-workers [147] that some ion peaks could be interpreted in terms of two compositions differing by about 2 u, a difference too small to determine with the TOF analyzer. A mass measurement accuracy to within 1 u is necessary to assign a unique composition to those ions such as with higher resolution offered by reflectron or magnetic sector instruments. The MALDI results show that besides the main component, each HPLC fraction also contained several minor

Table 3.7: MALDI-TOFMS molecular mass measurements for PMP-derivatized glycans from ovalbumin.

No[a]	Observed m/z[b] $[M+H]^+$	Mrs of oligosaccharides from experiments	Possible sugar composition
22#	920 (3)[c]	590	$(Hex)_1(GlcNAc)_2$ (587)
23	1082 (3)	752	$(Hex)_2(GlcNAc)_2$ (749)
24	1407(4)	1077	$(Hex)_4(GlcNAc)_2$ (1073)
25	1448 (4)	1118	$(Hex)_3(GlcNAc)_3$ (1114)
21	1613 (4)	1283	$(Hex)_4(GlcNAc)_3$ (1276)
2	1654 (4)	1324	$(Hex)_3(GlcNAc)_4$ (1317)
26	1769 (3)	1439	$(Hex)_5(GlcNAc)_3$ (1438)
27#	2120 (4)	1790	$(Hex)_5(GlcNAc)_4(Fuc)$ (1788) $(Hex)_6(GlcNAc)_4$-H_2O (1785)

[a] # these glycans have not been reported in the literature.

[b] We estimated an error of ± 7 on measured *m/z* values due to broadening of the peaks by the presence of Na^+ adducts.

[c] The numbers in the parentheses indicate RP-HPLC fractions.

components, possibly originating from incomplete resolution of HPLC peaks [157] or from structural heterogeneity [165] since isomeric glycans have similar structures which have similar interactions with RP-HPLC column so that they are not easily separated from each other. Our MALDI data agree with earlier work [134]: PMP-sugars are eluted in the order of decreasing molecular weight and polarity in RP-HPLC. In addition, generally, oligosaccharides with increasing numbers of GlcNAc residues elute later in the chromatogram as indicated earlier [141].

Overall, listed in Tables 3.5, 3.6 and 3.7, are twenty seven oligosaccharides with their respective suggested compositions. Nine of those have not been previously reported. However, at least four of them detected by off-line HPLC/MALDI and ESI-MS are possibly truncated sugar fragments generated during the workup or due to in-source fragmentation. The M_r values measured by MALDI-MS and ESI-MS can only suggest possible $(Hex)_x(GlcNAc)_y(Fuc)_z$ structures. In our hands, MS and MS/MS were also not able to differentiate oligosaccharides with same M_r but different compositions or different isomers with different linkage position, i.e. isomers with the same composition. For example, another possible composition for the oligosaccharide 10, which has been described as $Hex_3HexNAc_7$ in Table 3.6, could be $Hex_8HexNAc_3$, and its expected M_r, 1923, would be more closer to the observed value (1922). The results from direct ESI-MS analysis of intact ovalbumin are considered more reliable than those involving cleavage and derivatization chemistry since oligosaccharides were kept intact in the former. More specific information on carbohydrate structure has however been obtained in other laboratories by MALDI-TOFMS, with detection in the post-source decay (PSD) mode

[97,166] or by ESI-CID-MS/MS [11,33]. It has however been reported that better mass resolution of low M_r oligosaccharides detached from ovalbumin allowed determination of more glycoforms of ovalbumin than could be directly determined from the mass spectrum of the intact glycoprotein [43]. In our ESI-MS analyses of cleaved oligosaccharide mixtures, enhanced sensitivity could be achieved after derivatization with PMP, resulting in detection of seven oligosaccharides which have not been reported before. However, it should be mentioned here that there has been growing confusion about which of the reported structures in fact belong to ovalbumin and which are constituents of contaminating proteins [142]. As previously indicated by Reinhold and co-workers [164], successful profiling relies on complete deglycosylation and derivatization chemistry. Although glycan release by hydrazinolysis always appears complete, usually 5-10 times more material is required for hydrazinolysis than if enzymatic treatment is used for the same purpose, when ESI-MS is to be used as the characterization method. In addition, side products and background of this hydrazinolysis chemistry may interfere with electrospray ionization and reducing end labeling. Enzymatic cleavage methods are more costly than hydrazinolysis, but more reliable by not cleaving the sugars into smaller portions. In our case, truncation of the trimannosyl core by hydrazinolysis was shown to occur at the reducing end of oligosaccharides, however, it is not known if any truncation occurs at the non-reducing end.

CONCLUSION

In this project, a combination of derivatization, HPLC, and mass spectrometry, as well as off-line and on-line coupling of HPLC with mass spectrometry has been used to characterize glycans from a glycoprotein, ovalbumin. Derivatization with suitable chromophores allows enhanced HPLC detection. In addition, derivatization often gives rise to more structural information available from mass spectrometric experiments. Improved sensitivity and enhanced fragmentation are especially useful when the available chromatographic methods are not able to provide complete separation of major and minor components.

In the preliminary work, small sugars were used to prepare PA- and PMP-derivatives. Both PA- and PMP-derivatization methods involve reactions which are quantitative and simple to carry out. PA- and PMP-derivatization allowed sensitive detection of carbohydrates in both UV absorption and MS (FAB, ESI, and MALDI). The PMP-derivatives showed better chromatographic resolution and selectivity than PA-labeled sugars. In addition, PMP-derivatives of small sugars produced improvements in MS sensitivity of a factor up to 100 relative to underivatized sugars, and up to ten relative to PA-derivatives. PMP-labeling method was chosen to carry out work further on tetraglucose and larger standard oligosaccharides obtained commercially. ESI-MS results show that PMP-labeling increases the positive mode ESI sensitivity by a factor of 10 in the case of a neutral sugar. For a N-linked oligosaccharide containing GlcNAc moieties, no improvement in sensitivity has been achieved; however, PMP-derivatization made the fragmentation pattern much easier to interpret and gave more sequence information than

that provided with native sugars. This methodology was further applied to a glycoprotein with only one glycosylation site, ovalbumin. The sugar content of ovalbumin was characterized by ESI-MS combined with other techniques with and without glycans being detached from the glycoprotein. Electrospray of intact ovalbumin provided reliable and qualitative information on the glycoforms of the molecule. Hydrazinolysis caused truncation of some glycans, even when performed carefully for sugar removal from the peptide backbone. However, it is an inexpensive method relative to enzymatic cleavage, although the latter is more advisable to use, especially if less than 1 mg of gycoprotein is initially available. Characterization of PMP-derivatized N-glycans from ovalbumin by full-scan ESI confirmed some of the sugar compositions found by ESI of the intact glycoprotein, and also allowed identification of the compositions of some sugars which have not been reported in the literature, based on $(Hex)_x(GlcNAc)_y(Fuc)_z$ formula. This procedure also clearly demonstrated that hydrazinolysis had caused some sugar truncation among the glycan mixture. Finally, ESI-CID-MS/MS experiments on three PMP-glycans, chosen as precursors from the PMP-glycan mixture, did not provide detailed information of the sugar structures, but rather helped to confirm some truncations and verify the identity of PMP-glycans. These results are also complementary to those obtained by linear mode MALDI-TOF-MS. According to the results obtained with NGA3, a standard N-linked oligosaccharide, on-line coupling of HPLC with ESI-MS seems very promising in determining the structures of glycans from glycoproteins among the techniques applied in this project. The molecular mass of each component in a mixture can be measured, and the structure can be studied by MS/MS. This method is useful for elucidation of complex

mixtures, especially when some difficulty exists in separation by HPLC. HPLC and MS are complementary to each other. If HPLC cannot provide satisfactory separation, LC/MS and MS/MS render it possible to distinguish isobaric structures of different components which appear as coeluted peaks.

Oligosaccharides derivatized with PMP possess unmodified nonreducing termini and therefore are amenable to subsequent investigation using high sensitivity analytical methods such as exoglycosidase digestion. Exoglycosidase digestion in combination with the analysis of the truncated oligosaccharide from enzymatic digestion by mass spectrometry could be the avenue to future work for obtaining additional structural data.

REFERENCES

1. J. Darnell, H. Lodish, and D. Baltimore, *Molecular Cell Biology*, Scientific American Books, Inc. Ch. 3, pp51-104 (1986).

2. C. W. Sutton, J. A. O'Neill, and J. S. Cottrell, *Anal. Biochem.* **218**, 34-46 (1994).

3. O.P. Bahl in H. J. Allen and E. C. Kisailus (Editor), *Glycoconjugates: Composition, Structure, and Function*, Marcel Dekker, Inc. Ch. 1, pp1-12 (1992).

4. Oxford GlycoSystems Ltd., in "*Tools for Glycobiology*", *Catalog and Technical Notes*, Rosedale, NY (1992).

5. J. Keesey, *Biochemica Information*, Boehringer Mannheim Biochemicals, Indianapolis, IN.

6. U. Bahr, A. Pfenninger, M. Karas, and B. Stahl, *Anal. Chem.* **69**, 4530-4535 (1997).

7. G. S. Jacob, and P. Scudder, *Methods Enzymol.* **230**, 280-299 (1994).

8. R. Kornfeld, and S. Kornfeld, *Annu. Rev. Biochem.* **45**, 217-237 (1976).

9. R. J. Cotter, *Time -of-flight Mass Spectrometry Instrumentation and Applications in Biological Research*, ACS Professional Reference Books, American Chemical Society, Washington, DC, (1997).

10. A. Kobata, *Eur. J. Biochem.* **209**, 483-501 (1992).

11. V. N. Reinhold, B. B. Reinhold, and C. E. Costello, *Anal. Chem.* **67**,1772-1784 (1995).

12. William S. Hancock, A. *Methods Enzymol.* **271**, 403-427 (1996).

13. R. R. Townsend, M. Alai, M. R. Hardy, and C. C. Fenselau, *Anal. Biochem.* **171**, 180-191 (1988).

14. S. Hirani, R. J. Bernasconi, and J. R. Rasmussen, *Anal. Biochem.* **162**, 485-492 (1987).

15. A. J. Mort and M. L. Pierce. in Z. E. Rassi (Editor), *Carbohydrate Analysis, J. Chromatogr. Library* Vol. 58, Elsevier, Amsterdam, Ch. 1, pp. 3-37 (1995).

16. A. L. Tarentino and T. H. Plummer Jr., *Methods Enzymol.* **230**, 44-57 (1994).

17. R. B. Parekh, *Methods Enzymol.* **230**, 340-348 (1994).

18. R. R. Townsend in Z. E. Rassi (Editor), *Carbohydrate Analysis, J. Chromatogr. Library* Vol. 58, Elsevier, Amsterdam (1995) Ch. 5, pp. 181-209.

19. B. Nilsson and S. Svensson, *Carbohydr. Res.* **62**, 377-380 (1978).

20. S. Takasaki, T. Mizuochi, and A. Kobata, *Methods Enzymol.* **83**, 263-268 (1982).

21. T. Patel, J. Bruce, A. H. Merry, J.C. Bigge, M. R. Wormald, and R.B.Parekh, *Biochem.* **32**, 679-693 (1993).

22. T. P. Patel and R.B. Parekh, *Methods Enzymol.* **230**, 57-66 (1994).

23. B. Bendiak and D. A.Cumming, *Carbohydr. Res.* **151**, 89-103 (1986).

24. A. Kobata and K. Furukawa in H. J. Allen and E. C. Kisailus (Editor), *Glycoconjugates: Composition, Structure, and Function*, Marcel Dekker, Inc. Ch. 3, pp33-69 (1992).

25. Oxford GlycoSystems Ltd., in "*N-glycan Recovery Kit*", Rosedale, NY (1993).

26. M. L. Rasilo and O. Renkonen, *FEBS Letters*, **135** (1), 38-42 (1981).

27. S. I. Ogata and K. O. Lloyd, *Anal. Biochem.* **119**, 351-359 (1982).

28. L. M. Likhosherstov, O. S. Novikova, V. A. Derevitskaya and N. K. Kochetkov, *Carbohydr. Res.* **199**, 67-76 (1990).

29. L. M. likhosherstov, O. S. Novikova, V. E. Piskarev, E. E. Trusikhina, V. A. Derevitskaya, and N. K. Kochetkov, *Carbohydr. Res.* **178**, 155-163 (1988).

30. B. Nilsson and S. Svensson, *Carbohydr. Res.* **72**, 183-190 (1979).

31. H. V. Halbeek, *Methods Enzymol.* **230**, 132-168 (1994).

32. Y. Zhang, R. A. Cedergren, T. J. Nieuwenhuis, and R. I. Hollingsworth, *Anal. Biochem.* **208**, 363-371 (1993).

33. V. N. Reinhold, B. B. Reinhold, and S. Chan, *Methods Enzymol.* **271**, 377-402 (1996).

34. R. Barker, H. A. Nunez, P. Rosevear, and A.S. Serianni, *Methods Enzymol.* **83**, 58-69 (1982).

35. T. A. W. Koerner, J. H. Prestegard, and R. K. Yu, *Methods Enzymol.* **138**, 38-59 (1987).

36. A. S. Serianni in H. J. Allen and E. C. Kisailus (Editor), *Glycoconjugates: Composition, Structure, and Function*, Marcel Dekker, Inc. (1992) Ch. 4 pp71-102.

37. Y. C. Lee, *Anal. Biochem.* **189**, 151-162 (1990).

38. M. R. Hardy and R. R. Townsend, *Methods Enzymol.* **230**, 208-225 (1994).

39. J. Marc Lo-Guidice and M. Lhermitte, *Biomed. Chromatogr.* **10**, 290-296 (1996).

40. S. B. Levery, and S-I. Hakomori, *Methods Enzymol.* **138**, 13-25 (1987).

41. P. C. Elwood, W. K. Reid, P. D. Marcell, R. H. Allen, and J. F. Kolhouse, *Anal. Biochem.* **175**, 202-211(1988).

42. M. Okamoto, K. Takahashi and T. Doi, *Rapid Commun. Mass Spectrom.* **9**, 641-643 (1995).

43. K. L. Duffin, J. K. Welply, E. Huang and J. D. Henion, *Anal. Chem.* **64**, 1440-1448 (1992).

44. F. Hillenkamp, M. Karas, R. C. Beavis and B. T. Chait, *Anal. Chem.* **63**, 1193A-1203A (1991).

45. J. Lemoine, F. Chirat and B. Domon, *J. Mass Spectrom.* **31,** 908-912 (1996).

46. T. Takao, Y. Tambara, A. Nakamura, K. Yoshino, H. Fukuda, M. Fukuda and Y. Shimonishi, *Rapid Commu. Mass Spectrom.* **10,** 637-640 (1996).

47. G. R. Gary, *Methods Enzymol.* **138**, 26-38 (1987).

48. Y.C. Lee, *J. Chromatogr. A* **720**, 137-149 (1996)

49. C. J. Edge, T. W. Rademacher, M. R. Wormald, R. B. Parekh, T. D. Butters, D. R. Wind, and R. A. Dwek, *Proc. Natl. Acad. Sci. USA.* **89**, 6338-6342 (1992).

50. A. Kobata, *Anal. Biochem.* **100**, 1-14 (1979).

51. P.M Rudd, et al. *J. Biol. Chem.* **272**, 7229-7244 (1997).

52. T. Mizuochi, K. Yonemasu, K. Yamashita, and A. Kobata, *J. Biol. Chem.* **253**, 7404-7409 (1978).

53. S. Takasaki and A. Kobata, *Biochem.* **25**, 5709-5715 (1986).

54. S. Ogata, Y. Misumi, K. Miki and Y. Ikehara, *Eur. J. Biochem.* **161**, 315-320 (1986).

55. G. R. Guile, P. M. Rudd, D. R. Wing, S. B. Prime, and R. A. Dwek, *Anal. Biochem.* **240**, 210-226 (1996).

56. O. Iourin, T. S. Mattu, N. Mian, G. Keir, B. Winchester, R. A. Dwek and P. M. Rudd, *Glyco. J.* **13**, 1031-1042 (1996).

57. S. Suzuki, K. Kakehi and S. Honda, *Anal. Chem.* **68**, 2073-2083 (1996).

58. S. Hase, in Z. E. Rassi (Editor), *Carbohydrate Analysis, J. Chromatogr. Library* Vol. **58**, Elsevier, Amsterdam (1995) Ch. 15, p. 555-571.

59. M. S. F. Ross, *J Chromatogr.* **141**, 107-119 (1977).

60. K. Mopper and L. Johnson, *J. Chromatogr.* **256,** 27-38 (1983).

61. W. F. Alpenfels, *Anal. Biochem.* **114**, 153-157 (1981).

62. G. R. Her, S. Santikarn, V. N. Reinhold and J. C. Williams, *J. Carbohydr. Chem.* **6**, 129-139 (1987).

63. S. Hase, T. Ibuki and T. Ikenaka, *J. Biochem.* **95**, 197-203 (1984).

64. A. Kondo, J. Suzuki, N. Kuraka, S. Hase, I. Kato and J. Ikenaka, *Agric. Biol. Chem.* **54**, 2169-2170 (1990).

65. S. Hase, S. Koyama, H, Daiyasu, H. Taakemoto, et al. *J. Biochem.* **100**, 1-10 (1986).

66. N. Tomiya, J. Awaya, M. Kurono,et al. *Anal. Biochem.* **171**, 73-90 (1988).

67. J. S. Sawada, Y. Umeda, A. Kondo, and I. Kato, *Anal. Biochem.* **207**, 203-207 (1992).

68. S. Hase and T. Ikenaka, *Anal. Biochem.* **184**, 135-138 (1990).

69. Y. C. Lee, B. I. Lee, N. Tomiya, and N. Takahashi, *Anal. Biochem.* **188**, 259-266 (1990).

70. K. Kakehi, S. Suzuki, S. Honda and Y. C. Lee, *Anal. Biochem.* **199**, 256-268 (1991).

71. S. Honda, E. Akao, S. Suzuki, M. Okuda, K. Kakehi and J. Nakamura, *Anal. Biochem.* **180**, 351-357 (1989).

72. D. J. Strydom, *J. Chromatogr.* A **678**, 17-23 (1994).

73. D. Fu and R. A. O'Neill, *Anal. Biochem.* **227**, 377-384 (1995).

74. D. H. Hawke, K. Hsi, L. R. Zieske, L. Chen and P. Yuan, in R. H. Angeletti (Editor).

Techniques in Protein Chemistry III, Academic Press, Inc. (1992).

75. K. Kakehi and S. Honda, *Applied Biochem. and Biotech.* **43,** 55-71 (1993).

76. K. Kakehi, M. Ueda, S. Suzuki and S. Honda, *J. Chromatogr.* **630**, 141-146 (1993).

77. A. Dell, A. J. Reason, K. Khoo, M. Panico, R. A. McDowell, and H. R. Morris, *Methods Enzymol.* **230**, 108-132 (1994).

78. M. Barber, R. S. Bordoli, R. D. Sedgwick, and A. N. Tyler, *Nature* **293**, 270-275 (1981).

79. W. E. Seifert, Jr. and R. M. Carrioli, *Methods Enzymol.* **270**, 453-486 (1996).

80. J. P. Kamerling, W. Heerma, J. F. G. Vliegenthart, B. N. Green, I. A. S. Lewis, G. Strecker and G. Spik, *Biomed. Mass Spectrom.* **10**, 420-425 (1983).

81. A. Dell, *Adv. Carbohydr. Chem. Biochem.* **45**, 19-72 (1987).

82. C. A. Settineri and A. L. Burlingame, in Z. E. Rassi (Editor), *Carbohydrate Analysis*, J. Chromatogr. Vol. 58, Elsevier, Amsterdam (1995) Ch. 12, pp. 447-514.

83. Yuanda Zhang, *Part 1. Derivatives for the Isolation, Purification and Mass Spectrometric Characterization of Homo and Hetero Oligosaccharides*, Michigan State Univ., Ph. D Thesis, (1993).

84. G. Siuzdak (Editor), *Mass Spectrometry for Biotechnology*, Academic Press, Inc. (1996) Ch. 1, pp 4-31.

85. L. Poulter, and A. L. Burlingame, *Methods Enzymol.* **193**, 661-689 (1990).

86. J. A. Loo, H. R. Udseth, and R. D. Smith, *Anal. Biochem.* **179**, 404-412 (1989).

87. S. A. Hofstadler, R. Bakhtiar, and R. D. Smith, *J. Chem Edu.* **73** (4), A83-88 (1996).

88. R. Bakhtiar, S. A. Hofstadler, and R. D. Smith, *J. Chem. Edu.* **73**(6), A118-123

(1996).

89. Y. Ohashi, in R. B. Cole (Editor), *Electrospray Ionization Mass Spectrometry of Carbohydrates and Lipids*, John Wiley & Sons, Inc. Ch.13, pp. 459-498 (1997).

90. B. L. Gillece-Castro and A. L. Burlingame, *Methods Enzymol.* **193**, 689-712 (1990).

91. B. Domon, and C. E. Costello, *Glyco. J.* **5**, 397-409 (1988).

92. M. Karas and F. Hillenkamp, *Anal. Chem.* **60**, 2299-2301(1988).

93. C. E. Costello, H. Perreault and L.C. Ngoka in "Mass Spectrometry in the Biological Sciences" A. L. Burlingame and S. A. Carr, Ed., Humana Press, Totowa, NJ (1996) pp. 365-384.

94. J. J. Pitt, and J. J. Gorman, *Rapid Commu. Mass Spectrom.* **10**, 1786-1788 (1996).

95. W. C. Sutton, J. A. O'Neil and J. S. Cottrell, *Anal. Biochem.* **218**, 34-46 (1994).

96. B. Spengler, D. Kirsch, R. Kaufmann and J. Lemoine, *Org. Mass Spectrom.* **29**, 782-787 (1994).

97. D. J. Harvey, T. J. P. Naven, B. Kuster, R. H. Bateman, M. R. Green and G. Critchley, *Rapid Commun. Mass Spectrom.* **9**, 1556-1561 (1995).

98. R. J. Anderegg, *Mass Spectrom. Rev.* **7**, 395-424 (1988).

99. Daniel R. Knapp, *Methods Enzymol.* **193**, 314-329 (1990).

100. A. Dell and P. R. Tiller, *Biochem. Biophys. Res. Commun.* **135**, 1126-1134 (1986).

101. A. Cophie, and Bo Nilsson, *Methods Enzymol.* **193**, 587-607 (1990).

102. G. J. V. Berkel and K. Asano, *Anal. Chem.* **66**, 2096-2102 (1994).

103. J. M. E. Quirke, C. L. Adams, and G. J. V. Berkel, *Anal. Chem.* **66**, 1302-1315 (1994).

104. B. Fournet, G. Strecker, Y. Leroy, and J. Montreuil , *Anal. Biochem.* **116**, 489-502 (1981).

105. C. G. Hellerquist, B. Lindberg, S. Svensson, T. Holme and A. A. Lindberg, *Carbohydr. Res.* **8**, 43-55 (1968).

106. S. Hakomori, *J. Biochem.* (Tokyo) **55**, 205-208 (1964).

107. F. G. Hanisch, *Biol. Mass Spectrom.* **23**, 309-312 (1994).

108. R. Geyer and H. Geyer, *Methods Enzymol.* **230**, 86-108 (1994).

109. D. Rolf and G. R. Gray, *J. Am. Chem. Soc.* **104**, 3539-3541 (1982).

110. G. R. Gray, *Method Enzymol.* **193**, 573-587 (1990).

111. D. Rolf, J. A. Bennek, and G. R. Gray, *Carbohydr. Res.* **137**, 183-196 (1985).

112. J. G. Jun and G. R. Gray, *Carbohydr. Res.* **163**, 247-261 (1987).

113. K. K. Haschemie, A. Renger and H. Steinhart, *Carbohydr. Polymers* **30**, 31-35 (1996).

114. C. M. John and B. W. Gibson, *Anal. Biochem.* **187**, 281-291 (1990).

115. A. Dell, *Methods Enzymol.* **193**, 647-661 (1990).

116. A. Dell, N. H. Carman, P. R. Tiller and J. E. Thomas-Oates, *Biomed. Environ. Mass Spectrom.* **16**, 19-24 (1988).

117. B. Domon, D. R. Mueller and W. J. Richter, *Org. Mass Spectrom.* **29**, 713-719 (1994).

118. I. J. Goldstein, G. W. Hay, B. A. Lewis, and F. Smith, *Methods Carbohydr. Chem.* **5**, 361-370 (1965).

119. A. Angel, amd B. Nilsson, *Biomed. Environ. Mass Spectrom.* **19**, 721-730 (1990).

120. A. Angel, F. Lindh and B. Nilsson, *Carbohydr. Res.* **168**, 15-31 (1987).

121. R. S. Pappas, B. J. Sweetman, S. Ray, and C. G. Hellerqvist, *Carbohydr. Res.* **197**, 1-14 (1990).

122. H. Krotkiewski, and E. Lisowska, *Carbohydr. Res.* **184**, 27-38 (1988).

123. A. S. Angel, P. Lipniunas, K. Erlansson, and B. Nilsson, *Carbohydr. Res.* **221**, 17-35 (1991).

124. E. A. Nothnagel, M. McNeil, P. Albersheim, and A. Dell, *Plant Physiol.* **71**, 916-926 (1983).

125. Linda Poulter, R. Karren, and A. L. Burlingame, *Anal. Biochem.* **195**, 1-13 (1991).

126. L. Poulter, J. P. Earnest, R. M. Stroud, and A. L. Burlingame, *Proc. Natl. Acad. Sci. USA* **86**, 6645-6649 (1989).

127. W. T. Wang, N. C. LeDonne, Jr., B. Ackerman, *Anal. Biochem.* **141**, 366-381 (1984).

128. A. Dell, J. P. Earnest, R. M. Stroud, and A. L. Burlingame, *Biomed. Environ. Mass Spectrom.* **16**, 25-30 (1988).

129. S. A. Carr and V. N. Reinhold, *Biomed. Mass Spectrom.* **12**, 288-295 (1985).

130. J. Gu, T. Hiraga, and Y. Wada, *Biol. Mass Spectrom.* **23**, 212-217 (1994).

131. S. F. Osman and P. D. Hoagland, *Carbohydr. Res.* **128**, 361-365 (1984).

132. A. M. Lawson, W. Chai, G. C. Cashmore, *Carbohydr. Res.* **200**, 47-57 (1990).

133. S. Honda, K. Kakehi, T. Ohmura, and M. Morita, *Biomed. Environ. Mass Spectrom.* **15**, 233-237 (1988).

134. D. S. Ashton, C. R. Beddell, D. J. Cooper, and A. C. Lines, *Anal. Chim. Acta* **306**,

43-48 (1995).

135. A. D. Nisbet, R. H. Saundry, A. J. G. Moir, L. A. Fothergill, and J. E. Fothergill. *Eur. J. Biochem.* **115**, 335-345 (1981).

136. T. Tai, K. Yamashita, S. Ito, and A. Kobata, *J. Biol. Chem.* **252**, 6687-6694 (1977).

137. M.-G. Yet, C. C. Q. Chin and F.Wold, *J. Biol. Chem.* **263**, 111-117 (1988).

138. L. -M. Chen, M. -G. Yet and M. -C. Shao, *FASEB J.* **2,** 2819-2824 (1988).

139. S. Honda, A. Makino, S. Suzuki, and K. Kakeki, *Anal. Biochem.* **191,** 228-234 (1990).

140. K. Kakeki and S. Honda, *Applied Biochem. and Biotech.* **43,** 55-71 (1993).

141. M. L. Corradi Da Silva, H. J. Stubbs, T. Tamura, and K. G. Rice, *Archives Biochem. Biophys.* **318**, 465-475 (1995).

142. B. Kuster, T. J. P. Naven and D. J. Harvey, *J. Mass Spectrom.* **31**, 1131-1140 (1996).

143. Y. Mechref, and M. V. Novotny, *Anal. Chem.* **70**, 455-463 (1998).

144. T. Tai, K. Yamashita, M. Ogata-Arakawa, N. Koide, T. Muramatsu, S. Twashita, Y. Inoue, and A. Kobata, *J. Biol. Chem.* **250** , 8569-8575 (1975).

145. K. Yamashita, Y. Tachibana, and A. Kobata, *J. Biol. Chem.* **253**, 3862-3869 (1978).

146. T.J. P. Naven and D. J. Harvey, *Rapid Commun. Mass Spectrom.* **10**, 1361-1366 (1996).

147. D. J. Harvey, P. M. Rudd, R. H. Bateman, R. S. Bordoli, K. Howes, J. B. Hoyes and R. G. Vickers, *Org. Mass Spectrom.* **29**, 753-765 (1994)

148. T. H. Wang, T. F. Chen, and D. F. Barofsky, *Biomed. Environ. Mass Spectrom.* **16,**

335-338 (1988).

149. S. Hase, *Methods Enzymol.* **230**, 225-237 (1994).

150. J. Toyota, K. Omichi, K. Fukase, S. Kusumoto and S. Hase, *Biosci. Biotech. Biochem.* **58**, 567-569 (1994).

151. J. Suzuki, A. Kondo, I. Kato, S. Hase and T. Ikenaka, *Agric. Biol. Chem.* **55**, 283-284 (1991).

152. D. R. Wing, T.W. Rademacher, M. C. Field, R. A. Dwek, B. Schmitz, G. Thor and M. Schachner, *Glyco. J.* **9**, 293-301 (1992).

153. *Bio-Gel P Polyacrylamide Gel Instruction Manual*, BIO-RAD.

154. W. Ens, V. Spicer, K. G. Standing and J. Zhou, *Org. Mass Spectrom.* **28**, 1430-1434 (1993).

155. S. Hase, S. Natsuka, H. Oku, and T. Ikenaka, *Anal. Biochem.* **167**, 321-326 (1987).

156. H. Takemoto, S. Hase, and T. Ikenaka, *Anal. Biochem.* **145**, 245-250 (1985).

157. J. W. Webb, K. Jiang, B. L. Gillece-Castro, A. L. Tarentino, T. H. Plummer, J. C. Byrd, S. J. Fisher, and A. L. Burlingame, *Anal. Biochem.* **169**, 337-349 (1988).

158. M. Kussmann, E. Nordhoff, H. Rahbek-Nielsen, S. Haebel, M. Rossel-Larsen, L. Jakobsen, J. Gobom, E. Mirgorodskaya, A. Kroll-Kristensen, L. Palm and P. Roepstorff, *J. Mass Spectrom.* **32**, 593-601(1997).

159. M.E. Hemling, G. D. Roberts, W. Johnson, S. A. Carr, *and* T. R. Covey, *Biomed. Environ. Mass Spectrom.* **19**, 677-691 (1990).

160. D. Garozzo, V. Nasello, E. Spina, and L. Sturiale, *Rapid Commun. Mass Spectrom.* **11**, 1561-1566 (1997).

161. C. Sottani, M. Fiorentino and C. Minoia, *Rapid Commun. Mass Spectrom.* **11**, 907-913 (1997).

162. A.Tsarbopoulos, B. N. Pramanik, M. Karas, U. Bahr, and J. Ru, and Z. Stahl, *Rapid Commun. Mass Spectrom.* July, S207 (1995).

163. M. Karas and U. Bahr, *Mass Spectrom. Rev.* **10**, 335-357 (1991).

164. K. B. Linsley, S. Y. Chan, S. Chan, B. B. Reinhold, P. J. Lisi, and V. N. Reinhold, *Anal. Biochem.* **219**, 207-217 (1994).

165. E. Coles, V. N. Reinhold and S. A. Carr, *Carbohydr. Res.* **139**, 1-11 (1985).

166. G. Talbo and M. Mann, *Rapid Commun. Mass Spectrom.* **10**, 100-103 (1996).

IMAGE EVALUATION
TEST TARGET (QA–3)

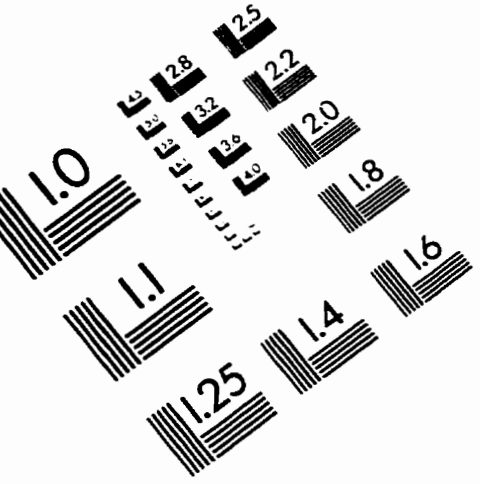

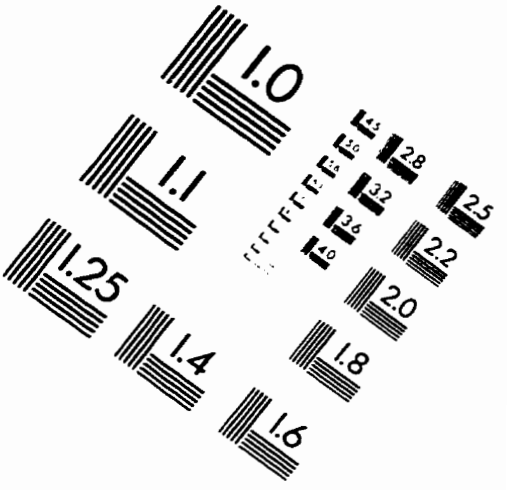

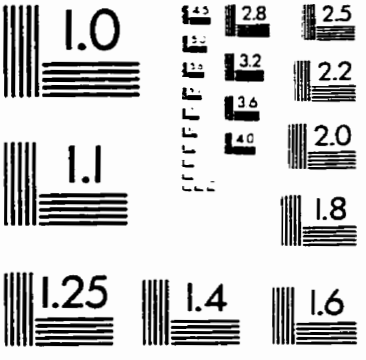

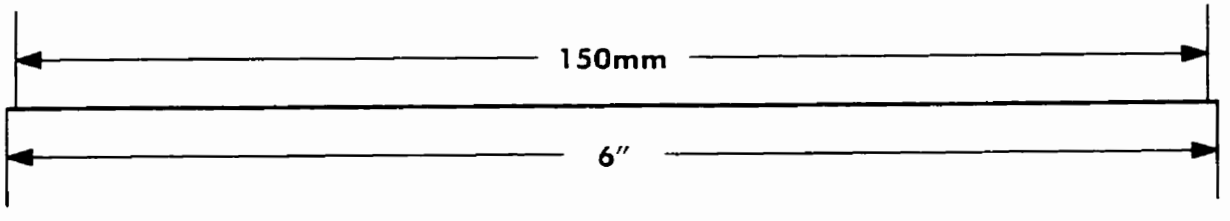

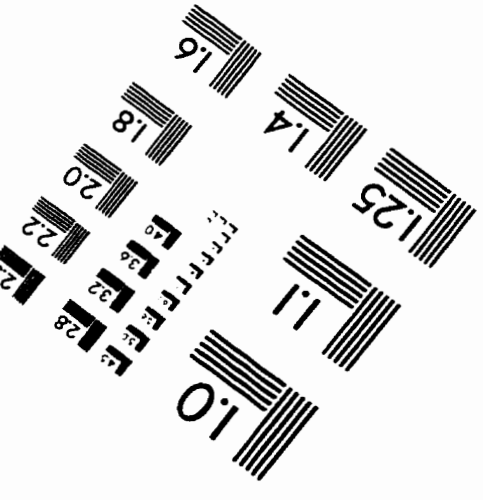

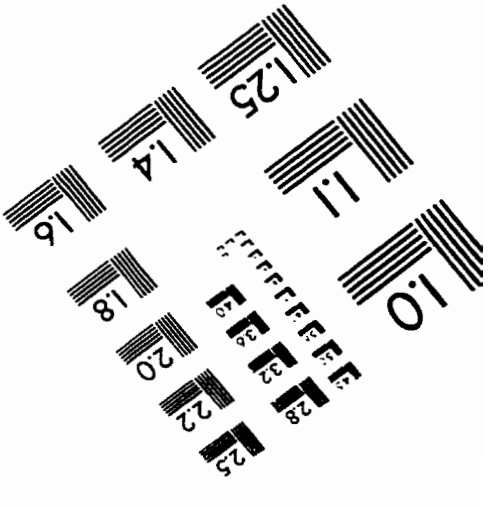

APPLIED IMAGE . Inc
1653 East Main Street
Rochester, NY 14609 USA
Phone: 716/482-0300
Fax: 716/288-5989